

Distribution Agreement

In presenting this thesis or dissertation as a partial fulfillment of the requirements for an advanced degree from Emory University, I hereby grant to Emory University and its agents the non-exclusive license to archive, make accessible, and display my thesis or dissertation in whole or in part in all forms of media, now or hereafter known, including display on the world wide web. I understand that I may select some access restrictions as part of the online submission of this thesis or dissertation. I retain all ownership rights to the copyright of the thesis or dissertation. I also retain the right to use in future works (such as articles or books) all or part of this thesis or dissertation.

Signature:

Lenore Monterroza

Date

EZH2 and STING as therapeutic targets in immunologically cold breast and lung tumors

By

Lenore Monterroza

Doctor of Philosophy

Graduate Division of Biological and Biomedical Sciences

Cancer Biology

Periasamy Selvaraj, Ph.D., Co-Advisor

Rabindra M. Tirouvanziam, Ph.D., Co-Advisor

Chrystal M. Paulos, Ph.D., Committee Member

Curtis J. Henry, Ph.D., Committee Member

Wei Zhou, Ph.D., Committee Member

Accepted:

Kimberly Jacob Arriola, Ph.D.

Dean of the James T. Laney School of Graduate Studies

Date

EZH2 and STING as therapeutic targets in immunologically cold breast and lung tumors

By

Lenore Monterroza

B.S., University of Texas at El Paso

Advisors:

Periasamy Selvaraj, Ph.D.

Rabindra Tirouvanziam, Ph.D.

An abstract of

A dissertation submitted to the Faculty of the James T. Laney School of Graduate Studies of
Emory University in partial fulfillment of the requirements for the degree of

Doctor of Philosophy

in the Graduate Division of Biological and Biomedical Sciences

Cancer Biology

2024

Abstract

EZH2 and STING as therapeutic targets in immunologically cold breast and lung tumors

By

Lenore Monterroza

Despite therapeutic advances, cancer remains a leading cause of morbidity and mortality worldwide. In early tumor development, cancer cells often coopt immune cells to promote angiogenesis and avoid immune attacks. They mutate to resist therapy, evade anti-tumor immunity, and metastasize. Cancer cells' interactions with tumor-infiltrating neutrophils (TINs) have historically received less attention than anti-tumor CD8+ T cells. This dissertation examines the influence of TINs in two treatment-resistant cancers, triple negative breast cancer (TNBC) and lung adenocarcinoma (LUAD). At the molecular level, we highlight the role of enhancer of zeste homolog 2 (EZH2), a pro-tumor methyltransferase, and one of its immunological targets, the stimulator of interferon genes (STING).

First, we used CRISPR to develop EZH2 gene knockout (KO) and overexpression (OE) clones of the 4T1 TNBC mouse model and examined downstream effects on invasive and replicative capacities of cancer cells *in vitro* and *in vivo*. We observed significant reductions in tumor growth and lung metastasis, as well as dramatic reductions in the ratios of TINs to both CD4+ and CD8+ T cells when EZH2 was knocked out. Results suggest that EZH2 is not only important for tumor growth and metastasis, but that its expression in tumor cells can alter the infiltration and relative role of pro- and anti-tumor immune subsets in the microenvironment.

Second, we tested whether chemical inhibition of EZH2 or activation of STING altered LUAD/TIN interplay. We utilized a novel *in vitro* co-culture model based on human neutrophil migration through LUAD cells grown at an air-liquid interface. Treatment with MSA-2 (STING agonist) resulted in high induction of IL-29 (interferon λ 3) secretion in EZH2-high LUAD/TIN co-cultures. In contrast, treatment with EPZ6438 and MS1943 (EZH2 inhibitors) modestly influenced mediator secretion without any change in IL-29. Results suggest that STING activation and interferon signaling can be restored by drugs in EZH2-high LUAD/TIN.

Collectively, our findings provide insights into the role of TINs, offering novel perspectives on their interactions with cancer cells and other immune cells in the tumor microenvironment. They also advance our knowledge on EZH2 and STING pathway modulation and inform the development of more effective immunotherapeutic approaches for treatment-resistant cancer.

Keywords: CD4+ T-cell, CD8+ T-cell, EZH2, IL-29, lung adenocarcinoma, invasion, metastasis, STING, triple-negative breast cancer, tumor-infiltrating neutrophils

EZH2 and STING as therapeutic targets in immunologically cold breast and lung tumors

By

Lenore Monterroza

B.S., University of Texas at El Paso

Advisors:

Periasamy Selvaraj, Ph.D.

Rabindra Tirouvanziam, Ph.D.

A dissertation submitted to the Faculty of the James T. Laney School of Graduate Studies of
Emory University in partial fulfillment of the requirements for the degree of

Doctor of Philosophy

in the Graduate Division of Biological and Biomedical Sciences

Cancer Biology

2024

Acknowledgments

The work presented in this dissertation is the result of collaborative efforts from multiple investigators and the invaluable guidance of my dedicated mentors. Throughout my graduate training, I have grown as both a scientist and a professional through hard work and dedication. However, I owe a deep gratitude to many individuals who have supported and mentored me along the way, both before and during my time as a graduate student.

As an undergraduate at the University of Texas at El Paso, I was fortunate to build a strong foundation as an aspiring biomedical researcher. I would like to thank Dr. Armando Varela for giving me the opportunity to work in his research laboratory. Starting as a sophomore and continuing until my graduation, I gained critical skills, like cell culture and drug fabrication, in a drug screening lab that have been invaluable to my career. In addition, Dr. Varela taught me the importance of honest work and openness to feedback. I would also like to thank Dr. Marc Cox for his patience and support in helping me seek professional opportunities, apply to graduate school, and for encouraging me to speak up for myself. Additionally, I am grateful to Dr. Charles Spencer, who was always willing to listen and reinforced my self-confidence. During the summers, I had the privilege of training at Washington University in St. Louis with Dr. Lilliana Solnica-Kresel. Her guidance taught me that women can excel in science and that determination can overcome obstacles. This experience instilled in me the values of discipline and commitment. Furthermore, I trained at the Gorgas Commemorative Institute of Health Studies in Panama City, Panama. The field research in the remote jungles of El Tapon de Darien particularly was one of the most rewarding of my life. It taught me resilience, empathy, and the hard work required to protect populations from viral hazards.

I have been fortunate to work with an outstanding team of researchers in the Selvaraj and Tirouvanziam Labs over the past six years. As a new student, I learned about mouse models and flow cytometry from Luiz Munoz, who has been an essential peer mentor and friend. I thank fellow graduate

student Sarah Samaranayake, who has been a great source of support during long experimental shifts as well as a great friend. Sarah has been my partner to many adventures as we share a passion for serving underserved communities in Georgia. I am also grateful to Justin Hosten and Sarah Mansour, who have been excellent lab mates and special friends to walk through graduate school with. Our research specialists, Ramireddy Bommireddy and Milagros Aldeco, have provided tremendous experience and often saved us from disaster. I am thankful for the guidance and feedback from my thesis committee, including Dr. Chrystal Paulos, Dr. Curtis Henry, Dr. Wei Zhou, and my mentors Dr. Periasamy Selvaraj and Dr. Rabindra Tirouvanziam. Their participation in committee meetings provided crucial support and motivation. Each member, with their unique backgrounds, gave me the tools to feel empowered and energized to continue my research.

Among all the mentors I have had at Emory, I owe the most gratitude to Dr. Periasamy Selvaraj and Dr. Rabindra Tirouvanziam. They have played crucial roles at different stages of my training and instilled values I will carry forward. I am sure I will never meet someone like Selva again in my life; he is one of those people that lives a simple life but holds a million stories within him. Dr. Selvaraj taught me about personalized cancer immunotherapy and the importance of being a responsible and resourceful scientist. Training under Dr. Tirouvanziam made me a better scientist—capable of thinking critically, ready to take any challenge, and able to defend my work. His innovative ideas and ambitious projects have constantly inspired me. Thank you, Selva and Rabin, for creating so many opportunities for me, for standing behind me when challenges seemed overwhelming, for trusting me when I wanted to try new things, and for guidance and protection when I needed it the most.

I dedicate this thesis work to the women in my life. To my grandmothers, who dedicated their lives to serving their families and their communities, fostering a sense of home and safety. My mother, Nohemi, a steadfast lawyer whose faith and discipline always inspired me to believe in myself and go the extra mile. I also extend my gratitude to all female scientists I have worked with for their sacrifice, dedication, and the recognition they deserve for their contributions to science.

Table of contents

Chapter 1: Introduction	1
Overview of the cancer development process	2
Anti-tumor immunity.....	5
Cold tumors	6
Hot tumors	8
Tumor-infiltrating neutrophils (TINs)	10
Detailed account of tumor-TIN crosstalk at different cancer stages.....	13
Local invasion	13
Intravasation.....	15
Transport in circulation	16
Arrest in microvessels and extravasation	17
Formation of micro- / macro-metastases.....	18
Role of the EZH2 pathway in anti-tumor immunity.....	19
Research focus of this thesis manuscript	23
References	25
Chapter 2: Research manuscript #1	35
Abstract.....	36
Introduction	37
Materials and methods.....	39

Results	45
Discussion.....	49
Acknowledgments	54
Figures	55
References	64
Chapter 3: Research manuscript #2.....	70
Abstract.....	71
Introduction	72
Materials and methods.....	75
Results	78
Discussion.....	81
Acknowledgments	85
Figures	86
References	95
Chapter 4: Conclusions and perspectives	99
Foreword.....	100
EZH2, a potential TNBC therapeutic target	101
STING agonism and IL-29 induction are promising immunotherapeutic routes for human LUAD....	104
References	109

List of figures

Chapter 1	Page No.
Figure 1.1	3
Figure 1.2	7
Figure 1.3	12
Figure 1.4	14
Figure 1.5	21
Chapter 2	
Figure 2.1	55
Figure 2.2	56
Figure 2.3	57
Figure 2.4	58
Figure 2.5	59-60
Figure 2S1	61
Figure 2S2	62
Figure 2S3	63
Chapter 3	
Figure 3.1	86
Figure 3.2	87-88
Figure 3.3	89
Figure 3.4	90-91
Figure 3.5	92
Figure 3S1	93
Figure 3S2	94
Chapter 4	
Figure 4.1	102-103
Figure 4.2	106

List of abbreviations

Acronym	Expansion
APC	Antigen-presenting cells
CAR-T	Chimeric antigen T-cell
CRISPR	Clustered regularly interspaced short palindromic repeats
CTCs	Circulating tumor cells
DAMPs	Damage-associated molecular patterns
DTCs	Disseminated tumor cells
ECM	Extracellular matrix
EMT	Epithelial-to-mesenchymal transition
ENA-78	Epithelial neutrophil-activating peptide 78
EZH2	Enhancer of zeste homolog 2
G-CSF	Granulocyte colony-stimulating factor
GM-CSF	Granulocyte macrophage colony stimulating factor
ICAM	Intercellular adhesion molecule 1
ICIs	Immune checkpoint inhibitors
IFN	Interferon
IL	Interleukin
IL-1RA	Interleukin-1 receptor antagonist
IP-10	Interferon gamma-induced protein 10
KO	Knockout
LUAD	Lung adenocarcinoma
LKB1	Liver kinase B1
MCP-I	Monocyte chemoattractant protein 1
MET	Mesenchymal-to-epithelial transition
MHC	Major histocompatibility complex
MIP-1β	Macrophage inflammatory protein 1-beta
MMPs	Matrix metalloproteases
NE	Neutrophil elastase
NSCLC	Non-small cell lung cancer
OE	Overexpression
PD-1	Programmed death 1
PD-L1	Programmed death-ligand 1
PRC2	Polycomb repressive complex 2
STING	Stimulator of interferon genes
TILs	Tumor-infiltrating lymphocytes
TINs	Tumor-infiltrating neutrophils
TMB	Tumor mutational burden
TME	Tumor microenvironment
TNBC	Triple negative breast cancer
TNF-α	Tumor necrosis factor alpha
TRAIL	TNF-related apoptosis-inducing ligand
VEGFA	Vascular endothelial growth factor A

Chapter 1: Introduction

Overview of the cancer development process

Cancer is an aggressive heterogeneous disease that is long-lasting and recurring. Approximately, 1,958,310 new cancer cases and 609,820 cancer deaths were estimated to occur in the United States in 2023 [1]. Cancer development is a multistep process in which normal cell physiology is altered to enable the acquisition of functional capabilities that are crucial for the formation of malignant tumors. Inherent divergence in cancer pathogenesis and in the resulting acquired malignant phenotypes lead to multiple tissue-specific tumor types, subtypes and underlying mechanisms of tumor survival.

Among the fourteen identified hallmarks of cancer, “tumor-promoting inflammation” [2], and “genomic instability and mutation” [3] are fundamental to successful tumor development and disease progression [4]. Genomic instability and mutation enable the activation of proto-oncogenes and inhibition of tumor suppressor genes that underlie the transformation of *preneoplastic cells* into tumor cells. Tumor-promoting inflammation provides metabolic resources to the nascent tumor and allows for early immune escape. As the *nascent tumor* grows, a complex heterogeneous ecosystem referred to as the tumor microenvironment (TME) is formed around it. The TME comprises tumor cells and infiltrated immune cells, as well as fibroblasts, endothelial cells, and other stromal cell types; all which participate in tumorigenesis (**Figure 1.1**) [5-8]. With further growth and evolution of the tumor into more *mature stages*, the TME becomes more complex, allowing for the recruitment of cells that can be either tumor-suppressive or supportive. Primary tumors are generally detected at such mature stages, where their complex and variable cellular makeup will significantly affect the efficacy of anti-cancer therapies.

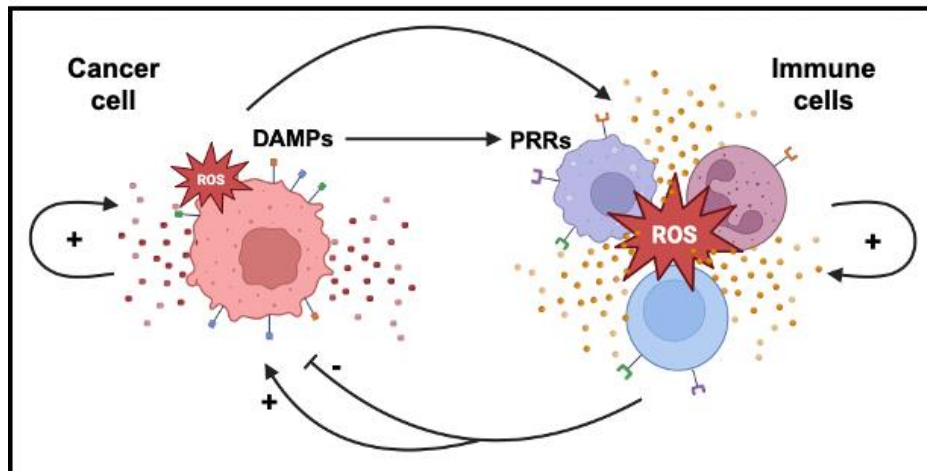


Figure 1.1. Genomic instability and inflammation are hallmarks of cancer development.

These two factors are driving forces in the transcriptomic heterogeneity of cancer cells, activation of survival mechanisms, metabolic support, and immune escape. Relationships between cancer and immune cells include sensing of cancer cell damage-associated molecular patterns (DAMPs) by pattern recognition receptors (PRRs) on immune cells, and major metabolic changes in the TME including the massive production of reactive oxygen species (ROS) by activated immune cells.

Although cancer mortality rates have recently declined, rising incidence for certain subtypes emphasize the need for better therapeutic approaches to prevent disease progression and recurrence [1]. Conventional cancer treatments include chemotherapy (using agents toxic to rapidly dividing cells), radiation therapy (damaging open chromatin), and hormone therapy (if appropriate for certain organs like breast and prostate). Those treatment modalities are efficient at debulking tumor mass before surgical resection. However, several critical mechanisms operating at the cellular level may limit the efficacy of those therapies. These include epigenetic alterations and DNA repair (nuclear compartment), activation of pro-survival and inhibition of

pro-apoptotic pathways (mitochondrial and cytosolic compartments), and multi-drug resistance (cytosolic conjugating enzymes and cell surface efflux pumps), to name a few. These mechanisms ultimately determine resistance to therapy [9-11]. In addition, the use of conventional therapies is limited by the multitude of known genotoxic and physiological side effects they are associated with. Chemotherapy targets not only cancer cells but also healthy, rapidly dividing cells in the bone marrow and gastrointestinal tract, leading to side effects that can significantly reduce patients' quality of life [12]. Some chemotherapies can cause DNA lesions (e.g. interfere DNA replication or RNA transcription), damage specific organs or cell types (e.g., cell differentiation), and induce toxicity. These adverse effects can vary widely among patients [13]. More than 50% of patients experience decreased appetite, nausea, vomiting, fatigue, dry mouth, constipation, and hair loss during the first cycle of chemotherapy. Additionally, despite the variation in side effects among different cancer types, 66.7% of all patients report experiencing six or more types of side effects during their treatment [14, 15]. Overall, side effects can significantly impact the continuation of treatment. To improve management of toxicity and mitigate the acceleration of aging features, it is vital to expand our knowledge of the medications used during cancer treatment. A deeper understanding of the mechanisms of action, dosage, and organ-specific toxicity is essential for the early identification of adverse effects, adjustment of treatment protocols, and enhancement of drug efficacy in anti-cancer therapy.

In the past two decades, novel therapies leveraging the immune system to combat cancers have emerged, which allow to overcome cancer resistance to conventional therapies. Examples of cancer immunotherapies include chimeric antigen receptor (CAR) T-cell therapies, which provide custom-engineered anti-tumor T cells recognizing specific molecular determinants on

tumor cells with high affinity, and immune checkpoint inhibitors (ICIs), which broadly function by counteracting inhibitory receptors (e.g., PD-1, CTL-4) on anti-tumor T cells. While these novel therapies have benefitted many patients who failed conventional therapies, treatment response is still limited by various factors. For example, both ICIs and CAR-T cells can lead to overactive T cells resulting in acute inflammation and autoimmunity. Also, the efficacy of CAR-T therapy may also be limited by tumor cell dormancy leading to the downregulation of surface antigens or by hypermutability (reflected by the tumor mutational burden -TMB). ICIs may be overcome also by tumor cell dormancy, and by the presence of other immune cells in the TME that may obfuscate T-cells via other pathways than those targeted by ICIs. The relative presence of T-cells to other immune cells in the TME is reflected by the classification of tumors into the “cold”, T-cell poor, and “hot”, T-cell rich, subgroups [16-18], which are detailed in the next section.

Anti-tumor immunity

Typically, when tumors reach a mature stage, an anti-tumor immune response is triggered leading to immunogenic cell death (ICD), which depends on the activation and expansion of T cells in the TME. This process involves alterations in the cell membrane of dying cancer cells, promoting the release of soluble mediators known as damage-associated molecular patterns (DAMPs) that act as danger signals or “alarmins” to the innate immune system [19]. These signals include high mobility group box 1 (HMGB1) release (from the nucleus), calreticulin translocation (from the endoplasmic reticulum), heat shock protein 70/90 (Hsp70/Hsp90) expression (from the cytoplasm), and ATP leakage (chiefly from mitochondria), all which have

immunostimulatory effects. The interaction of DAMPs with pattern recognition receptors (PRRs) on scavenger cells like macrophages and dendritic cells (DCs) induce their maturation as antigen-presenting cells (APCs).

Potent stimulation of T cells ensues, which traffic to the tumor site and initiate an anti-tumor immune response. In particular, CD8⁺ cytotoxic T cells infiltrating into the tumor niche recognize antigen peptide-MHC complexes on the surface of tumor cells and release perforin and granzyme effector molecules, which induce tumor cell death and further amplify antigen presentation and antitumoral T-cell responses [19-21]. Moreover, CTLs can activate alternative death mechanisms in tumor cells through the Fas/FasL pathway, leading to ferroptosis or pyroptosis [22]. This interaction also starts an activation loop in which dying tumor cells release antigens that will be detected by APCs and further amplify T-cell responses. The potency of T-cell anti-tumor responses depends on intrinsic properties of tumors, resulting in “cold” vs. “hot” phenotypes (**Figure 1.2**).

Cold tumors

T-cell poor tumors, also called cold tumors, are defined by the absence of CD8⁺ T cells and their poor localization at invasive margins. From a molecular standpoint, cold tumors typically exhibit a low mutational load, and low expression of genes associated with antigen presentation, like class I MHC [23]. In some cancers, activation of the PI3K/AKT pathway by loss of tumor suppressor PTEN reduces lipidation of the autophagosome protein LC3, decreasing autophagy and inhibiting downstream T-cell activation. Low levels of tumor antigens necessary for APC stimulation results in an insufficient release of immune mediators essential for antitumor immunity like interferon (IFN)- γ , and interleukin (IL)-12, IL-18, and TNF- α [18] and limit the

influx of T cells into the tumor. T-cell recruitment to the tumor may be also inhibited by the limited production of the chemokine CCL4 via the WNT/ β -catenin pathway, resulting in decreased recruitment of DCs to the TME, and low secretion of CXCL9/CXCL10 chemokines that are key to CD8⁺ T-cell recruitment [24]. As another example, the MYC oncogene can increase expression of surface CD47 (“don’t eat me” signal), preventing phagocytosis of tumor cells and antigen uptake by APCs, PD-L1 expression is also upregulated on tumors cells leading to T-cell exhaustion by binding to PD-1 [1, 22]. From a structural standpoint, alterations of fibronectin and collagen in the dense extracellular matrix (ECM) that surround the tumor, inhibit the mobility, penetration, adherence, and communication of T cells with tumor cells.

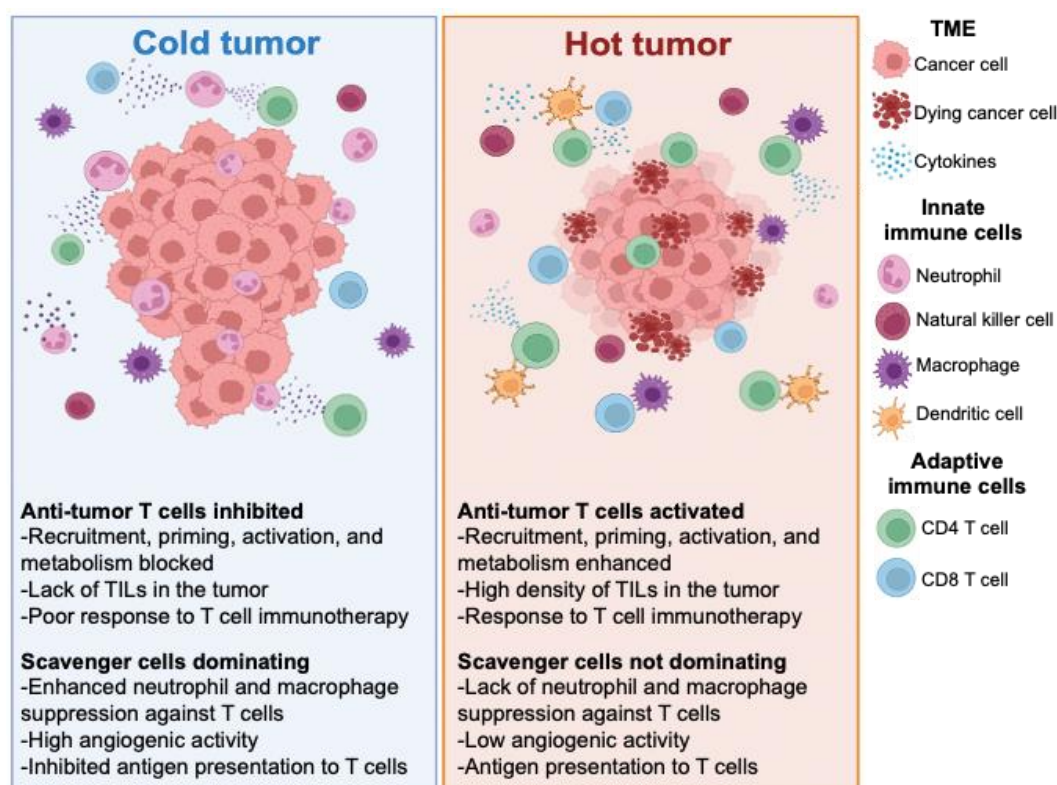


Figure 1.2. Summary of immunogenic “cold” and “hot” tumor phenotypes. Cold tumors are characterized by the high density of innate immune cells in the TME leading to inhibition of anti-tumor T cells. In the contrary, hot tumors promote anti-tumor T cell activation and decrease

activity of scavenger cells. Based on the distribution of innate and adaptive immune cells the tumor microenvironment can develop immunosuppressive or pro-tumorigenic mechanisms that will be central to control disease progression and effective response to immunotherapy.

Although T cell-tumor communication is impaired in cold tumors, innate immune cells do establish communication with tumor cells and infiltrate the TME in cold tumors. Tumor-infiltrating neutrophils (TINs) and macrophages (TIMs) exert metabolic blockade over effector T cells via metabolic enzymes such as arginase-1 (Arg-1) and indoleamine deoxygenase-1 (IDO-1), which deplete arginine and tryptophan, respectively (**Figure 1.2**) [22, 25-27]. Suppression of effector T-cell activity is also achieved via TIN/TIM surface expression of PD-L1 and production of reactive nitrogen species which induce T-cell exhaustion and trapping in the stroma [28]. Cold tumors may actively coopt innate cells (TINs/TIMs) to dampen T-cell responses. For example, oncogenic K-RAS mutations in tumors can activate MAPK/PI3K signaling and induce NLRP3 inflammasome activation in TINs/TIMs, leading to the release of immune mediators (IL-6, IL-8 and IL-10) and chemokines (CCL5 and CCL9) that promote innate (TIN/TIM-mediated) over adaptive (T cell-mediated) responses. The lack of tumor antigens, defects in antigen presentation, absence of T cell activation, and abundance of innate immune suppression make immunotherapy for cold tumors a major ongoing challenge.

Hot tumors

T-cell rich tumors, also called hot tumors, are characterized by the high infiltration of effector CD8⁺ T cells, helper CD4⁺ T cells, APCs (macrophages, dendritic cells), and natural killer (NK) cells (**Figure 1.2**) [29]. From a molecular standpoint, hot tumors exhibit high genomic instability leading to high expression of mutated antigens (neoepitopes) and

cancer/testis antigens normally restricted to the male reproductive tract. Unlike cold tumors, innate immune cell participation in hot tumors is mostly restricted to the recognition of tumor DAMPs in the microenvironment for antigen presentation and secretion of pro-inflammatory cytokines. The production of high levels of intra-tumoral chemokines like CCL4, CCL5 and CXCL9, and others, further enhance T-cell recruitment and ensuing ICD [18, 22, 30]. This triggers potent immune responses, characterized by high IFN- γ signaling activating APCs and T cells.

Activation of IFN- γ in the presence of effector CD8⁺ T cells induce expression of tumor inflammation gene signatures, comprising transcription factors (e.g., STAT1), cell priming receptors (HLA, CD27, and LAG3), inhibitory molecules (PD-L1, PD-L2, and TIGIT), and chemokines (CCL5, CXCR6, and CXCL9) which impact T-cell immunity [23, 28]. However, IFN- γ secretion also activates different feedback mechanisms and suppressor pathways like PD-L1, IDO-1, and regulatory T cell (Treg) infiltration that can suppress adaptive immunity impacting the recruitment of effector CD8⁺ T cells into the tumor niche and invasive margins [23]. For this reason, hot tumors demonstrate better responses to T-cell focused immunotherapies (e.g., by CAR T-cells and ICIs), due to the higher infiltration of T-cells within the tumor and antigen-specific responses to immune checkpoint inhibitory signals like PD-1 and CTLA-4. Currently, the expression of tumor inflammation signatures like PD-L1, and the high mutational load in tumors are used as predictive markers to determine patient responsiveness to immunotherapy. Another predictive marker is the relative proportion of neutrophils to lymphocytes in blood, itself linked to the prevalence of TINs, which we expand on in the next section.

Tumor-infiltrating neutrophils (TINs)

In humans, neutrophils are the most abundant leukocyte subset in the bone marrow (the primary site of hematopoiesis) and in blood, representing approximately 40-70% of all leukocytes. Endowed with a short half-life of approximately 18-24 hours, mature neutrophils turn over rapidly and hence are produced in large quantities in the bone marrow ($\sim 10^{11}$ cells/day) [31, 32]. Under homeostatic conditions, neutrophils assume the first line of defense within the innate arm of the immune system by rapidly infiltrating tissues undergoing sterile injury or infection. Neutrophils display potent scavenging and antimicrobial functions including phagocytosis, degranulation of toxic effectors, and the release of DNA-histone-cationic effector molecule complexes in the form of neutrophil extracellular traps (NETs). Mature neutrophils leave the bone marrow with a characteristic condensed (polylobulated) chromatin, which has led to the dogma that they are largely transcriptionally silent. However, overwhelming evidence has been produced in the past decade that tissue-recruited neutrophils are transcriptionally active, and able to unfold complex responses upon exposure to tissue cues. For example, tissue-recruited neutrophils are capable of producing a large array of mediators (e.g., IL-1 α/β , IFNs, and TNF- α), regulating the recruitment and activation of neighboring cells (e.g., CCL3, CXCL9 and CXCL10), attracting suppressive immune cells (e.g., CCL17, IFNs, and IL-10), and actively participating in ECM and capillary remodeling (e.g., via matrix metalloproteases -MMPs-, VEGF, and neutrophil elastase -NE-) [31].

In the context of cancer, the lifespan of neutrophils is extended, their production in the bone marrow and number in the circulation increase, and their phenotype changes, engaging in all stages of the tumor development as the diseases advances (**Figure 1.3**) [33-35]. Over the past decade, the presence of neutrophils in the blood of cancer patients (and their ratio to

lymphocytes), especially those with advanced-stage disease, has gained relevance as a biomarker for poor clinical prognosis [36, 37]. Neutrophils are recruited into the TME through chemokine/cytokine signaling and undergo discrete epigenetic, transcriptomic, proteomic and functional adjustments that differ from naïve cells. Cold tumors can polarize TINs to induce further recruitment of additional waves of neutrophils, monocytes, and macrophages that will unleash pro- and/or anti-tumor functions based on their own response to the TME [38]. In general, during the early stages of tumor development, neutrophils display an anti-tumorigenic phenotype, secreting pro-inflammatory cytokines (e.g., IL-1 β , TNF- α , IL-6 and IL-12) that promote T-cell recruitment and proliferation. Anti-tumorigenic TINs can also kill tumor cells via direct cytotoxicity through the exocytosis of effector enzymes or antibody-dependent cell cytotoxicity (using anti-tumor antibodies as bridges between their Fc receptors and surface proteins expressed on tumor cells) [39]. In addition, TINs are endowed with pro-oxidative enzymes such as NADPH oxidase, (NOX) myeloperoxidase (MPO) and nitric oxide synthase (NOS) which can kill tumor cells, and/or reduce their growth and metastasis [40].

As tumors grow and metastasize, TINs may switch to a supportive phenotype, providing survival advantages to tumor cells. Pro-tumor TINs can release various chemokines (e.g., CCL2, CCL5 and CXCL15), as well as enzymes such as Arg-1 (which depletes extracellular arginine), and proteases such as neutrophil elastase (NE) [41], cathepsin G (CG) [42], and/or matrix metalloproteinase-9 (MMP-9), which remodel the ECM and promote angiogenesis, tumor growth, and metastasis (**Figure 1.3**) [43] Pro-tumor TINs can also attract Tregs by secreting high levels of CCL17 to assist in the inhibition of effector T cells and continue to support tumor cell motility, migration and invasion [44]. Moreover, the production of oxidants by TINs can play a pro-tumor role by inducing DNA damage and additional mutations [45]. Of note, some of

the factors that TINs produce such as $\text{TNF}\alpha$ may take on either pro- or anti- tumor functions, depending on which receptor they interact with (TNFR1 or TNFR2 in the case of $\text{TNF}\alpha$). TINs are highly adaptable and can undergo phenotypic differentiation, leading to a multiplicity of discrete subsets in humans affected by cancer and murine cancer models. TIN subset identification is an area of active research using omics methods to characterize essential pathways that may be targeted therapeutically to benefit patients.

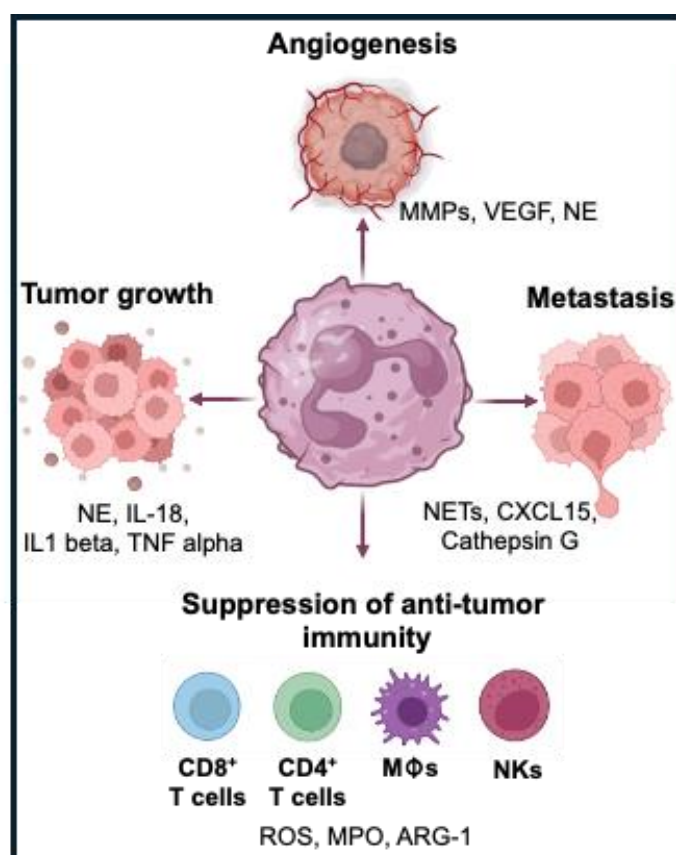


Figure 1.3. Tumor-infiltrating neutrophils (TINs) exert a variety of pro/anti-tumor roles.

Depending on the cues received, TINs may directly impact: (i) growth and metastasis of tumor cells; (ii) properties of the TME, including the ECM and capillary network; and (iii) anti-tumor immunity, either on their own, or via other immune cells such as CD8⁺ / CD4⁺ T cells, macrophages and NK cells, which they either empower or suppress.

Detailed account of tumor-TIN crosstalk at different cancer stages

Local invasion

As they begin to grow, tumors ensure proper vascularization by co-opting tissue vessels or promoting angiogenesis (**Figure 1.4**). In spite of this, rapid tumor expansion often results in metabolic depletion of oxygen and tissue hypoxia [4]. Hypoxic TMEs push tumors to undergo a metabolic switch from oxidative phosphorylation (which requires oxygen as a final electron acceptor) to anaerobic glycolysis (Warburg effect). This leads to lactic acid accumulation in the extracellular fluid, which inhibits the activation, proliferation, and cytotoxic activity of effector T cells [46]. Insufficient vascularization limits availability of critical nutrients, altering translational control and inducing hypoxia-mediated epigenetic and transcriptomic adaptations. For example, hypoxia reduces the activity of TET demethylases, resulting in hypermethylation [47]. Chemokines released under this tumor hypoxia enhance the recruitment of Treg cells that support immunosuppression. Additionally, hypoxic tumor cells develop further resistance to cytotoxic CD8⁺ T cells by undergoing autophagy and upregulating PD-L1 expression.

Epigenetic changes may enhance the invasive capacity of tumor cells and support their phenotypic conversion in the case of epithelial tumors through a multistep process termed epithelial-to-mesenchymal transition (EMT). EMT involves the downregulation of adherence and tight junctions, along with the loss of cell polarity [48, 49]. This process dissociates epithelial cell sheets into individual cells that upregulate the expression of invasive transcription factors and EMT-defining genes (e.g., Slug, Snail, and Twist). The release of TGF- β derived from TINs can induce EMT of tumor cells, increasing their invasiveness [33, 50]. Moreover, signaling through TLR4 on TINs in response to the ECM structural regulator hyaluronan,

promotes motility and migration of tumor cells [51]. This causes further alterations in chromatin state and represses E-cadherin, thus stabilizing the newly acquired mesenchymal phenotype of tumor cells until they switch back to their epithelial phenotype via mesenchymal-to-epithelial transition (MET) [52, 53].

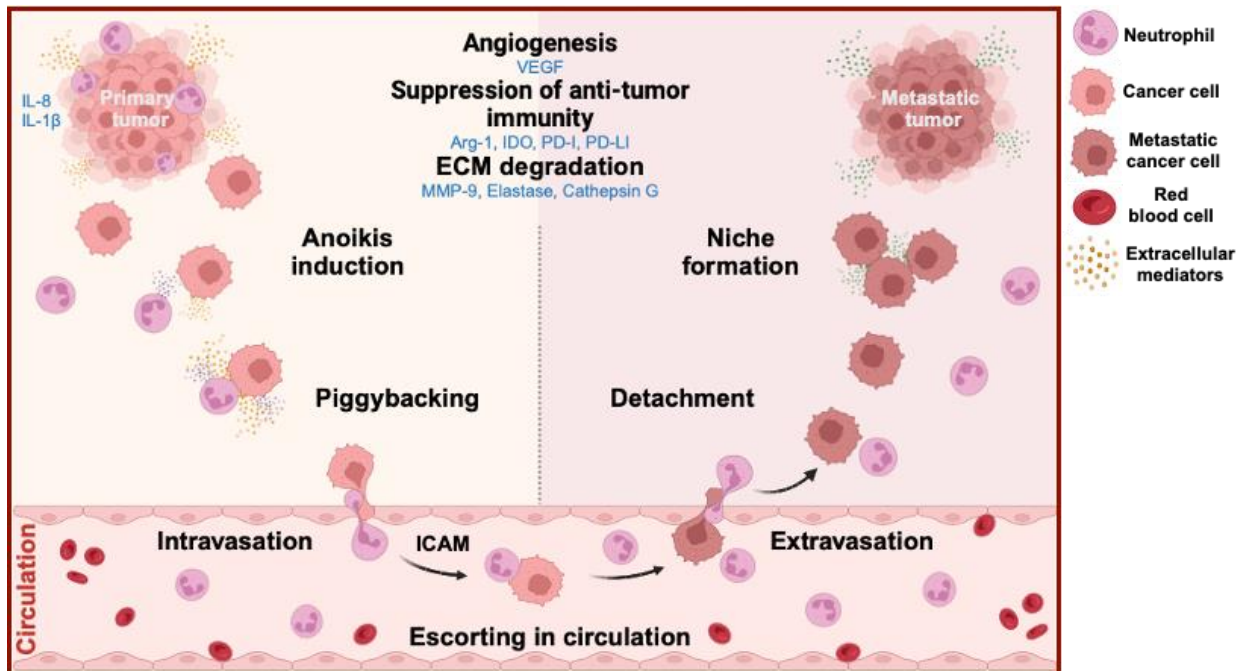


Figure 1.4. Tumor-TIN crosstalk in cancer initiation and metastatic outgrowth. Pro-tumor functions of TINs play key roles at different cancer stages. After initial phases of growth in the primary tumor sites, tumor cells can undergo anoikis and piggyback on TINs to become disseminated tumor cells (DTCs) that may intravasate in the circulation. While in circulation, circulating tumor cells (CTCs) continue to interact closely with neutrophils which escort them to new tissues, and help them extravasate therein. Secretion of pro-inflammatory markers (IL-8 and IL-1 β), proteases (MMPs, elastase, and cathepsin G), cell-cell interaction (ICAM), and immune suppression (IL-10 and Arg-1) mediate some key steps in tumor-TIN interactions leading to the formation of a metastatic niche.

Tumor cells can proteolytically dissolve basement membranes, facilitating interactions with tumor-associated stromal cells and recruited innate immune cells during the invasion-metastasis cascade. For example, TINs are recruited to the TME by IL-8 induction following NF- κ B signaling in genomically unstable K-RAS mutated tumors [54]. Effector proteins are released by TINs, including Arg-1, which inhibits CD8⁺ T cells activation and proliferation, as mentioned before, as well as MMP-9, cathepsin G and NE which can upregulate tumor cell proliferation [44, 50, 55, 56]. For example, extracellular TIN-derived NE can be endocytosed by tumor cells and intracellularly bind to the insulin receptor substrate-1, enhancing cellular proliferation by activating the phosphatidylinositol 3-kinase (PI3K)/Akt/mTOR anabolic pathway. In addition to inducing cell proliferation, TIN-derived proteases such as MMP-9 can degrade the ECM, releasing bound VEGF- α and inducing a pathological signaling loop in the TME through the secretion of GM-CSF and oncostatin M (an IL-6 family member) [39, 57]. Adapting to this new environment conveys various challenges, including the deprivation of integrin-dependent adhesion to the ECM, which is necessary for cell survival. Without attachment to the ECM, epithelial cells generally undergo anoikis -an apoptotic response that is metabolically modulated and is triggered by loss of anchoring to a surface-, but tumor cells can survive anoikins induction [58, 59].

Intravasation

When tumor cells acquire the necessary molecular mechanisms to leave the primary site and travel to an ectopic environment to seed secondary growths, they become disseminated tumor cells (DTCs) [60]. The transendothelial migration of DTCs into the lumina of lymphatic or blood vessels is known as intravasation [61]. This process is supported by the structural features of tumor-associated blood vessels, which are formed via VEGF pathway activation and neo-

angiogenesis. Neovasculature produced by tumor cells undergoes constant reconfiguration and is prone to formation of leaky blood vessels, facilitating DTC passage into the circulation [5, 52]. Additional mediators identified to stimulate the formation of leaky vessels in some cancers include cyclooxygenase-2, epiregulin, MMP-1, and MMP-2 [62]. Evidence shows that tumor development at this stage is determined by the rate of TIN influx, which facilitates the intravasation of DTCs and their survival in circulation. Both contact-independent and contact-dependent (piggybacking) interactions between tumor cells and TINs allows tumor cells to migrate into the bloodstream by penetrating endothelial tight junctions (**Figure 1.4**).

Transport in circulation

After disseminating through the blood and lymphatic vessels, DTCs transform into circulating tumor cells (CTCs) (**Figure 1.4**), which upregulate integrins and other adhesion molecules to survive transport in the circulation [63, 64]. The duration that CTCs remain in circulation remains uncertain; however, with a diameter of 20-30 μm compared to the 8 μm mean luminal diameter of capillaries, they are likely to become trapped in capillary beds or exit the bloodstream early on [52]. In circulation, the majority of CTCs are eliminated by shear stress of blood flow and immune-mediated attacks. To withstand damage from hemodynamic shear forces and evade immune detection, tumor cells recruit neutrophils through vascular cell adhesion molecule 1 (VCAM1) and glypican-3 expression. In this context, neutrophils facilitate cell-cell aggregation, forming clusters that shield CTCs from immune surveillance and mitigate fluidic challenges, thereby altering the local environment to facilitate uninterrupted circulation [5]. A subset of CTCs may thus manage to survive, by promoting stemness via upregulation of Yamanaka transcription factors Nanog, Sox2, and Oct4, and by piggybacking on neutrophils, which are proficient at traveling through circulation [33]. Platelets also cooperate with

neutrophils to shield CTCs from natural killer cells by forming platelet-rich thrombi, secreting chemokines, and transferring MHC-class I containing vesicles to the surface of tumor cells to prevent their recognition by adaptive immune cells [65].

Arrest in microvessels and extravasation

Tumor cells undergo multiple cycles of replication, mutations, and selection for competitive fitness to adhere to the endothelium, induce transendothelial migration, and extravasate into distant organs [66]. Once CTCs interact with the vasculature, they may initiate intraluminal growth and microcolony formation, aiming to rupture surrounding vessel walls and establish direct contact with the tissue parenchyma. CTCs can penetrate pericyte layers separating vessel lumens from the stromal microenvironment, facilitating their exit from circulation. Adhesion of CTCs in tissue microvasculature is facilitated by proteases, degradative enzymes, and ligand-receptor interactions with luminal walls, enabling organ-specific arrest [5]. To overcome physical barriers in tissues with low intrinsic microvessel permeability and facilitate extravasation, tumor cells may secrete factors that induce hyperpermeability. These include angiopoietin-like-4, cyclooxygenase-2, epithelial growth factor, epiregulin, VEGF, and various MMPs (e.g., MMP-1, 2, 3, and 10). Other mediators like osteonectin induce actin remodeling and bind membrane-bound amyloid precursor protein on tumor cells to endothelial death receptor 6, causing endothelial cell death and creating gaps in epithelial junctions for CTC escape [52, 67]. Neutrophils directly interact with CTCs to support extravasation via IL-8 dependent ICAM-integrin signaling (**Figure 1.4**). This involves the adhesion of ICAM-1 on tumor cells to $\beta 2$ integrins on neutrophils, activating migration pathways like focal adhesion kinase and p38-MAPK in tumor cells. Neutrophils can also secrete IL-1 β and MMPs to activate endothelial cells and enhance CTC dissemination [39, 44, 68, 69].

Formation of micro- / macro-metastases

Metastasis accounts for over 90% of cancer-related deaths [70]. There are two fundamental models of metastasis in cancer: linear and parallel progression. In the linear progression model, when the primary tumor is at a mature stage, tumor cells disseminate to form metastatic colonies at distant sites, retaining molecular characteristics similar to the primary tumor. By contrast, the parallel progression model posits that tumor cells undergo somatic evolution early in their development, seeding secondary growths independently from the primary tumor [71]. To prepare distant microenvironments for colonization, primary tumors release systemic signals as lysyl oxidase, which mobilize hematopoietic progenitor cells and stimulate integrins and chemoattractants like stromal cell-derived factor to establish a “pre-metastatic niche” [52, 72]. Once CTCs extravasate, they acquire molecular traits necessary to become metastatic founder cells. During this growth phase, metastatic cells must adapt to the new environment using cell-autonomous programs, becoming highly malignant to initiate micrometastasis formation. If of epithelial origin they may undergo a reversal of their initial EMT through MET, allowing them to regain epithelial cell-to-cell junctions and successfully colonize secondary sites [73]. To overcome stromal challenges, metastasizing cells secrete cytokines like IL-6 and IFN- α , and activate pro-inflammatory pathways such as STAT1, STAT3 and NF- κ B. As an alternative strategy, tumor cells coming into secondary sites may enter dormancy in response to stressful stimuli to evade immune surveillance and cytotoxicity. Metabolic homeostasis in quiescent tumors is maintained by downregulating key pathways like RAS–MEK–ERK/MAPK and PI3K–Akt, which are later upregulated upon reactivation [74]. If micrometastasis persists, a lesion no larger than 0.2-2 mm will form, allowing its evolution to macrometastasis, resulting in larger tumor deposits with dimensions larger than 2 mm. At this

stage, tumor cells are not guaranteed to proliferate *in situ*, but may further propagate into secondary metastases, perpetuating disease progression [75]. Studies indicate that DTCs initially lodge in lymph nodes or bone marrow prior to forming metastatic colonies, with certain aggressive tumor cells showing preference for specific organs; a phenomenon known as organotropic metastasis. For example, breast cancer tends to metastasize to bone [76], lung [77], liver [78], and brain [79], while colorectal cancer often metastasizes to the liver [5, 80].

TINs play a significant role in the pre-metastatic niche by creating an immunosuppressive environment that facilitates the survival and extravasation of CTCs. Metastatic tumors secrete chemokines (e.g., CXC11, CXC12, and CXC15) and amplify SDF-1 and TLR3 signaling to attract neutrophils to the pre-metastatic niche. Within the metastatic niche, NE released from TINs can enhance PI3K signaling supporting tumor cell survival and proliferation. Additionally, neutrophils contribute to metastatic progression by secreting fibroblast growth factor 2 to enhance vascular branching and attract other scavenger cells like monocytes which can amplify MMP-9 production. TINs also assist in modulating the immune response by producing nitric oxide, IL-10, and suppressing NK cell cytotoxic activity via ROS [68, 81, 82]. In sum, TINs are major cellular mediators in all stages of cancer initiation and metastatic growth. Targeting therapies at TINs could be a promising strategy to combat cancer progression and inhibit DTCs / CTCs during metastasis.

Role of the EZH2 pathway in anti-tumor immunity

During cancer development and treatment, tumor cells closely interact with immune cells. Subtypes of tumor-infiltrating immune cells can modify the TME into either pro- or anti-tumorigenic phenotypes, influencing the therapeutic response. Their differentiation, proliferation,

and activation are often associated with direct and indirect epigenetic modifications mediated by the enhancer of zeste homolog 2 (EZH2). EZH2 is a histone methyltransferase frequently mutated in cancer cells and expressed in immune cells at various stages of cancer progression. It belongs to the Polycomb group (PcG) protein family and often serves as a subunit of the Polycomb repressive complex 2 (PRC2), although it can also function independently of the PRC2 complex. EZH2 activation is central to the epigenetic regulation of genes involved in several mechanisms, including cell cycle and differentiation (modulates cyclins, cyclin-dependent kinases, and Rb proteins) [83], DNA damage repair (regulates DNA repair genes RAD51 and BRCA1) [84], autophagy (via transcriptional regulation), apoptosis (regulate pro-apoptotic factors), and immune modulation (modulates STING and other critical immune cell activation pathway) (**Figure 1.5**) [85]. Within tumor cells, EZH2 is the catalytic subunit of the PRC2 complex responsible for inhibiting transcription of key anti-oncogenic genes, including tumor suppressors. Conversely, it can directly activate proto-oncogenes such as cyclin D1, c-Myc, and Notch1. Pro-survival and growth signaling pathways most influenced by EZH2 include Wnt/ β -catenin, MERK/ERK, Notch, PI3K/Akt and checkpoint kinase 1 [86-89]. Overall, dysregulation of EZH2 correlates with poor prognosis in solid tumors, leading to higher tumor grade, increased metastasis, and lower disease-free survival.

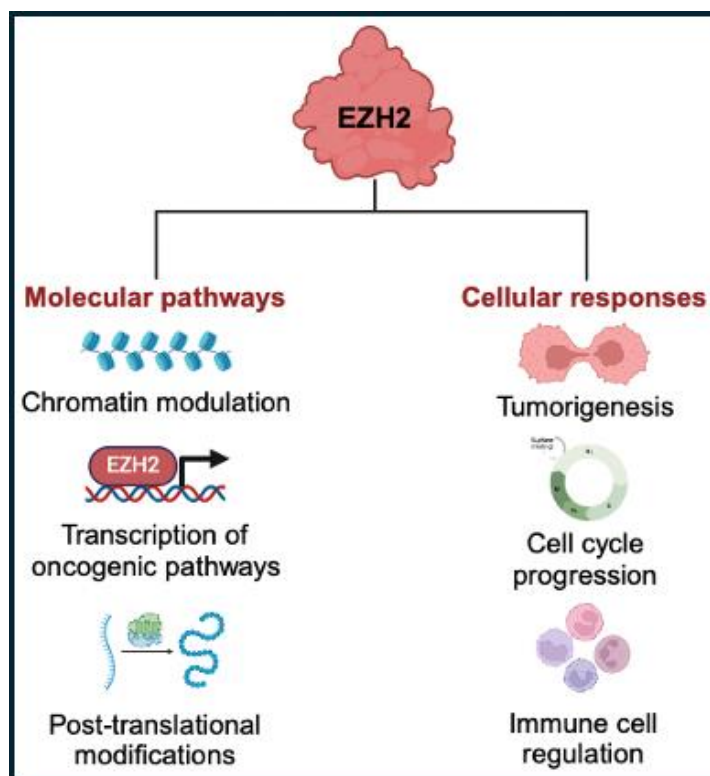


Figure 1.5. Mechanisms mediated by EZH2 in cancer initiation, metastasis, immunity, metabolism, and drug resistance. EZH2 expression at the genetic, epigenetic, and post-translational modification in cancer cells leads to the activation of pro-oncogenic pathways that promote cancer, alter cell cycle progression and support metastasis. Such mechanisms can negatively impact recruitment of adaptive immune cells into the tumor microenvironment, further promoting tumorigenesis.

In tumor-associated immune cells, EZH2 is a double-edged sword that can either support or suppress immune activation and proliferation and impact tumor growth. In adaptive immune cells, EZH2 is required for CD8⁺ T cell proliferation by suppressing negative regulators like cyclin-dependent kinase inhibitor (CDKN) 2A and CDKN1C. However, EZH2 can also inhibit CD4⁺ T cell differentiation and plasticity between T-cell functional subsets by silencing lineage-

specific genes (e.g., T-bet, GATA3, and Eomes) through H3K27me3 modification [90, 91]. Additionally, EZH2 can suppress secretion of CXCL10, a chemokine released in response to IFN- γ , which binds to CXCR3 on effector T cells to promote recruitment to the TME [85, 92]. EZH2 is also critical for maintaining Treg stability and immunosuppressive function. Indeed, genetic deletion of EZH2 in Tregs results in failure to maintain immune tolerance, and dysfunctional immune homeostasis, leading to inflammation and a CD4⁺/CD8⁺ T-cell enriched TME [85]. EZH2 impacts innate immune cells as well, e.g., by indirectly polarizing macrophages to a pro-tumor phenotype, promoting the differentiation of myeloid-derived suppressor cells (MDSCs) from bone marrow precursors, and decreasing NK cell precursors. Collectively, EZH2 induction gives tumor a significant advantage (directly and indirectly via coopting pro-tumor and blocking anti-tumor immune functions), supporting their growth and dissemination.

EZH2 mutations in cancer cells, whether they result in gain- or loss-of-function, are associated with aggressive disease progression in melanoma, prostate, breast, bladder, and endometrial cancer [93-95]. The oncogenic activity of EZH2 in cancer cells confers a proliferative advantage over non-cancer cells, leading to poor prognosis in solid tumors. In some cases, EZH2 is implicated in the transcriptional activation of specific genes regulated by signaling pathways that drive disease progression. For instance, in breast cancer, EZH2 regulates genes through estrogen receptor (ER) and Wnt signaling [96]. In breast cancer patients, high EZH2 protein levels are negatively correlated with overall survival; the 10-year disease-free survival rate for patients with high EZH2 levels is 24.76%, compared to 58.92% for those with lower levels [95]. Other critical genes whose expression by EZH2 in various cancers include disabled homolog 2 interacting protein (impacting cell proliferation and survival), E-cadherin

(modulating cell-cell adhesion), HIF-1 α (regulation adaptations to hypoxia during growth and invasion), SNAIL (involved in EMT) and stimulator of interferon genes (STING, a transcription factor that serves as a master regulator of stress responses in cancer and infection). EZH2 also impacts drug resistance, via suppressed expression of the DNA-damaged repair factor Schlafen 11, suppressed phosphorylation of receptor tyrosine kinases, and inhibition of poly ADP-ribose polymerase [97, 98]. In sum, while the precise mechanisms by which EZH2 plays pro- or anti-tumor roles are under active investigation, its dysregulation in cancer patients can help predict treatment outcomes [99, 100]. Therefore, EZH2 represents a *bona fide* target for therapy in both tumor cells and infiltrating immune cells.

Research focus of this thesis manuscript

This first introductory chapter contrasted hot and cold tumors and listed mechanisms, including immunosuppressive TIN activities, making the latter unresponsive to T-cell immunotherapies [22, 24]. Thus, there is a critical unmet therapeutic gap for patients with cold tumors. EZH2 has been identified as a potential target in this regard because of multiple pro-oncogenic effects fueling cold tumor progression [1, 85, 96]. Ideally, new treatment strategies targeting EZH2 may be able to directly antagonize cold tumors or turn into hot tumors, making them responsive to existing ICIs and CAR-T modalities to improve clinical outcomes. Designing improved therapeutic combinations that successfully cold tumors require a better understanding of the nature, dynamics and roles of immune cell infiltrates at the tumor niche and their interactions with cancer cells. Herein, we investigated whether EZH2 inhibition in cold tumors would exert anti-tumor activity and impact the activity of TINs at the TME. For this purpose, we focused our efforts on triple negative breast cancer (TNBC) and lung adenocarcinoma (LAUD),

both identified to have cold tumor phenotypes. First, we generated EZH2 gene knockout (KO) and overexpression (OE) lines from a 4T1 murine TNBC model and proceeded to measure disease invasiveness, metastatic capabilities, TINs, and T-cell infiltration (Chapter 2) [101]. Second, we tested the efficacy of two EZH2 inhibitors currently in human cancer trials along with the activation of STING in two human LUAD cell lines (Chapter 3). Collectively, our findings provide important insights into the communication between tumor cells and TINs, and how it may be reprogrammed for therapeutic benefit, providing future directions to advance cancer treatment (put in perspective in Chapter 4).

References

1. Siegel, R.L., et al., Cancer statistics, 2023. *CA Cancer J Clin*, 2023. **73**(1): p. 17-48.
2. Khusnurokhman, G. and F.F. Wati, Tumor-promoting inflammation in lung cancer: A literature review. *Ann Med Surg (Lond)*, 2022. **79**: p. 104022.
3. Negrini, S., V.G. Gorgoulis, and T.D. Halazonetis, Genomic instability--an evolving hallmark of cancer. *Nat Rev Mol Cell Biol*, 2010. **11**(3): p. 220-8.
4. Hanahan, D., Hallmarks of Cancer: New Dimensions. *Cancer Discov*, 2022. **12**(1): p. 31-46.
5. de Visser, K.E. and J.A. Joyce, The evolving tumor microenvironment: From cancer initiation to metastatic outgrowth. *Cancer Cell*, 2023. **41**(3): p. 374-403.
6. Baghban, R., et al., Tumor microenvironment complexity and therapeutic implications at a glance. *Cell Commun Signal*, 2020. **18**(1): p. 59.
7. Dominiak, A., et al., Communication in the Cancer Microenvironment as a Target for Therapeutic Interventions. *Cancers (Basel)*, 2020. **12**(5).
8. Bejarano, L., M.J.C. Jordao, and J.A. Joyce, Therapeutic Targeting of the Tumor Microenvironment. *Cancer Discov*, 2021. **11**(4): p. 933-959.
9. Mansoori, B., et al., The Different Mechanisms of Cancer Drug Resistance: A Brief Review. *Adv Pharm Bull*, 2017. **7**(3): p. 339-348.
10. Lei, Z.N., et al., Understanding and targeting resistance mechanisms in cancer. *MedComm (2020)*, 2023. **4**(3): p. e265.
11. Sarkar, S., et al., Cancer development, progression, and therapy: an epigenetic overview. *Int J Mol Sci*, 2013. **14**(10): p. 21087-113.

12. Tilsed, C.M., et al., Cancer chemotherapy: insights into cellular and tumor microenvironmental mechanisms of action. *Front Oncol*, 2022. **12**: p. 960317.
13. Maleki Vareki, S., High and low mutational burden tumors versus immunologically hot and cold tumors and response to immune checkpoint inhibitors. *J Immunother Cancer*, 2018. **6**(1): p. 157.
14. Bozyk, A., et al., Tumor Microenvironment-A Short Review of Cellular and Interaction Diversity. *Biology (Basel)*, 2022. **11**(6).
15. Kroemer, G., et al., Immunogenic cell death in cancer therapy. *Annu Rev Immunol*, 2013. **31**: p. 51-72.
16. Krysko, D.V., et al., Immunogenic cell death and DAMPs in cancer therapy. *Nat Rev Cancer*, 2012. **12**(12): p. 860-75.
17. Zhou, J., et al., Immunogenic cell death in cancer therapy: Present and emerging inducers. *J Cell Mol Med*, 2019. **23**(8): p. 4854-4865.
18. Liu, Y.T. and Z.J. Sun, Turning cold tumors into hot tumors by improving T-cell infiltration. *Theranostics*, 2021. **11**(11): p. 5365-5386.
19. De Guillebon, E., et al., Beyond the concept of cold and hot tumors for the development of novel predictive biomarkers and the rational design of immunotherapy combination. *Int J Cancer*, 2020. **147**(6): p. 1509-1518.
20. Bonaventura, P., et al., Cold Tumors: A Therapeutic Challenge for Immunotherapy. *Front Immunol*, 2019. **10**: p. 168.
21. Wang, M., et al., Therapeutic strategies to remodel immunologically cold tumors. *Clin Transl Immunology*, 2020. **9**(12): p. e1226.

22. Duan, Q., et al., Turning Cold into Hot: Firing up the Tumor Microenvironment. *Trends Cancer*, 2020. **6**(7): p. 605-618.
23. van der Woude, L.L., et al., Migrating into the Tumor: a Roadmap for T Cells. *Trends Cancer*, 2017. **3**(11): p. 797-808.
24. Wang, L., et al., Hot and cold tumors: Immunological features and the therapeutic strategies. *MedComm (2020), 2023*. **4**(5): p. e343.
25. Gajewski, T.F., H. Schreiber, and Y.X. Fu, Innate and adaptive immune cells in the tumor microenvironment. *Nat Immunol*, 2013. **14**(10): p. 1014-22.
26. Gajewski, T.F., et al., Cancer Immunotherapy Targets Based on Understanding the T Cell-Inflamed Versus Non-T Cell-Inflamed Tumor Microenvironment. *Adv Exp Med Biol*, 2017. **1036**: p. 19-31.
27. Rosales, C., Neutrophil: A Cell with Many Roles in Inflammation or Several Cell Types? *Front Physiol*, 2018. **9**: p. 113.
28. Furze, R.C. and S.M. Rankin, Neutrophil mobilization and clearance in the bone marrow. *Immunology*, 2008. **125**(3): p. 281-8.
29. Wu, L., S. Saxena, and R.K. Singh, Neutrophils in the Tumor Microenvironment. *Adv Exp Med Biol*, 2020. **1224**: p. 1-20.
30. Ocana, A., et al., Neutrophils in cancer: prognostic role and therapeutic strategies. *Mol Cancer*, 2017. **16**(1): p. 137.
31. Quail, D.F., et al., Neutrophil phenotypes and functions in cancer: A consensus statement. *J Exp Med*, 2022. **219**(6).
32. Shaul, M.E. and Z.G. Fridlender, Tumour-associated neutrophils in patients with cancer. *Nat Rev Clin Oncol*, 2019. **16**(10): p. 601-620.

33. Sagiv, J.Y., et al., Phenotypic diversity and plasticity in circulating neutrophil subpopulations in cancer. *Cell Rep*, 2015. **10**(4): p. 562-73.
34. Kim, J. and J.S. Bae, Tumor-Associated Macrophages and Neutrophils in Tumor Microenvironment. *Mediators Inflamm*, 2016. **2016**: p. 6058147.
35. Hurt, B., et al., Cancer-promoting mechanisms of tumor-associated neutrophils. *Am J Surg*, 2017. **214**(5): p. 938-944.
36. Masucci, M.T., M. Minopoli, and M.V. Carriero, Tumor Associated Neutrophils. Their Role in Tumorigenesis, Metastasis, Prognosis and Therapy. *Front Oncol*, 2019. **9**: p. 1146.
37. Sato, T., et al., Neutrophil elastase and cancer. *Surg Oncol*, 2006. **15**(4): p. 217-22.
38. Wilson, T.J., et al., Cathepsin G-mediated enhanced TGF-beta signaling promotes angiogenesis via upregulation of VEGF and MCP-1. *Cancer Lett*, 2010. **288**(2): p. 162-9.
39. Egeblad, M. and Z. Werb, New functions for the matrix metalloproteinases in cancer progression. *Nat Rev Cancer*, 2002. **2**(3): p. 161-74.
40. Uribe-Querol, E. and C. Rosales, Neutrophils in Cancer: Two Sides of the Same Coin. *J Immunol Res*, 2015. **2015**: p. 983698.
41. Raftopoulou, S., et al., Tumor-Mediated Neutrophil Polarization and Therapeutic Implications. *Int J Mol Sci*, 2022. **23**(6).
42. Lu, H., R.A. Forbes, and A. Verma, Hypoxia-inducible factor 1 activation by aerobic glycolysis implicates the Warburg effect in carcinogenesis. *J Biol Chem*, 2002. **277**(26): p. 23111-5.
43. Petrova, V., et al., The hypoxic tumour microenvironment. *Oncogenesis*, 2018. **7**(1): p. 10.

44. Ribatti, D., R. Tamma, and T. Annese, Epithelial-Mesenchymal Transition in Cancer: A Historical Overview. *Transl Oncol*, 2020. **13**(6): p. 100773.
45. Kalluri, R. and R.A. Weinberg, The basics of epithelial-mesenchymal transition. *J Clin Invest*, 2009. **119**(6): p. 1420-8.
46. Deryugina, E.I. and J.P. Quigley, Tumor angiogenesis: MMP-mediated induction of intravasation- and metastasis-sustaining neovasculature. *Matrix Biol*, 2015. **44-46**: p. 94-112.
47. Wu, Y., et al., Neutrophils promote motility of cancer cells via a hyaluronan-mediated TLR4/PI3K activation loop. *J Pathol*, 2011. **225**(3): p. 438-47.
48. Valastyan, S. and R.A. Weinberg, Tumor metastasis: molecular insights and evolving paradigms. *Cell*, 2011. **147**(2): p. 275-92.
49. Roche, J., The Epithelial-to-Mesenchymal Transition in Cancer. *Cancers (Basel)*, 2018. **10**(2).
50. Brat, D.J., A.C. Bellail, and E.G. Van Meir, The role of interleukin-8 and its receptors in gliomagenesis and tumoral angiogenesis. *Neuro Oncol*, 2005. **7**(2): p. 122-33.
51. Masson, V., et al., Contribution of host MMP-2 and MMP-9 to promote tumor vascularization and invasion of malignant keratinocytes. *FASEB J*, 2005. **19**(2): p. 234-6.
52. Bekes, E.M., et al., Tumor-recruited neutrophils and neutrophil TIMP-free MMP-9 regulate coordinately the levels of tumor angiogenesis and efficiency of malignant cell intravasation. *Am J Pathol*, 2011. **179**(3): p. 1455-70.
53. Yan, M., et al., Roles of tumor-associated neutrophils in tumor metastasis and its clinical applications. *Front Cell Dev Biol*, 2022. **10**: p. 938289.

54. Adeshakin, F.O., et al., Mechanisms for Modulating Anoikis Resistance in Cancer and the Relevance of Metabolic Reprogramming. *Front Oncol*, 2021. **11**: p. 626577.
55. Paoli, P., E. Giannoni, and P. Chiarugi, Anoikis molecular pathways and its role in cancer progression. *Biochim Biophys Acta*, 2013. **1833**(12): p. 3481-3498.
56. Dasgupta, A., A.R. Lim, and C.M. Ghajar, Circulating and disseminated tumor cells: harbingers or initiators of metastasis? *Mol Oncol*, 2017. **11**(1): p. 40-61.
57. Zavyalova, M.V., et al., Intravasation as a Key Step in Cancer Metastasis. *Biochemistry (Mosc)*, 2019. **84**(7): p. 762-772.
58. Gupta, G.P., et al., Mediators of vascular remodelling co-opted for sequential steps in lung metastasis. *Nature*, 2007. **446**(7137): p. 765-70.
59. Chiang, S.P., R.M. Cabrera, and J.E. Segall, Tumor cell intravasation. *Am J Physiol Cell Physiol*, 2016. **311**(1): p. C1-C14.
60. Plaks, V., C.D. Koopman, and Z. Werb, Cancer. Circulating tumor cells. *Science*, 2013. **341**(6151): p. 1186-8.
61. Schlesinger, M., Role of platelets and platelet receptors in cancer metastasis. *J Hematol Oncol*, 2018. **11**(1): p. 125.
62. Chen, M.B., et al., Mechanisms of tumor cell extravasation in an in vitro microvascular network platform. *Integr Biol (Camb)*, 2013. **5**(10): p. 1262-71.
63. Strilic, B. and S. Offermanns, Intravascular Survival and Extravasation of Tumor Cells. *Cancer Cell*, 2017. **32**(3): p. 282-293.
64. Spiegel, A., et al., Neutrophils Suppress Intraluminal NK Cell-Mediated Tumor Cell Clearance and Enhance Extravasation of Disseminated Carcinoma Cells. *Cancer Discov*, 2016. **6**(6): p. 630-49.

65. Sokeland, G. and U. Schumacher, The functional role of integrins during intra- and extravasation within the metastatic cascade. *Mol Cancer*, 2019. **18**(1): p. 12.
66. Hudock, N.L., et al., Future trends in incidence and long-term survival of metastatic cancer in the United States. *Commun Med (Lond)*, 2023. **3**(1): p. 76.
67. Klein, C.A., Parallel progression of primary tumours and metastases. *Nat Rev Cancer*, 2009. **9**(4): p. 302-12.
68. Psaila, B. and D. Lyden, The metastatic niche: adapting the foreign soil. *Nat Rev Cancer*, 2009. **9**(4): p. 285-93.
69. van Zijl, F., G. Krupitza, and W. Mikulits, Initial steps of metastasis: cell invasion and endothelial transmigration. *Mutat Res*, 2011. **728**(1-2): p. 23-34.
70. Fares, J., et al., Molecular principles of metastasis: a hallmark of cancer revisited. *Signal Transduct Target Ther*, 2020. **5**(1): p. 28.
71. Apple, S.K., Sentinel Lymph Node in Breast Cancer: Review Article from a Pathologist's Point of View. *J Pathol Transl Med*, 2016. **50**(2): p. 83-95.
72. Kang, Y., et al., A multigenic program mediating breast cancer metastasis to bone. *Cancer Cell*, 2003. **3**(6): p. 537-49.
73. Minn, A.J., et al., Genes that mediate breast cancer metastasis to lung. *Nature*, 2005. **436**(7050): p. 518-24.
74. Tabaries, S., et al., Claudin-2 is selectively enriched in and promotes the formation of breast cancer liver metastases through engagement of integrin complexes. *Oncogene*, 2011. **30**(11): p. 1318-28.
75. Bos, P.D., et al., Genes that mediate breast cancer metastasis to the brain. *Nature*, 2009. **459**(7249): p. 1005-9.

76. Kow, A.W.C., Hepatic metastasis from colorectal cancer. *J Gastrointest Oncol*, 2019. **10**(6): p. 1274-1298.
77. Leach, J., J.P. Morton, and O.J. Sansom, Neutrophils: Homing in on the myeloid mechanisms of metastasis. *Mol Immunol*, 2019. **110**: p. 69-76.
78. Smith, H.A. and Y. Kang, The metastasis-promoting roles of tumor-associated immune cells. *J Mol Med (Berl)*, 2013. **91**(4): p. 411-29.
79. Colon, T., et al., Enzyme-independent role of EZH2 in regulating cell cycle progression via the SKP2-KIP/CIP pathway. *Sci Rep*, 2024. **14**(1): p. 13389.
80. Yang, Q., et al., The Polycomb Group Protein EZH2 Impairs DNA Damage Repair Gene Expression in Human Uterine Fibroids. *Biol Reprod*, 2016. **94**(3): p. 69.
81. Shao, F.F., B.J. Chen, and G.Q. Wu, The functions of EZH2 in immune cells: Principles for novel immunotherapies. *J Leukoc Biol*, 2021. **110**(1): p. 77-87.
82. Liu, Y. and Q. Yang, The roles of EZH2 in cancer and its inhibitors. *Med Oncol*, 2023. **40**(6): p. 167.
83. Wen, Y., et al., EZH2 activates CHK1 signaling to promote ovarian cancer chemoresistance by maintaining the properties of cancer stem cells. *Theranostics*, 2021. **11**(4): p. 1795-1813.
84. Manning, C.S., S. Hooper, and E.A. Sahai, Intravital imaging of SRF and Notch signalling identifies a key role for EZH2 in invasive melanoma cells. *Oncogene*, 2015. **34**(33): p. 4320-32.
85. Fujii, S., et al., MEK-ERK pathway regulates EZH2 overexpression in association with aggressive breast cancer subtypes. *Oncogene*, 2011. **30**(39): p. 4118-28.

86. He, S., et al., Ezh2 phosphorylation state determines its capacity to maintain CD8(+) T memory precursors for antitumor immunity. *Nat Commun*, 2017. **8**(1): p. 2125.
87. Zhao, E., et al., Cancer mediates effector T cell dysfunction by targeting microRNAs and EZH2 via glycolysis restriction. *Nat Immunol*, 2016. **17**(1): p. 95-103.
88. Tumes, D.J., et al., The polycomb protein Ezh2 regulates differentiation and plasticity of CD4(+) T helper type 1 and type 2 cells. *Immunity*, 2013. **39**(5): p. 819-32.
89. Varambally, S., et al., The polycomb group protein EZH2 is involved in progression of prostate cancer. *Nature*, 2002. **419**(6907): p. 624-9.
90. Bachmann, I.M., et al., EZH2 expression is associated with high proliferation rate and aggressive tumor subgroups in cutaneous melanoma and cancers of the endometrium, prostate, and breast. *J Clin Oncol*, 2006. **24**(2): p. 268-73.
91. Kleer, C.G., et al., EZH2 is a marker of aggressive breast cancer and promotes neoplastic transformation of breast epithelial cells. *Proc Natl Acad Sci U S A*, 2003. **100**(20): p. 11606-11.
92. Kim, K.H. and C.W. Roberts, Targeting EZH2 in cancer. *Nat Med*, 2016. **22**(2): p. 128-34.
93. Gan, L., et al., Epigenetic regulation of cancer progression by EZH2: from biological insights to therapeutic potential. *Biomark Res*, 2018. **6**: p. 10.
94. Chang, C.J. and M.C. Hung, The role of EZH2 in tumour progression. *Br J Cancer*, 2012. **106**(2): p. 243-7.
95. Guo, B., X. Tan, and H. Cen, EZH2 is a negative prognostic biomarker associated with immunosuppression in hepatocellular carcinoma. *PLoS One*, 2020. **15**(11): p. e0242191.

96. Bai, Y.K., et al., The clinicopathological and prognostic significances of EZH2 expression in urological cancers: A meta-analysis and bioinformatics analysis. *Oncol Lett*, 2023. **26**(1): p. 315.
97. Monterroza, L., et al., Tumor-Intrinsic Enhancer of Zeste Homolog 2 Controls Immune Cell Infiltration, Tumor Growth, and Lung Metastasis in a Triple-Negative Breast Cancer Model. *Int J Mol Sci*, 2024. **25**(10).

Chapter 2: Research manuscript #1

The data and results from this chapter are modified from an original manuscript published in the International Journal of Molecular Sciences (Monterroza et al. Int J Med Sci. 2024)

Title:

Tumor-intrinsic enhancer of zeste homolog 2 controls immune cell infiltration, tumor growth, and lung metastasis in a triple-negative breast cancer models

Authors:

Lenore Monterroza, Maria M Parrilla, Sarah G Samaranayake, Dormarie E Rivera-Rodriguez, Sung Bo Yoon, Ramireddy Bommireddy, Justin Hosten, Luisa Cervantes Barragan, Adam Marcus, Brian S Dobosh, Periasamy Selvaraj, Rabindra Tirouvanziam

Abstract

Triple-negative breast cancer (TNBC) is an aggressive and highly metastatic type of tumor. TNBC is often enriched in tumor-infiltrating neutrophils (TINs), which support cancer growth in part by counteracting tumor-infiltrating lymphocytes (TILs). Prior studies identified the enhancer of zeste homolog 2 (EZH2) as a pro-tumor methyltransferase in primary and metastatic TNBCs. We hypothesized that EZH2 inhibition in TNBC cells per se would exert antitumor activity by altering the tumor immune microenvironment. To test this hypothesis, we used CRISPR to generate EZH2 gene knockout (KO) and overexpressing (OE) lines from parent (wild-type—WT) 4T1 cells, an established murine TNBC model, resulting in EZH2 protein KO and OE, respectively. In vitro, EZH2 KO and OE cells showed early, transient changes in replicative capacity and invasiveness, and marked changes in surface marker profile and cytokine/chemokine secretion compared to WT cells. In vivo, EZH2 KO cells showed significantly reduced primary tumor growth and a 10-fold decrease in lung metastasis compared to WT cells, while EZH2 OE cells were unchanged. Compared to WT tumors, TIN:TIL ratios were greatly reduced in EZH2 KO tumors but unchanged in EZH2 OE tumors. Thus, EZH2 is key to 4T1 aggressiveness as its tumor-intrinsic knockout alters their in vitro secretome and in vivo primary tumor growth, TIN/TIL poise, and metastasis.

Keywords: CD4⁺ T-cell, CD8⁺ T-cell, invasion, myeloid derived suppressor cell, triple-negative breast cancer, tumor-infiltrating neutrophils

Introduction

Breast cancer is a global health problem affecting 2.3 million individuals globally [1]. Defined as estrogen- and progesterone-receptor negative and lacking HER2 overexpression, triple-negative breast cancer (TNBC) holds the poorest prognosis among breast cancer types [2]. This aggressive form occurs in 15–20% of patients, accounting for ~170,000 cases worldwide [3]. TNBC is comprised of different subtypes, characterized by distinct molecular signatures. Common treatments include chemotherapy, radiation, and surgical resection. Patients with T-cell-rich or non-refractory (“hot”) tumors also benefit from newly developed immune checkpoint inhibitor (ICI) and chimeric antigen receptor (CAR) T-cell therapies [4]. Unfortunately, a large proportion of TNBC patients are refractory to ICI therapy (designated as “cold”) [3,5]. Consequently, primary tumors and metastatic outgrowth from chemotherapy-resistant TNBC are a major cause of mortality [6].

Genetic and epigenetic alterations in TNBC are some of the main obstacles for successful responses to therapy [7]. Among the TNBC markers identified as potential therapeutic targets, the methyltransferase enhancer of zeste homolog 2 (EZH2) holds significant promise, as its overexpression is associated with poor prognosis and short disease-free survival in patients [8–11]. This may occur in part through the increased stability of EZH2 due to upstream regulatory pathways leading to its post-translational modification in aggressive TNBCs [12]. Upregulated EZH2 contributes to tumor development, progression, and metastasis via multiple downstream pathways, including but not limited to the modulation of stimulator of interferon genes (STINGs) [13], transforming growth factor β (TGF β) [14], signal transducer and activator of transcription 3 (STAT3) [15], and Wnt [16] signaling. Thus, EZH2 inhibitors have been tested in combination with ICIs and other chemotherapies [17]. A confounding factor, however, is that the expression

of EZH2 occurs in both tumor cells and in tumor-associated innate and adaptive immune cells (e.g., tumor-infiltrating neutrophils (TINs) and lymphocytes (TILs), respectively) [7].

In this study, we probed the role of EZH2 in primary and metastatic TNBCs [18] using a 4T1 murine TNBC model. EZH2 was previously shown to be significantly upregulated in 4T1 compared to normal mouse breast epithelial cells [10]. To this end, we used CRISPR technology to drive EZH2 gene knockout (KO) and overexpression (OE) in stable cell lines derived from parent wild-type (WT) 4T1 cells, resulting in EZH2 protein KO and OE, respectively. While the replicative and invasive capacities of EZH2 KO and OE cells did not broadly differ from those of WT 4T1 cells *in vitro*, the former but not the latter showed significantly decreased primary growth and lung metastasis *in vivo*, along with dramatic reductions in the ratios of TINs to both CD4⁺ and CD8⁺ T cells.

Materials and methods

Cell lines. The parent WT 4T1 (CRL-2539) cell line [18] was purchased from ATCC and cultured at 37 °C and 5% CO₂ in DMEM high-glucose medium (Sigma Aldrich, St Louis, MO, USA), supplemented with 10% fetal bovine serum (FBS, HyClone, purchased from Avantor, Radnor, PA, USA), 1% HEPES (Thermo Fisher Scientific, Hampton, NH, USA), 1% L-glutamine (Sigma Aldrich), and penicillin–streptomycin (100 U mL⁻¹, Sigma Aldrich). Expression constructs were made using a modified GoldenGate Assembly protocol [35]. Murine EZH2 was amplified from pINTO-NFH: mEZH2 (Addgene #65925; gift from Roberto Bonasio [36]) and cloned into pBD170abc, a level 0 destination vector for the downstream cloning of an open reading frame. Then, a level 1 expression construct (pBD320) was cloned with a CMV promoter, BetaGlobin 3'UTR, into a position 1 destination vector (pTW324; Addgene #115955; gift from Ron Weiss) using BsaI and T4 DNA ligase. Puromycin alone (pBD324) or mScarlet-IRES[EMCV]-puromycin (pBD332) expression vectors under the control of a PGK promoter were cloned into a position 2 destination vector (pTW325; Addgene #115956; gift from Ron Weiss). Then, pBD320 was combined with a minimal linker and pBD324 or pBD332, respectively, to generate level 2 dual-expression constructs pBD321 and pBD333. For KO plasmids, the murine EZH2 sequences from AOI-WT-Cas9-sq-mouse Ezh2-E18-GFP and AOI-WT-Cas9-sq-mouse Ezh2-E10-GFP (Addgene #91880 and Addgene #91879; gift from Martine Roussel [37]) were cloned into pSPCas9(BB)-2A-Puro (Addgene #62988; gift from Feng Zhang [38]). Plasmids were transfected into 4T1 cells using lipofectamine 3000 (Thermo Fisher Scientific) following the manufacturer's protocol and selected using puromycin at a concentration of 5 µg/mL. Stable OE clones were continually grown in puromycin; KO clones

were only exposed to puromycin for up to a week. Cells were then isolated into 96-well plates and the clones selected.

Western blot. Cell lysates were prepared using the Minute Total Protein Extraction Kit (Invent Biotechnologies, Plymouth, MN, USA). The provided denaturing buffer was supplemented with Halt's protease and phosphatase inhibitor cocktail at a 3× concentration (Thermo Fisher Scientific). Lysates were passed through spin columns to remove viscosity. Total protein concentration was measured using the Pierce Rapid Gold BCA protein assay kit (Thermo Fisher Scientific), concentration was normalized across treatments with denaturing buffer, then a Laemmli sample buffer (Bio-Rad Laboratories, Hercules, CA, USA) supplemented with β-mercaptoethanol was added. Samples were then boiled at 95 °C for 5 min and lysates were separated by SDS-PAGE on Any-KD gels (Bio-Rad Laboratories). Protein transfer to nitrocellulose membranes (LI-COR Biosciences, Lincoln, NE, USA) was performed at 4 °C by wet transfer in Towbin buffer (25 mM Tris, 192 mM glycine, and 20% MeOH (v/v) without SDS). After transfer, the membrane was rinsed three times with double-distilled H₂O. Blocking was performed using Intercept (TBS) blocking buffer (LI-COR Biosciences) for one hour at room temperature in motion. Primary antibodies to EZH2 and α-tubulin (from Cell Signaling Technologies, Danvers, MA, USA, used at 1:1000) were added to an Intercept T20 antibody diluent (LI-COR) at 4 °C overnight in motion. Secondary IRDye 800CW donkey anti-rabbit IgG antibody (from LI-COR Biosciences, used at 1:15,000) was added to the Intercept antibody diluent (LI-COR Biosciences) for 1 h at 37 °C on a shaker. Membranes were analyzed using an Odyssey CLx imager and Image Studio software (version 5.5, LI-COR Biosciences).

Cell proliferation assay. EZH2 KO, EZH2 OE, and WT 4T1 cells were harvested, resuspended in DMEM-complete medium, and counted. Then, 5×10^5 cells were plated on a T25 flask in 5 mL of medium and cultured at 37 °C and 5% CO₂. At 24, 48, and 72 h, the cells were harvested and stained with propidium iodide to determine the cell count and viability using a hemocytometer.

3D spheroid invasion assay. To generate EZH2 KO, EZH2 OE, and WT 4T1 cell spheroids, 3000 cells were plated in 200 μ L on a Spheroid Nunclon 96-well plate (Thermo Scientific) and centrifuged at 450 \times g for 5 min at 4 °C and incubated at 37 °C and 5% CO₂. After 48–72 h of incubation, spheroids were collected, embedded in 3 mg/mL collagen type I (Corning, Glendale, AZ, USA), and then plated in a 35 mm glass-bottom dish (Cellvis, Mountain View, CA, USA) for incubation overnight at 37 °C. After collagen was polymerized, complete DMEM (Thermo Fisher Scientific) was added to cover the collagen matrix and spheroids. An IX51 microscope (Olympus, Center Valley, PA, USA) at a 10 \times magnification (equal to 1.5 pixels/ μ m) with an Infinity2 charge-coupled device camera was used for 3D spheroid imaging. Spheroid circulatory and invasiveness were measured by ImageJ, <https://imagej.net/ij/download.html> (accessed on 1 August 2023), as previously described [19].

Extracellular mediator assay. Supernatants from in vitro cultures of EZH2 KO, EZH2 OE, and WT 4T1 cells were collected and stored at –80 °C until use. Extracellular mediators were quantified using a U-PLEX multiplexed chemiluminescent ELISA assay (Meso Scale Discovery, Rockville, MD, USA), following the manufacturer’s protocol. Plates were acquired on the

QuickPlex SQ 120MM reader and later analyzed using Discovery Workbench 4.0 software (both from Meso Scale Discovery).

Animals. BALB/c mice (females, 6–8 weeks old) were purchased from Jackson Laboratories and maintained in the Division of Animal Resources facilities at Emory University. Experiments were performed in accordance with the Emory University Institutional Animal Care and Use Committee's approved protocol (DAR-2017-00-504). Female mice were chosen to match the strain and sex of origin of the parent WT 4T1 cell line. To establish the model, 5×10^5 cells were injected subcutaneously (s.c.) in the right flank as the location of the primary tumor [39]. Tumor size (mm²) was measured in two dimensions with Vernier calipers every 3 days. In some cases, WT and EZH2 KO cells were injected s.c. and animals were concomitantly treated with the synthetic STING agonist MSA-2 [40]. MSA-2 (benzothiophene oxobutanoic acid; Cat: HY-136927) was purchased from MedChemExpress (Monmouth Junction, NJ, USA) and dissolved in 20% sulfobutylether- β -cyclodextrin (SBE- β -CD, Cat: HY-17031, MedChemExpress) in 0.9% saline to a concentration of 25 mg/mL. This stock was stored at -20 °C in the dark until injection. MSA-2 at 25 mg/kg in SBE- β -CD in a 200 μ L volume was administered subcutaneously in the left flank. Doses were administered every third day [41], and the non-treated control group received 200 μ L of SBE- β -CD only.

Lung metastasis assay. Lungs were isolated under sterile conditions from tumor-bearing mice 21–28 days post-injection, then minced and digested in 1 mg/mL of collagenase IV (Millipore Sigma, Burlington, MA, USA) for 2 h at 37 °C under a rotating motion. After digestion, single-cell suspensions were filtered through a 70 μ m strainer and washed twice in selection medium

consisting of complete DMEM with 6-thioguanine (Millipore Sigma) at 60 μ M. Cells were resuspended in 8 mL of selection medium, and 1 mL was plated per well in a 6-well plate for each lung digestion. After 7 to 14 days of incubation in the selection medium (to kill lung fibroblasts without affecting tumor cells), as soon as one of the wells reached confluency, all wells were harvested and counted on a Cellometer T4 Automated Counter (Nexcelom, Lawrence, MA, USA) using trypan blue to discriminate dead cells.

Flow cytometry staining and data acquisition. For in vitro analyses, EZH2 KO, EZH2 OE, and WT 4T1 cells were thawed, resuspended in DMEM-complete medium, and cultured in T75 flasks. Before reaching confluency, the cells were harvested and counted using propidium iodide. For ex vivo analyses, tumors grown in the flank of mice were harvested, weighed, minced, and digested in liberase TL (Roche, Indianapolis, IN, USA) and DNase (Roche) for 30 min at 37 °C in motion. Cell suspensions were filtered through a 70 μ m strainer and washed with PBS. Total cell count was determined using a Cellometer T4 Automated Counter and trypan blue. All cells were pre-incubated with Fc receptor blocking antibody (Clone 24G2, BioLegend, San Diego, CA, USA) in an FACS buffer at room temperature for 10 min. Then, the cells were incubated with fluorochrome-conjugated antibodies for 30 min at 4 °C. The in vitro staining panel included antibodies to CD24 (clone M1/69), CD44 (clone IM7), CD80 (clone 16-10A1), ICAM-1 (clone YN1/1.7.4), MHC class I (clone M1/42), MHC class II (clone M5/114.15.2), and PD-L1 (clones 10F.9G2), all purchased from BioLegend. The ex vivo staining panel included, in addition to the above, antibodies to CD3 (clone 17A2), CD4 (clone GK15), CD8a (clone 53-6.7), CD11b (clone M1/70), CD11c (clone N418), CD19 (clone 6D5), CD45 (clone 30-F11), CD69 (clone H1.2F3), CD107a (clone 1D4B), F4/80 (clone BM8), Ly6C (clone HK1.4), Ly6G (clone 1A8), NK1.1

(clone PK136), and PD-1 (clone 29F.1A12), also purchased from BioLegend. The live dead fixable NIR (1:400 in PBS) was obtained from ThermoFisher Scientific. After incubation, the cells were washed three times with FACS buffer and analyzed using the Aurora Spectral Flow Cytometer (Cytek Biosciences, Fremont, CA, USA). Data were analyzed using FlowJo software (version 10.10, BD Biosciences, Franklin Lakes, NJ, USA).

Statistical analysis. All statistical analysis and graphs were performed using Prism software (version 10.2, GraphPad Software, Boston, MA, USA). Non-parametric methods were used for descriptive statistics (box plots with median line and interquartile range forming outside boundaries to illustrate distributions), and comparisons between conditions and or timepoints. One-way ANOVA was used to analyze differences between the three groups (EZH2 KO, EZH2 OE, and WT 4T1 cells) at fixed timepoints. Two-way ANOVA was used to test group differences across timepoints, e.g., for invasiveness in 3D spheroid assay over 3 days in vitro, or primary tumor growth in the range of 21–28 days in vivo. Values of $p < 0.05$ were considered significant (* $p < 0.05$, ** $p < 0.01$, *** $p < 0.001$, and **** $p < 0.0001$).

Results

EZH2 knockout and overexpressing lines derived from the 4T1 TNBC model behave similarly to the parent line in vitro. We generated multiple EZH2 gene KO and EZH2 gene OE clones from parent WT 4T1 cells using CRISPR/Cas9 and gene amplification followed by a round of sorting. Lysates were prepared from each clone and analyzed by Western blot, using α -tubulin as a normalization control. All KO and OE clones demonstrated a successful elimination and overexpression of the EZH2 protein, respectively (**Figure 2.1**). To characterize the effect of altered cell-intrinsic EZH2 expression on 4T1 behavior in vitro, we selected 4T1 EZH2 KO11 and EZH2 OE6 clones for further investigation. These two clones were selected because of their grossly normal morphology and viability compared to the WT. They were plated in parallel with the parent WT 4T1 cell line at 5×10^5 cells, and counts were performed at 24, 48, and 72 h post-plating, revealing no significant difference in replication (**Figure 2.2A**). Next, we used a 3D spheroid invasion assay to evaluate the invasive capacities of EZH2 KO, EZH2 OE, and WT 4T1 cells at 0, 24, 48, and 72 h post-plating (**Figure 2.2B**). EZH2 OE cells showed increased spheroid circularity at 24, 48, and 72 h (**Figure 2.2C**), but a decreased invasive area (another measure of invasiveness) at 24 h (**Figure 2.2D**). Conversely, compared to the WT cells in vitro, the EZH2 KO cells showed decreased spheroid circularity at 24 h (**Figure 2.2C**), but increased invasive areas at 0 and 24 h (**Figure 2.2D**). Note however that at 72 h, WT, EZH2 OE, and EZH2 KO cells showed equal invasive areas (**Figure 2.2D**).

EZH2 expression impacts surface phenotype and secreted mediators of 4T1 cells in vitro.

Using flow cytometry (**Figure 2S1A**), the expression of relevant markers on EZH2 KO, EZH2 OE, and WT 4T1 cells was assessed against unstained controls for positivity (**Figure 2S1B**), and

positively expressed markers were then quantified over multiple repeats across lines (**Figure 2.3A**). The expression levels of CD24, CD44, ICAM-1, MHC-I, and checkpoint inhibitor PD-L1 differed across 4T1 WT, EZH2 KO, and EZH2 OE cells. Specifically, expressions of CD24 and CD44 were lower on EZH2 KO compared to both the WT and EZH2 OE cells, and expressions of ICAM-1 and PD-L1 were lower in EZH2 KO than in EZH2 OE cells, while EZH2 OE cells were similar to the WT for all markers except for a lower MHC-I expression. When assessing their profiles of twelve secreted mediators (**Figure 2.3B**), we observed no significant difference between the WT or either EZH2 KO or EZH2 OE cells. However, EZH2 KO cells secreted higher levels of several mediators in comparison to EZH2 OE cells, with significant >4-fold increases for GM-CSF and MCP-1 and a >2-fold increase for IL1 β . Similar trends for the increased secretion in EZH2 KO vs. EZH2 OE cultures were observed for IFN α , IL-10, IP-10, and TNF α secretion, albeit non-significant.

EZH2 knockout reduces primary tumor growth and lung metastasis of 4T1 cells in vivo.

Because the in vivo growth of tumor cells occurs at longer intervals and also involves other factors (e.g., immune cells), the in vitro data on EZH2 OE and KO 4T1 cells may not be predictive of their growth and metastatic potential in animals. Thus, we next moved to test the impacts of EZH2 knockout and overexpression on 4T1 TNBC primary tumor growth and metastasis in vivo. To this end, we challenged mice with WT, EZH2 KO, and EZH2 OE cells. The cells were injected subcutaneously in the flank of BALB/c mice and allowed to grow over 21 days (**Figure 2.4A**). While the WT and EZH2 OE cells showed similar primary tumor growth across all timepoints, EZH2 KO cells grew significantly slower than both, resulting in a 2-fold-smaller size at day 21 (**Figure 2.4B**). Since the 4T1 TNBC model is spontaneously metastatic,

the lungs of tumor-bearing mice were isolated at the end of the in vivo challenge and processed for the quantification of metastatic cells. Strikingly, EZH2 KO showed a significantly reduced (approximately 10-fold lower) lung metastatic burden compared to the WT and EZH2 OE cells (**Figure 2.4C**). To confirm these results, we repeated the in vivo challenge comparing WT and EZH2 KO cells and extended the duration by a week. Again, EZH2 KO cells grew significantly slower than the WT, which was evident macroscopically by day 18 (**Figure S2A**). The difference in primary tumor size between EZH2 KO and WT groups reached 4-fold by day 28 (**Figure S2B**). Additionally, a 10-fold lower lung metastatic burden was again observed between EZH2 KO and WT cells (**Figure S2C**). To probe the potential implication of the EZH2-regulated STING pathway in the observed effects, we conducted parallel in vivo challenge with the longitudinal treatment of EZH2 KO- and WT-cell-injected animals with the STING agonist MSA-2. We observed that the MSA-2 agonism of STING significantly decreased the primary tumor growth (**Figure S2A, B**) and metastatic potential (**Figure S2C**) of WT cells. Interestingly, MSA-2 treatment did not decrease the primary tumor growth and metastatic potential in EZH2 KO cells compared to the WT.

Tumor-intrinsic EZH2 knockout alters the balance of neutrophils and CD4⁺ and CD8⁺ T cells in primary 4T1 tumors. To determine whether altering EZH2 expression affects immune cell infiltration into tumors, we prepared single-cell suspensions from WT, EZH2 KO, and EZH2 OE primary tumors, and quantified live infiltrating leukocytes through flow cytometry analysis and the sequential gating of relevant subsets (**Figure 2.5A**). While WT and EZH2 OE tumors had similar proportions across all leukocyte subsets measured, EZH2 KO tumors showed on average a 2-fold-lower proportion of neutrophils, and 2- and 10-fold-higher proportions of CD4⁺

and CD8⁺ T cells, respectively, than the WT and EZH2 OE tumors (**Figure 2.5B**). Consistently, EZH2 KO tumors showed on average 3- to 4-fold-higher proportions of CD3⁺ T cells (including both CD4⁺ and CD8⁺), while their lower proportions of infiltrated neutrophils included both mature and immature cells (**Figure 2S3**). The paradoxical effect of tumor-intrinsic EZH2 knockout on infiltrated neutrophils (decrease) as well as CD4⁺ and CD8⁺ T cells (increase) was even more striking when expressed as ratios, revealing a >20-fold decrease in the neutrophil:CD8⁺ T-cell ratio in EZH2 KO vs. WT and EZH2 OE tumors (**Figure 2.5B**).

Discussion

In this study, we report the successful CRISPR-aided generation of several EZH2 KO and EZH2 OE clones derived from the 4T1 murine TNBC cell line. Based on grossly normal morphology and viability compared to the WT, one EZH2 KO line and EZH2 OE line were selected for further phenotypic evaluations in vitro and in vivo. An analysis of in vitro proliferation on 2D plates and invasiveness in a 3D spheroid assay [19] showed no major differences between EZH2 KO, EZH2 OE, and WT 4T1 cell lines, suggesting the little regulatory impact of EZH2 on these properties. These results are consistent with prior data on the siRNA-aided knockdown of EZH2 in 4T1 cells, also reporting no apparent effect on cell proliferation or invasiveness [14]. Our study is the first to introduce EZH2 OE cells and shows that these and WT cells behaved very similarly, both in vitro and in vivo, suggesting that EZH2 expression may be already saturating with regards to downstream signaling in parent WT 4T1 cells.

In regard to the cell surface markers, only MHC class I was altered (lowered) in EZH2 OE cells compared to the WT, while EZH2 KO cells showed a decreased expression of multiple immune activation markers (CD24, CD44, ICAM, and PD-L1) compared to EZH2 OE cells, with intermediate levels in WT cells. The significantly altered secretion of GM-CSF, MCP-1, and IL1 β (all myeloid mediators) was observed in EZH2 KO culture supernatants, suggesting that EZH2 may impact immune crosstalk by 4T1 cells. Indeed, EZH2 KO tumors grown in vivo decreased the proportion of infiltrated neutrophils and increased those of infiltrated CD4 $^{+}$ and CD8 $^{+}$ T cells (culminating in a 20-fold reduction in the neutrophil:CD8 $^{+}$ T-cell ratio). Concomitantly, EZH2 KO tumors displayed significantly reduced growth in the primary tumor site (by 2 to 4 fold) and lung metastatic potential (by 10 fold). Together, our findings suggest

that, while baseline EZH2 expression in 4T1 TNBC cells does not seem to play a critical role in vitro, it is necessary to maintain high TIN:TIL ratios and their growth and metastatic potential in vivo.

There is ample evidence that EZH2 is involved in the epigenetic control of critical immune regulatory pathways [7], notably including the STING pattern recognition receptor [13,20]. STING plays multiple crucial roles in danger signaling, interferon secretion, and leukocyte infiltration in solid tumors [21]. Prior research on the 4T1 model demonstrated altered levels of pro-inflammatory and interferon-related cytokines in serum [22,23]. Our in vivo experiments using the STING agonist MSA-2 as a longitudinal treatment combined with either 4T1 WT or EZH2 KO cells showed significant reductions in primary tumor growth and metastasis potential for the former, but not the latter. Together, these findings suggest that high EZH2 expression in WT 4T1 cells may act in part via STING inhibition and can be overcome by MSA-2 treatment, while STING activity may be fully released in EZH2 KO cells, explaining the absence of additive antitumor effects of MSA-2. Future studies on our EZH2 KO and EZH2 OE lines will evaluate the relative roles of STING and other regulators of immune signaling by 4T1 cells.

Our in vivo findings are consistent with previous studies demonstrating that cells with high EZH2 expressions have an advantage in metastasizing, while EZH2 KO 4T1 tumor-bearing mice have significantly longer survival and decreased occurrence of metastatic colonies [24]. Previous work showed that metastasis in the 4T1 model is impacted by the capacity of circulating cancer cells to undergo epithelial–mesenchymal transition and successfully establish micrometastasis at a distant organ site [25]. Since EZH2 KO primary tumors likely have to undergo similar processes to WT cells to metastasize, our results suggest that EZH2 deficiency in

the former may not only negatively affect tumor cell mobilization and survival, but also the processes leading to metastasis. Prior studies have suggested multi-pronged roles of EZH2 in the modulation of TNBC aggressiveness [8–11].

TINs have emerged as key modulators of primary tumor growth and metastatic progression in TNBC [26]. As the most abundant leukocyte in human bone marrow and blood, neutrophils can infiltrate tumors in high numbers and acquire novel activities therein, promoting anti- and/or pro-tumorigenic functions [27]. In the context of TNBC patients, high levels of TINs are predictive of poor treatment responses and decreased survival [28,29]. TILs and TINs often play antagonistic roles, for example, TINs may inhibit the recruitment and/or activation of TILs via metabolic (e.g., arginase-mediated amino acid depletion) or cell–cell (e.g., PD-1/PD-L1 and TIM-3/Gal-9) interactions [30,31]. Because of these activities, TINs (whether derived from developmentally mature or immature neutrophils) are often categorized under the functional term “myeloid-derived suppressive cells” (MDSCs) [32].

Current therapeutic approaches face the challenge of alleviating cold tumor progression in the absence of T-cell activation. Although conventional anticancer treatments, like chemotherapy and radiotherapy, still have important roles to play in tumor burden reduction and preventing the selection of immune-resistant clones, the incorporation of improved therapies that suit the mutational burden in patients are much needed. In this context, increasing tumor sensitivity to ICI therapy by converting them from a “cold” to a “hot” phenotype may lead to better outcomes. Overall, limiting TIN infiltration to enable TIL antitumor activity (i.e., making cold tumors hot) is a major goal of current research [4]. Since EZH2 can be expressed in both TINs [33] and TILs [34], further understanding its role and impact as a tumor-intrinsic and/or

immune-associated factor is critical to overcoming TNBC resistance and improving patient outcomes.

We acknowledge several limitations to the present study. First, our *in vitro* experiments included descriptive assessments of WT, EZH2 KO, and EZH2 OE 4T1 cells via proliferation, invasion, secretome, and surface flow cytometry assays, but did not include an extensive analysis of the epigenetic (e.g., by ATAC-Seq), transcriptomic (e.g., by RNA-Seq), proteomic, or metabolic (e.g., by mass spectrometry) processes of these cell lines. Based on the profound *in vivo* differences in the growth and metastasis of these cells observed in this study, future investigations are warranted in which WT, EZH2 KO, and EZH2 OE cells may be grown *in vitro* and sorted after *in vivo* expansion to compare their molecular makeup. Second, this study revealed significant effects of tumor-intrinsic EZH2 knockout on TIN/TIL poise, but did not provide functional and/or signaling data on these tumor-associated immune cells. Future investigations will tackle this issue after sorting individual subsets (neutrophils and CD8⁺ and CD4⁺ T cells, notably) using downstream analysis by RNA-Seq. Third, our findings with *in vivo* MSA-2 treatment suggest that the 4T1 WT, EZH2 KO, and OE cells are amenable to the combined testing of drugs directed at key pathways not only including STING, but also other EZH2-regulated transcriptional regulators, such as TGF β [14], STAT3 [15], and Wnt [16]. One may also envision investigating systemic treatment with candidate EZH2 inhibitors [17], although our study highlighted that tumor-intrinsic, rather than the global inhibition of this pathway, may be beneficial. Fourth, it is important to bear in mind that, while CRISPR editing as used in our study is efficient at targeting specific sites in the genome, it is also affected by potential off-target effects, which would need to be ascertained by deep sequencing methods in follow-up investigations. Fifth, our study assessed tumor growth *in vivo* every 3 days, but

metastatic potential only at endpoint (21 or 28 days), and only in the lung. Future studies could measure metastatic potential at other timepoints and in other organs, such as the brain and liver. Ideally, it would be desirable in such extended studies to attempt a spatial transcriptomics analysis of human TNBC resection tissues from both primary tumor and metastatic sites to assess the potential association between EZH2 expression in tumor cells and the nearby presence of TILs vs. TINs, as suggested by our study using the 4T1 model.

Acknowledgments

The authors thank Emory University Pediatrics and Winship Flow Cytometry core, Emory Division of Animal Resources, and the Emory University Institutional Animal Care and Use Committee. The authors also thank Curtis Henry from the University of Colorado Anschutz Medical Campus, Rebecca Parker, and Diego Moncada Giraldo, James Lyles, and Wei Zhou from Emory University for their feedback and critical reading of the manuscript.

Figures

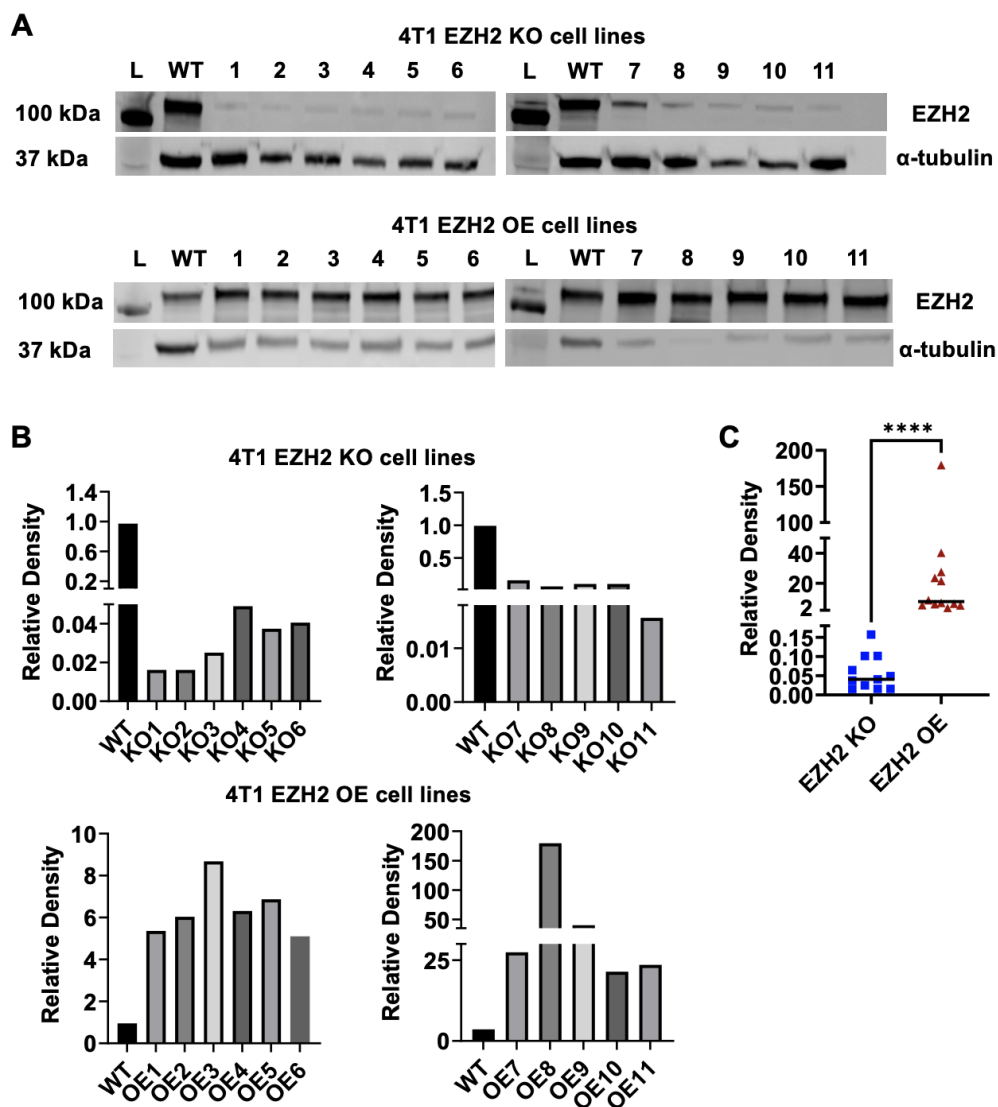


Figure 2.1. EZH2 knockout (KO) and overexpression (OE) cell clones were generated from the parent wild-type (WT) 4T1 TNBC line. (A) Western blots (L indicates protein ladder) and **(B)** densitometric analysis comparing 11 clones from each EZH2 KO (upper panel) and EZH2 OE (lower panel) lines to the 4T1 WT line (2 sets of blots for each), with alpha-tubulin as the normalization control. **(C)** Comparison of EZH2 protein expression between KO (blue squares) and OE (red triangles) groups by Wilcoxon rank-sum test, **** $p < 0.0001$.

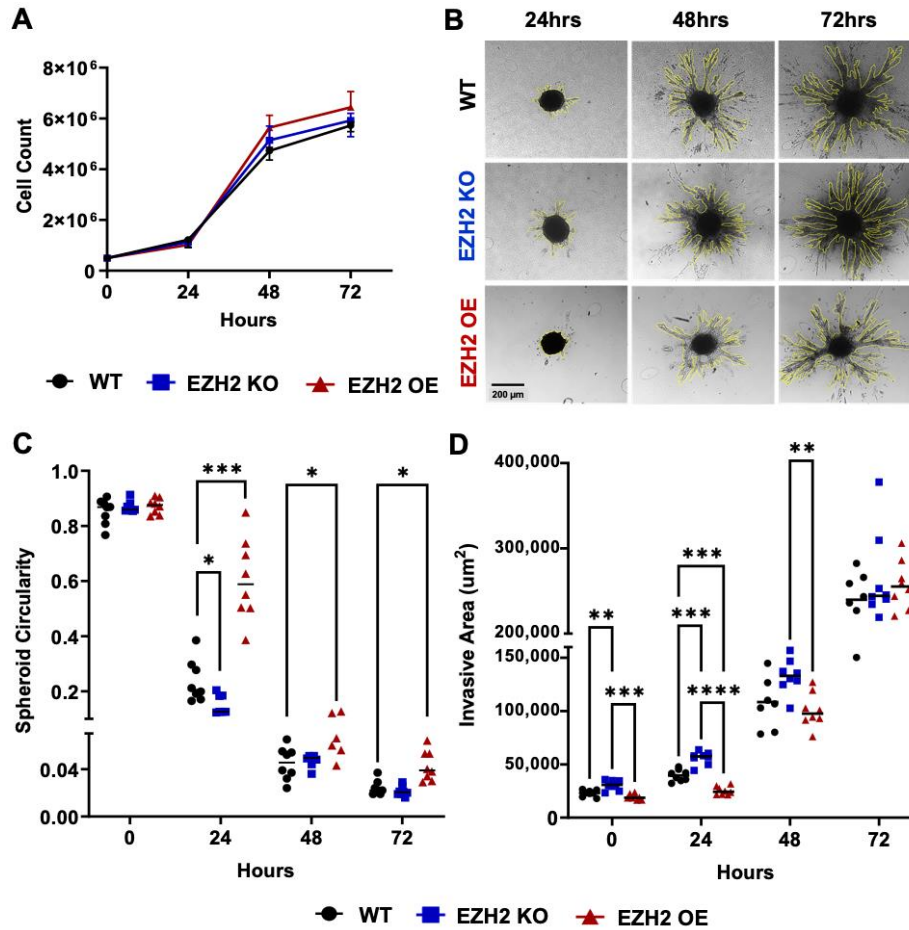


Figure 2.2. In vitro replicative and invasive behaviors of EZH2 KO and EZH2 OE

compared to parent WT 4T1 cells. (A) Counts of 4T1 WT, EZH2 KO, and EZH2 OE lines over 72 h of growth in 2D plates. **(B)** Representative images of spheroid for 4T1 WT, EZH2 KO, and EZH2 OE lines, and quantification of **(C)** circularity and **(D)** invasive area over 72 h of growth in a 3D invasion assay (n = 8 spheroids per group). Comparisons across groups and timepoints are by two-way ANOVA with Tukey's post-hoc test and shown as * p < 0.05, ** p < 0.01, *** p < 0.001, and **** p < 0.0001.

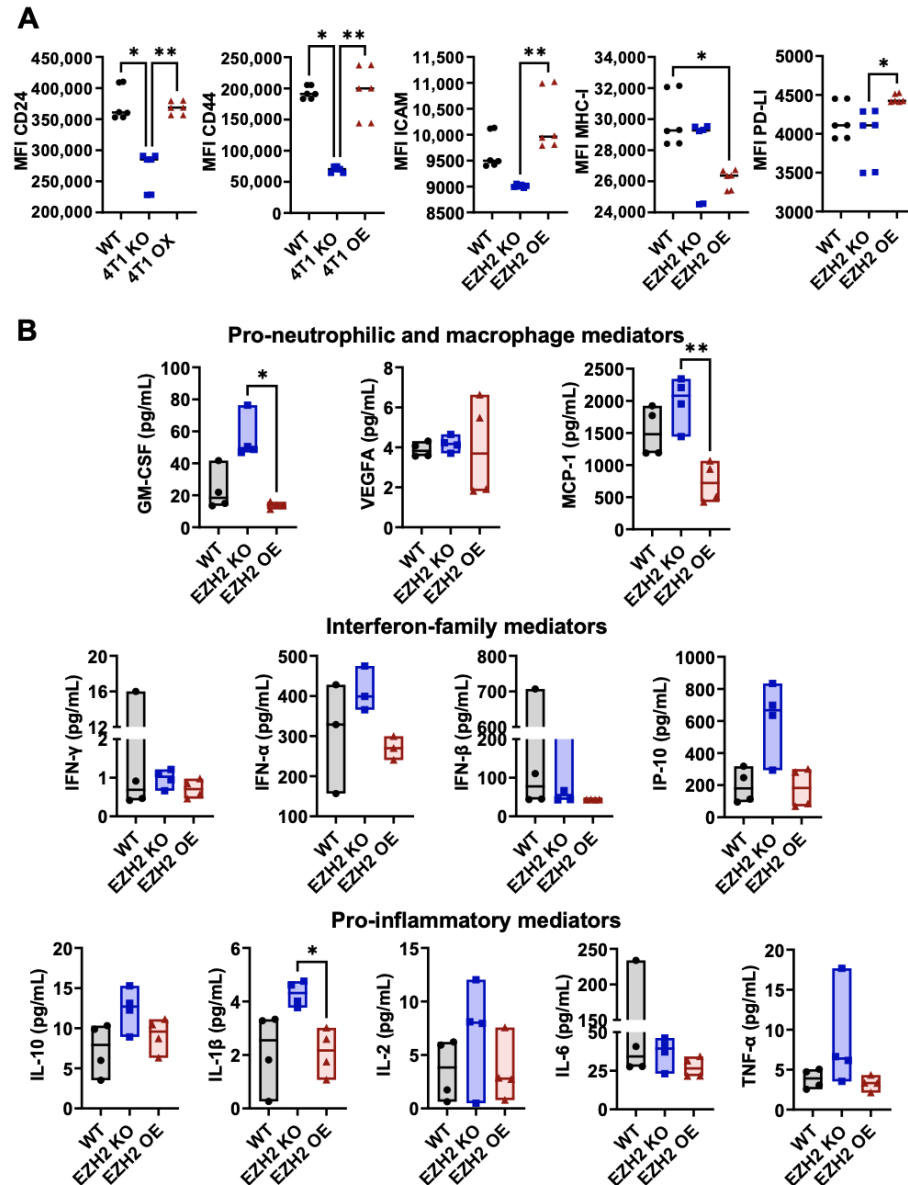


Figure 2.3. In vitro surface phenotype and secreted factors by EZH2 KO and EZH2 OE compared to parent WT 4T1 cells. (A) 4T1 WT (black circles), EZH2 KO (blue squares), and EZH2 OE (red triangles) lines were cultured in DMEM for 24 h and analyzed for the surface expression of relevant surface markers by flow cytometry (six repeats, see Methods and **(Figure 2S1 for details)**). (B) Culture supernatants were screened for relevant extracellular mediators via mesoscale assay (four repeats). Comparison between groups is by one-way ANOVA with Tukey's post-hoc test and shown as * $p < 0.05$, ** $p < 0.01$.

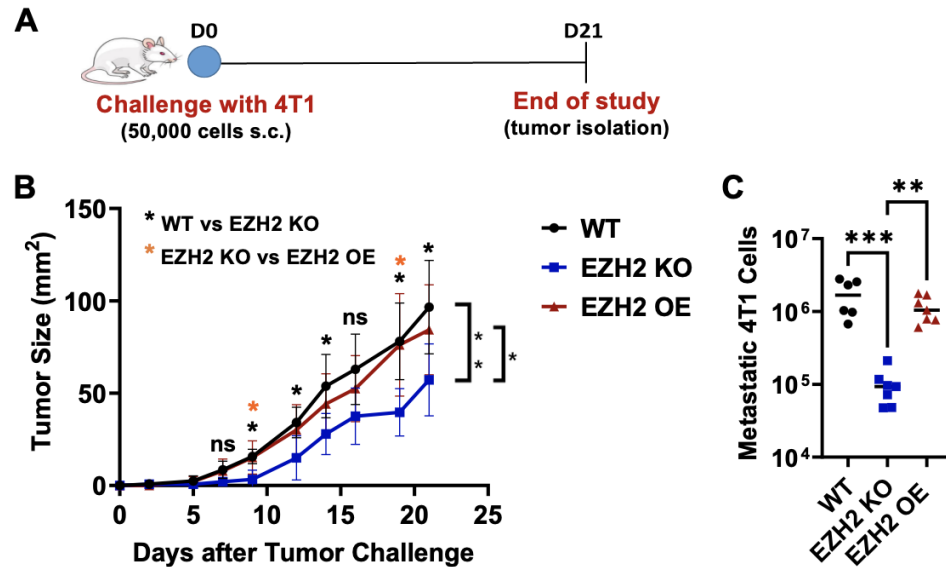


Figure 2.4. In vivo primary tumor growth and lung metastasis by EZH2 KO and EZH2 OE compared to parent WT 4T1 cells. (A) Experimental timeline of 4T1 WT, EZH2 KO, and EZH2 OE injections in mice. **(B)** Growth of 4T1 WT, EZH2 KO, and EZH2 OE primary tumors over 21 days post-injection (n = 6–7 mice per group). Comparisons across groups and timepoints are by two-way ANOVA with Tukey’s post-hoc test and shown as * p < 0.05 and ** p < 0.01 (brackets). Comparison between groups at each timepoint is by one-way ANOVA and shown as * p < 0.05 (as indicated for WT vs. EZH2 KO and EZH2 KO vs. EZH2 OE, above each timepoint). **(C)** Lung metastasis assays for 4T1 WT, EZH2 KO, and EZH2 OE lines. Comparisons between groups are by one-way ANOVA with Tukey’s post-hoc test and shown as ** p < 0.01 and *** p < 0.001.

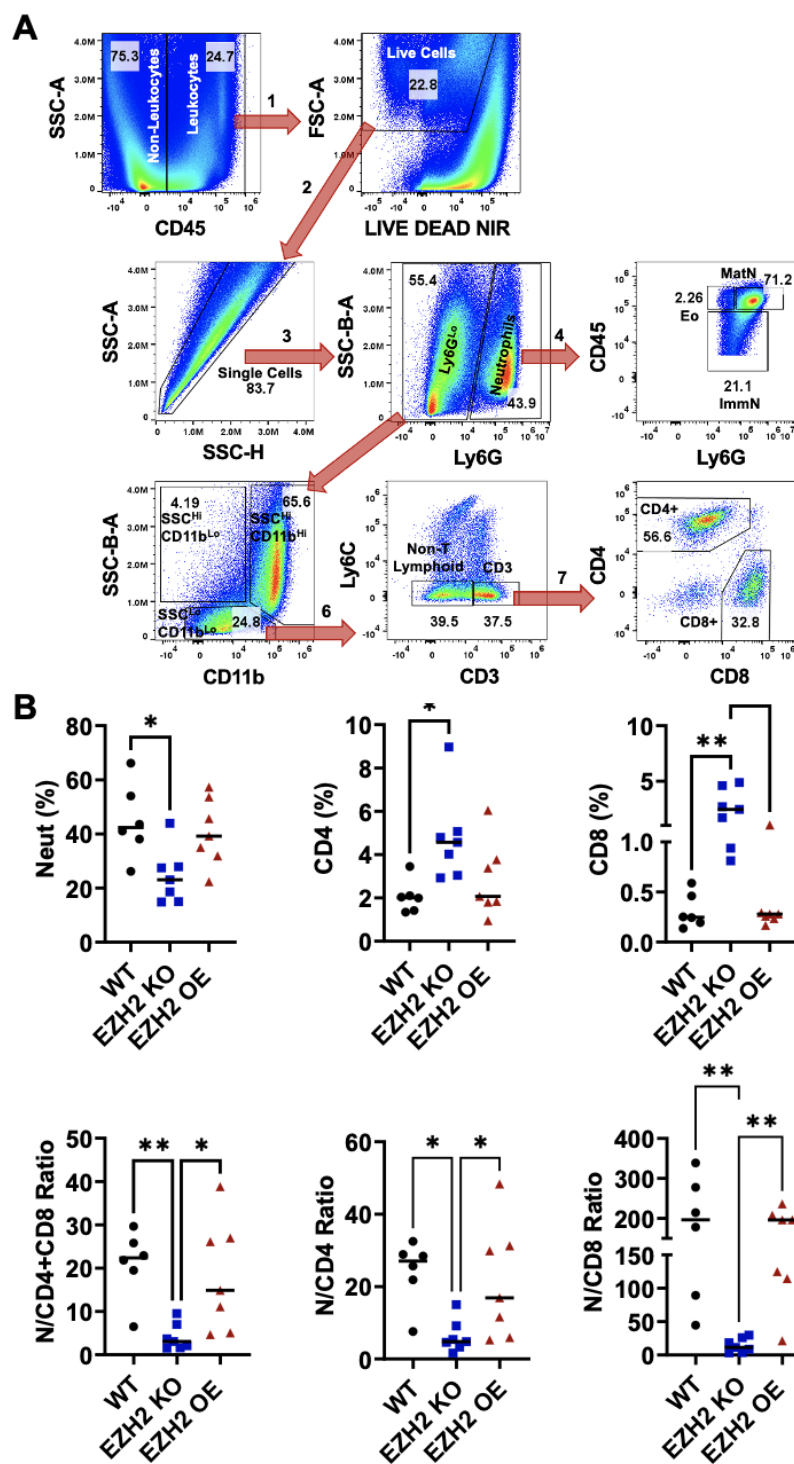


Figure 2.5. In vivo primary tumor infiltration by neutrophils and CD4⁺ and CD8⁺ T cells for EZH2 KO and EZH2 OE compared to parent WT 4T1 cells. (A) Flow cytometry strategy for gating of infiltrating leukocyte subsets in 4T1 WT, EZH2 KO, and EZH2 OE primary tumors,

with sequential steps 1 (leukocytes), 2 (live cells), 3 (singlets), 4 (granulocytes, including mature neutrophils, immature neutrophils, and eosinophils), 5 (non-granulocytes), 6 (T cells), and 7 (CD4+ and CD8+). **(B)** Relative percentages of infiltrating neutrophils and CD4+ and CD8+ cells among live leukocytes (top), and ratios between these subsets (bottom) in 4T1 WT (black circles), EZH2 KO (blue squares), and EZH2 OE (red triangles) primary tumors. Comparisons between groups are by one-way ANOVA with Tukey's post-hoc test and shown as * $p < 0.05$ and ** $p < 0.01$.

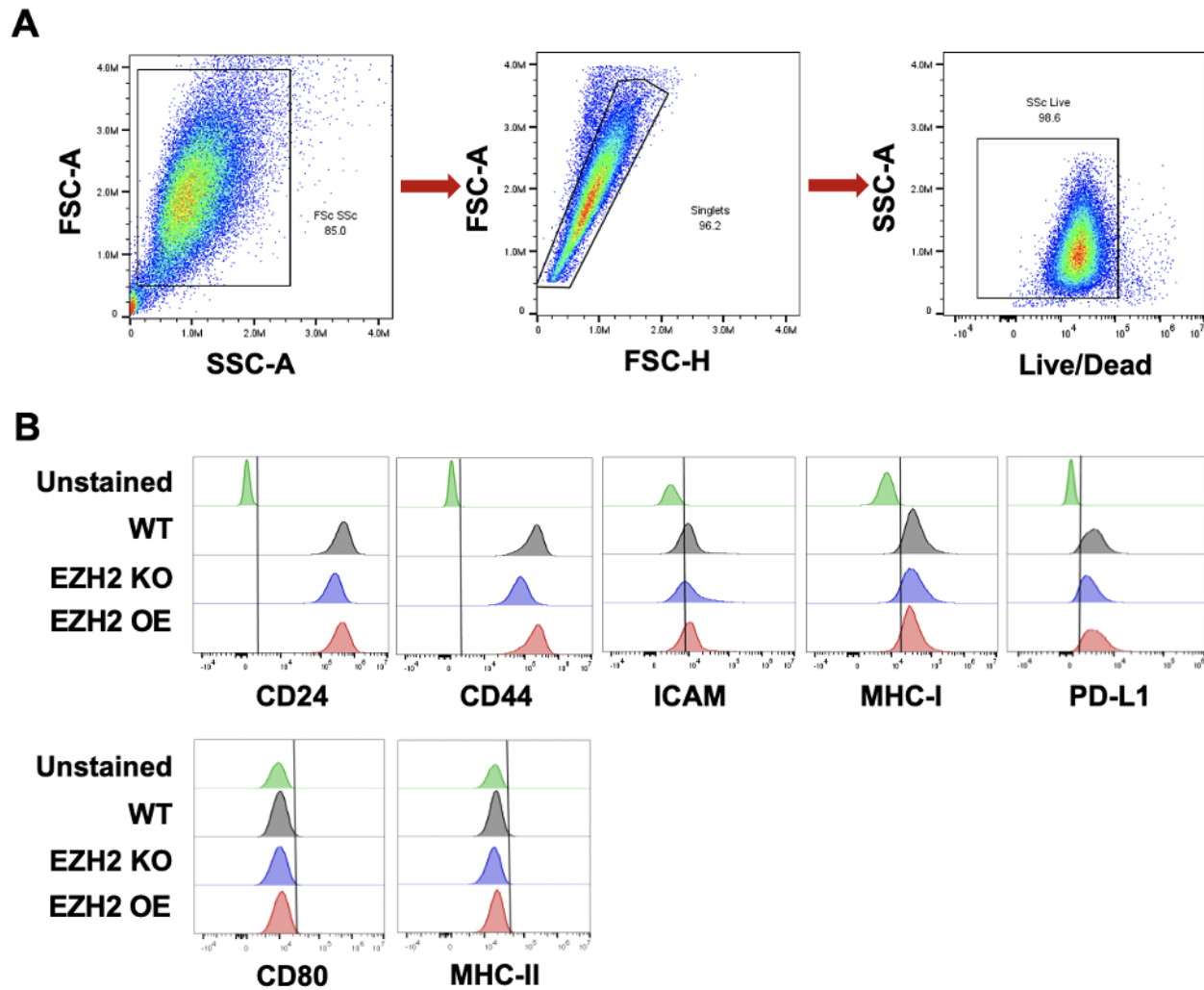


Figure 2S1. In vitro surface phenotype of EZH2 KO and EZH2 OE compared to parent

WT 4T1 cells. (A) Gating strategy showing sequential cells, singlets and live gates. (B)

Representative stacked histograms comparing expression levels of given phenotypic markers on stained EZH2 KO, EZH2 OE and WT 4T1 cell lines compared to unstained EZH2 KO cells (similar to EZH2 OE and WT 4T1 cells for baseline MFI in unstained samples). Dashed lines represent thresholds for marker positivity based on the upper boundary in respective unstained controls, revealing significantly expressed markers (top) and non-expressed markers (bottom).

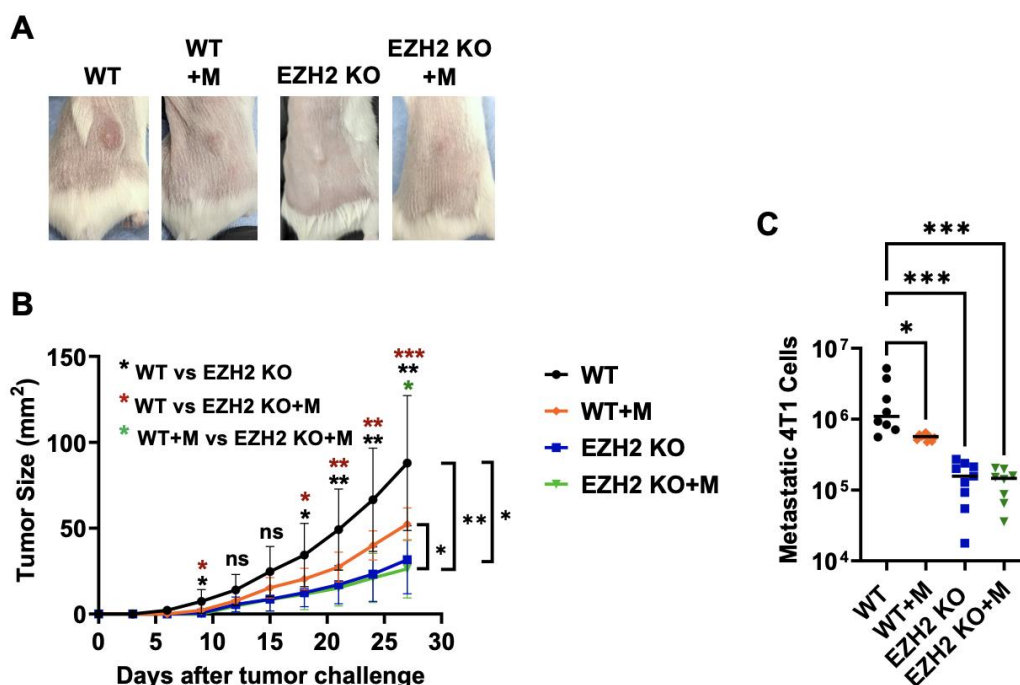


Figure 2S2. In vivo primary tumor growth and lung metastasis by EZH2 KO compared to parent WT 4T1 cells, in the absence or presence of STING agonist MSA-2. (A)

Representative images of 4T1 WT and EZH2 KO primary tumors at day 18 post-injection are shown, grow either in the absence of MSA-2 (same as experiment presented in **(Figure 2.2)**), or in the presence of MSA-2 (+M). **(B)** Growth of 4T1 WT and EZH2 KO primary tumors over 28 days post-injection (n=6-7 mice per group, left), in the absence of MSA-2 (repeat of experiment conducted over 21 days, shown in **(Figure 2.2)**), or in the presence of MSA-2 (+M). Comparison across groups and timepoints is by two-way ANOVA with Tukey post-hoc test and shown as *p<0.05, **p<0.01, and ***p<0.001 (brackets). Comparison between groups at each timepoint is by one-way ANOVA and shown as *p<0.05 and **p<0.01 (as indicated for WT vs EZH2 KO, WT vs EZH2 KO+M, and WT+M vs EZH2 KO+M, above each timepoint). **(C)** Lung metastasis assay for 4T1 WT and EZH2 KO lines grown in the absence or presence of MSA-2 (+M). Comparison between groups is by one-way ANOVA with Tukey post-hoc test and shown as *p<0.05, and ***p<0.001.

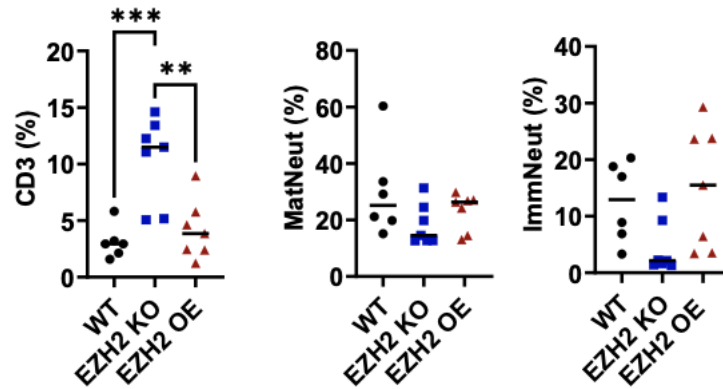


Figure 2S3. In vivo primary tumor infiltration by CD3+ T cells, mature and immature neutrophils for EZH2 KO and EZH2 OE compared to parent WT 4T1 cells. Relative percentages in 4T1 WT, EZH2 KO and EZH2 OE primary tumors of CD3+ T cells (left), mature neutrophils (middle) and immature neutrophils (right) gated among live leukocytes per **Figure 2.5A**. Comparison between groups is by one-way ANOVA with Tukey post-hoc test and shown as ** $p < 0.01$, and *** $p < 0.001$.

References

1. Arnold, M.; Morgan, E.; Rungay, H.; Mafra, A.; Singh, D.; Laversanne, M.; Vignat, J.; Gralow, J.R.; Cardoso, F.; Siesling, S.; et al. Current and future burden of breast cancer: Global statistics for 2020 and 2040. *Breast* 2022, 66, 15–23.
2. Zagami, P.; Carey, L.A. Triple negative breast cancer: Pitfalls and progress. *NPJ Breast Cancer* 2022, 8, 95.
3. Aysola, K.; Desai, A.; Welch, C.; Xu, J.; Qin, Y.; Reddy, V.; Matthews, R.; Owens, C.; Okoli, J.; Beech, D.J.; et al. Triple Negative Breast Cancer—An Overview. *Hered. Genet.* 2013, 2013 (Suppl S2), 001.
4. Wang, L.; Geng, H.; Liu, Y.; Liu, L.; Chen, Y.; Wu, F.; Liu, Z.; Ling, S.; Wang, Y.; Zhou, L. Hot and cold tumors: Immunological features and the therapeutic strategies. *MedComm (2020)* 2023, 4, e343.
5. Hong, R.; Xu, B. Breast cancer: An up-to-date review and future perspectives. *Cancer Commun.* 2022, 42, 913–936.
6. Peddi, P.F.; Ellis, M.J.; Ma, C. Molecular basis of triple negative breast cancer and implications for therapy. *Int. J. Breast Cancer* 2012, 2012, 217185.
7. Sun, S.; Yu, F.; Xu, D.; Zheng, H.; Li, M. EZH2, a prominent orchestrator of genetic and epigenetic regulation of solid tumor microenvironment and immunotherapy. *Biochim. Biophys. Acta Rev. Cancer* 2022, 1877, 188700.
8. Adibfar, S.; Elveny, M.; Kashikova, H.S.; Mikhailova, M.V.; Farhangnia, P.; Vakili-Samiani, S.; Tarokhian, H.; Jadidi-Niaragh, F. The molecular mechanisms and therapeutic potential of EZH2 in breast cancer. *Life Sci.* 2021, 286, 120047.

9. Inari, H.; Suganuma, N.; Kawachi, K.; Yoshida, T.; Yamanaka, T.; Nakamura, Y.; Yoshihara, M.; Nakayama, H.; Yamanaka, A.; Masudo, K.; et al. Expression of Enhancer of zeste homolog 2 correlates with survival outcome in patients with metastatic breast cancer: Exploratory study using primary and paired metastatic lesions. *BMC Cancer* 2017, 17, 160.
10. Liu, L.C.; Chien, Y.-C.; Wu, G.-W.; Hua, C.-H.; Tsai, I.-C.; Hung, C.-C.; Wu, T.-K.; Pan, Y.-R.; Yang, S.-F.; Yu, Y.-L. Analysis of EZH2 genetic variants on triple-negative breast cancer susceptibility and pathology. *Int. J. Med. Sci.* 2022, 19, 1023–1028.
11. Verma, A.; Singh, A.; Singh, M.P.; Nengroo, M.A.; Saini, K.K.; Satrusal, S.R.; Khan, M.A.; Chaturvedi, P.; Sinha, A.; Meena, S.; et al. EZH2-H3K27me3 mediated KRT14 upregulation promotes TNBC peritoneal metastasis. *Nat. Commun.* 2022, 13, 7344.
12. Li, Z.; Wang, D.; Lu, J.; Huang, B.; Wang, Y.; Dong, M.; Fan, D.; Li, H.; Gao, Y.; Hou, P.; et al. Methylation of EZH2 by PRMT1 regulates its stability and promotes breast cancer metastasis. *Cell Death Differ.* 2020, 27, 3226–3242.
13. Duan, D.; Shang, M.; Han, Y.; Liu, J.; Liu, J.; Kong, S.H.; Hou, J.; Huang, B.; Lu, J.; Zhang, Y. EZH2-CCF-cGAS Axis Promotes Breast Cancer Metastasis. *Int. J. Mol. Sci.* 2022, 23, 1788.
14. Zhang, L.; Qu, J.; Qi, Y.; Duan, Y.; Huang, Y. W.; Zhou, Z.; Li, P.; Yao, J.; Huang, B.; Zhang, S.; et al. EZH2 engages TGFbeta signaling to promote breast cancer bone metastasis via integrin beta1-FAK activation. *Nat. Commun.* 2022, 13, 2543.
15. Zhao, Y.; Hu, Z.; Li, J.; Hu, T. EZH2 exacerbates breast cancer by methylating and activating STAT3 directly. *J. Cancer* 2021, 12, 5220–5230.

16. Schrors, B.; Boegel, S.; Albrecht, C.; Bukur, T.; Bukur, V.; Holtsträter, C.; Ritzel, C.; Manninen, K.; Tadmor, A.D.; Vormehr, M.; et al. Multi-Omics Characterization of the 4T1 Murine Mammary Gland Tumor Model. *Front. Oncol.* 2020, 10, 1195.
17. Liu, Y.; Yang, Q. The roles of EZH2 in cancer and its inhibitors. *Med. Oncol.* 2023, 40, 167.
18. Pulaski, B.A.; Ostrand-Rosenberg, S. Mouse 4T1 breast tumor model. *Curr. Protoc. Immunol.* 2001, 39, 20.2.1–20.2.16.
19. Summerbell, E.R.; Mouw, J.K.; Bell, J.S.; Knippler, C.M.; Pedro, B.; Arnst, J.L.; Khatib, T.O.; Commander, R.; Barwick, B.G.; Konen, J.; et al. Epigenetically heterogeneous tumor cells direct collective invasion through filopodia-driven fibronectin micropatterning. *Sci. Adv.* 2020, 6, eaaz6197.
20. Mathenge, E.G.; Dean, C.A.; Clements, D.; Vaghar-Kashani, A.; Photopoulos, S.; Coyle, K.M.; Giacomantonio, M.; Malueth, B.; Nunokawa, A.; Jordan, J.; et al. Core needle biopsy of breast cancer tumors increases distant metastases in a mouse model. *Neoplasia* 2014, 16, 950–960.
21. Flood, B.A.; Higgs, E.F.; Li, S.; Luke, J.J.; Gajewski, T.F. STING pathway agonism as a cancer therapeutic. *Immunol. Rev.* 2019, 290, 24–38.
22. Walker Ii, W.H.; Borniger, J.C.; Surbhi; Zalenski, A.A.; Muscarella, S.L.; Fitzgerald, J.A.; Zhang, N.; Gaudier-Diaz, M.M.; DeVries, A.C. Mammary Tumors Induce Central Pro-inflammatory Cytokine Expression, but Not Behavioral Deficits in Balb/C Mice. *Sci. Rep.* 2017, 7, 8152.

23. DuPre, S.A.; Redelman, D.; Hunter, K.W. The mouse mammary carcinoma 4T1: Characterization of the cellular landscape of primary tumours and metastatic tumour foci. *Int. J. Exp. Pathol.* 2007, 88, 351–360.
24. Zhang, L.; Yao, J.; Wei, Y.; Zhou, Z.; Li, P.; Qu, J.; Badu-Nkansah, A.; Yuan, X.; Huang, Y.-W.; Fukumura, K.; et al. Blocking immunosuppressive neutrophils deters pY696-EZH2-driven brain metastases. *Sci. Transl. Med.* 2020, 12, eaaz5387.
25. Liu, X.; Li, J.; Cadilha, B.L.; Markota, A.; Voigt, C.; Huang, Z.; Lin, P.P.; Wang, D.D.; Dai, J.; Kranz, G.; et al. Epithelial-type systemic breast carcinoma cells with a restricted mesenchymal transition are a major source of metastasis. *Sci. Adv.* 2019, 5, eaav4275.
26. Zheng, C.; Xu, X.; Wu, M.; Xue, L.; Zhu, J.; Xia, H.; Ding, S.; Fu, S.; Wang, X.; Wang, Y.; et al. Neutrophils in triple-negative breast cancer: An underestimated player with increasingly recognized importance. *Breast Cancer Res.* 2023, 25, 88.
27. Arpinati, L.; Kaisar-Iluz, N.; Shaul, M.E.; Groth, C.; Umansky, V.; Fridlender, Z.G. Tumor-Derived Factors Differentially Affect the Recruitment and Plasticity of Neutrophils. *Cancers* 2021, 13, 5082.
28. Uribe-Querol, E.; Rosales, C. Neutrophils in Cancer: Two Sides of the Same Coin. *J. Immunol. Res.* 2015, 2015, 983698.
29. Hurt, B.; Schulick, R.; Edil, B.; El Kasmi, K.C.; Barnett, C., Jr. Cancer-promoting mechanisms of tumor-associated neutrophils. *Am. J. Surg.* 2017, 214, 938–944.
30. Brandau, S.; Dumitru, C.A.; Lang, S. Protumor and antitumor functions of neutrophil granulocytes. *Semin. Immunopathol.* 2013, 35, 163–176.
31. Liu, Y.; Hu, Y.; Xue, J.; Li, J.; Yi, J.; Bu, J.; Zhang, Z.; Qiu, P.; Gu, X. Advances in immunotherapy for triple-negative breast cancer. *Mol. Cancer* 2023, 22, 145.

32. Kim, I.S.; Gao, Y.; Welte, T.; Wang, H.; Liu, J.; Janghorban, M.; Sheng, K.; Niu, Y.; Goldstein, A.; Zhao, N.; et al. Immuno-subtyping of breast cancer reveals distinct myeloid cell profiles and immunotherapy resistance mechanisms. *Nat. Cell Biol.* 2019, 21, 1113–1126.
33. Kitchen, G.B.; Hopwood, T.; Ramamoorthy, T.G.; Downton, P.; Begley, N.; Hussell, T.; Dockrell, D.H.; Gibbs, J.E.; Ray, D.W.; Loudon, A.S.I. The histone methyltransferase Ezh2 restrains macrophage inflammatory responses. *FASEB J.* 2021, 35, e21843.
34. Koss, B.; Shields, B.D.; Taylor, E.M.; Storey, A.J.; Byrum, S.D.; Gies, A.J.; Washam, C.L.; Choudhury, S.R.; Ahn, J.H.; Uryu, H.; et al. Epigenetic Control of Cdkn2a.Arf Protects Tumor-Infiltrating Lymphocytes from Metabolic Exhaustion. *Cancer Res* 2020, 80, 4707–4719.
35. Wagner, T.E.; Becraft, J.R.; Bodner, K.; Teague, B.; Zhang, X.; Woo, A.; Porter, E.; Albuquerque, B.; Dobosh, B.; Andries, O.; et al. Small-molecule-based regulation of RNA-delivered circuits in mammalian cells. *Nat. Chem. Biol.* 2018, 14, 1043–1050.
36. Beck, D.B.; Narendra, V.; Drury, W.J.; Casey, R.; Jansen, P.W.T.C.; Yuan, Z.-F.; Garcia, B.A.; Vermeulen, M.; Bonasio, R. In vivo proximity labeling for the detection of protein-protein and protein-RNA interactions. *J. Proteome Res.* 2014, 13, 6135–6143.
37. Vo, B.T.; Li, C.; Morgan, M.A.; Theurillat, I.; Finkelstein, D.; Wright, S.; Hyle, J.; Smith, S.M.; Fan, Y.; Wang, Y.-D.; et al. Inactivation of Ezh2 Upregulates Gfi1 and Drives Aggressive Myc-Driven Group 3 Medulloblastoma. *Cell Rep.* 2017, 18, 2907–2917.
38. Ran, F.A.; Hsu, P.D.; Wright, J.; Agarwala, V.; Scott, D.A.; Zhang, F. Genome engineering using the CRISPR-Cas9 system. *Nat. Protoc.* 2013, 8, 2281–2308.
39. Munoz, L.E.; Huang, L.; Bommireddy, R.; Sharma, R.; Monterroza, L.; Guin, R.N.; Samaranyake, S.G.; Pack, C.D.; Ramachandiran, S.; Reddy, S.J.; et al. Metformin reduces PD-

L1 on tumor cells and enhances the anti-tumor immune response generated by vaccine immunotherapy. *J. Immunother. Cancer* 2021, 9, e002614.

40. Pan, B.S.; Perera, S.A.; Piesvaux, J.A.; Presland, J.P.; Schroeder, G.K.; Cumming, J.N.; Trotter, B.W.; Altman, M.D.; Buevich, A.V.; Cash, B.; et al. An orally available non-nucleotide STING agonist with antitumor activity. *Science* 2020, 369, eaba6098.

41. Yi, M.; Niu, M.; Wu, Y.; Ge, H.; Jiao, D.; Zhu, S.; Zhang, J.; Yan, Y.; Zhou, P.; Chu, Q.; et al. Combination of oral STING agonist MSA-2 and anti-TGF-beta/PD-L1 bispecific antibody YM101: A novel immune cocktail therapy for non-inflamed tumors. *J. Hematol. Oncol.* 2022, 15, 142.

Chapter 3: Research manuscript #2

Title:

Effects of EZH2 inhibition and STING agonism in a biomimetic model combining human lung adenocarcinoma cells and tumor-infiltrating neutrophils

Authors:

Lenore Monterroza, Periasamy Selvaraj, Rabindra Tirouvanziam.

Abstract

LKB1 is one of the most frequently mutated tumor suppressor genes in lung adenocarcinoma (LUAD), accounting for the majority of lung cancer cases. Due to poor T-cell infiltration, recently developed cancer immunotherapies such as chimeric antigen T-cell (CAR-T) and immune checkpoint inhibitors (ICIs) have not been effective at treating LKB1-mutant LUAD. This lack of response could also be attributed to the chronic recruitment of tumor-infiltrating neutrophils (TINs) at the tumor site. The enhancer of zeste homolog 2 (EZH2), a prominent methyltransferase in primary and metastatic lung tumors, is expressed in TINs. EZH2 is a direct target of LKB1, and an inhibitor of stress responses mediated by STING. However, the status of STING signaling and if it can be activated in TINs to overcome EZH2 expression in tumors is unknown. Here, we developed a novel human LKB1-mutant LUAD/TIN biomimetic model to address this question. We cultured H441 and H1944 LKB1-mutant LUAD lines at air-liquid interface on permeable scaffolds, followed by the transmigration of human blood neutrophils. Effects of the STING agonist MSA-2 and of EZH2 inhibitors EPZ6438 and MS1943 were assessed by flow cytometry and a 20-plex immune mediator assay. We observed that MSA-2, EPZ6438, and MS1943 treatments induced significant increases in STING-dependent mediators IL-6, IP-10 and MIP-1beta. Most strikingly, MSA-2 treatment induced 27-fold higher levels of the type III interferon mediator IL-29 (interferon lambda 3) compared to control, while neither type I nor type II interferons were induced. These findings in our novel model of LKB1-mutant LUAD/TIN interplay show responsiveness to STING activation and EZH2 inhibition through induction of type III interferon and other immune mediators and suggest that these drugs may be used to reactivate immune responses against LKB1-mutant LUAD.

Keywords: adenocarcinoma, EZH2, IL-29, LKB1, neutrophils, STING

Introduction

Lung cancer is one of the deadliest cancers worldwide with 1.8 million deaths and 2.5 million new cases each year [1]. Approximately 85% of lung cancer patients are diagnosed with non-small cell lung cancer (NSCLC), which is associated with a 5-year survival rate of less than 18%. LKB1, p53 and K-Ras are the most common genes whose expression is altered by mutations that drive lung cancer initiation and progression [2-5]. In particular, LKB1-mutant lung adenocarcinoma (LUAD) comprises ~40% of all lung cancer cases and is prone to develop metastasis during early stages [6]. Historically, patients with LUAD are treated with surgery, chemotherapy, radiation, tyrosine kinase inhibitors, and immune checkpoint inhibitors (ICIs), depending on the disease stage [7-10]. However, treatment inefficacy is common due to acquired resistance, insufficient T-cell infiltration, and loss of immunotoxic activities in the tumor niche. Moreover, high neutrophil-to-lymphocyte ratio in LUAD patients correlates with unfavorable clinical outcomes, higher rates of relapse and decreased survival [11, 12]. Thus, more effective treatments for LUAD are still needed, notably in the case of LKB1-mutant tumors.

Inflammation caused by the rapid proliferation of lung cancer cells results in tissue damage, which induces the recruitment of neutrophils from blood. Upon recruitment into this microenvironment, tumor-infiltrating neutrophils (TINs) adopt novel functions. TINs can promote cancer cell growth and invasion by stimulating pro-angiogenic factors, remodeling the extracellular matrix, and inducing cell aggregation that eventually contribute to extravasation and metastasis [13-15]. TINs can also support tumor growth by exerting immunosuppressive functions against other tumor-infiltrating immune cells through metabolic blockade (e.g., by arginine catabolism via arginase-1), checkpoint signaling (e.g., via PD-L1/PD-1 ligation), and neutrophil elastase (e.g., by cleavage of CD2, CD4, CD8 and CD25 surface receptors on T-cells)

[16-18]. Conversely, TINs may limit tumor growth via metabolic restriction (competition for glucose) and pro-apoptotic signaling (e.g., dependent on neutrophil elastase internalization) [19, 20]. Hence, modulating TINs with novel immunotherapeutics is a promising approach to overcoming current inefficiencies of LUAD treatments.

The enhancer of zeste homolog 2 (EZH2) is a prominent methyltransferase associated with the Polycomb repressive complex 2 (PRC2) that is aberrantly expressed in various cancers. EZH2 overexpression in LUAD promotes the initiation, progression, and immune dysregulation of primary and metastatic tumors [21, 22]. LKB1 normally inhibits EZH2, in turn affecting multiple downstream pathways such as the stimulator of interferon genes (STING), which is normally inhibited by EZH2. Loss-of-function mutations in LKB1 result in EZH2 overexpression and downstream STING inhibition, which enables mitochondrial damage and the presence of cytoplasmic double-stranded DNA in rapidly proliferating LUAD to avoid detection, downstream interferon induction and immune activation [2, 3, 23]. In addition to its intrinsic role in tumor cells, EZH2 is also expressed by TINs and influences their recruitment and immunoregulatory activities, notably in relation to T-cell recruitment to the tumor niche and activation therein [16]. Multiple studies have identified EZH2 as a clinical biomarker and potential therapeutic target in LUAD patients [24, 25]. However, it is unknown if STING activators or EZH2 inhibitors may disrupt LUAD/TIN interplay and positively impact tumor growth and clinical outcomes.

In prior work, our group developed a co-culture model based on the migration of primary blood neutrophils through a LUAD monolayer, resulting in the mass-production of human TINs and revealing profound transcriptional and functional reprogramming in these cells [26]. To better understand how EZH2 and/or STING modulation may directly impact TINs and control

their secretion of anti- or pro-tumor factors, we utilized this transmigration model in the presence or absence of small molecule EZH2 inhibitors and a STING agonist. Among other findings, our data reveal a strong (27-fold) induction in IL-29 secretion by the STING agonist MSA-2 in LUAD/TIN co-cultures, while EZH2 inhibitors EPZ6438 and MS1943 led to increased IL-6, IP-10 and MIP-1 β secretion, suggesting potential therapeutic use to reactivate anti-tumor immunity in conventionally treatment-resistant LUAD.

Materials and methods

LUAD cell culture. H441 (LKB1 wild-type, KRAS/TP53 and EGFR mutant LUAD; ATCC, Cat: HTB-174) and H1944 (ATCC, Cat: CRL-5907) cells were maintained in DMEM/F-12 media supplemented with 10% FBS (Corning), 2 mM glutamine (Sigma-Aldrich), and 100 U/mL-0.1 mg/mL penicillin/ streptomycin (Sigma-Aldrich) at 37 °C and 5% CO₂. For co-cultures, 2.5x10⁵ H441 or H1944 cells were cultured at air-liquid interface on Alvetex scaffolds (Reprocell) coated with rat tail collagen (Sigma-Aldrich) [27]. Every two days, basolateral medium DMEM/F-12 media supplemented with 2% Ultrosor G (Crescent Chemical Co.), 2 mM glutamine (Sigma-Aldrich) and 100 U/mL-0.1 mg/mL penicillin/streptomycin (Sigma-Aldrich) was replaced. After 14 days, membranes were inverted, allowing for fresh blood neutrophil loading on the basolateral side and transepithelial migration through H441 or H1944 monolayers, as detailed below.

Human neutrophil isolation and transmigration. Blood from healthy donors was collected by venipuncture in K2-EDTA tubes and placed on ice. Right after collection, blood neutrophils were isolated using Polymorphprep (Accurate Chemical) by centrifugation at 400xg for 42 min at RT with slow acceleration and minimal break. The neutrophil layer was collected with a Pasteur pipette, transferred to a 15 ml conical tube. After lysis of residual red blood cells, neutrophils were washed and were resuspended in RPMI-1640 medium (Corning) and count was determined using a Cellometer T4 Automated Counter with trypan blue. A total of 100 µL of purified blood neutrophils (1x10⁶ cells) were loaded on top of the filter of each well. Samples were incubated for 12 h to allow neutrophils to transmigrate towards the chemoattractant leukotriene B4 (LTB₄, 100 nM, Sigma-Aldrich) in the absence or presence of EZH2/STING

drugs (below) at 37 °C and 5% CO₂. After transmigration, neutrophils were collected, washed three times, and resuspended in RPMI-1640 for analysis by flow cytometry.

Drugs. EZP6438 (Cat:16174, Cayman Chemicals) was dissolved in dimethyl sulfoxide (DMSO) at a stock concentration of 1 mg/mL, aliquoted and stored at -20 °C until use. For transmigration, a concentration of 100 nM of EPZ6438 in 2 ml of DMEM per well was used. MS1943 (Cat: HY-133129, MedChemExpress) was dissolved in DMSO at a stock concentration of 5 mM, aliquoted and stored at -20 °C until use. For transmigration, a concentration of 5 μM in 2 mL of DMEM per well was used. MSA-2 (benzothiophene oxobutanoic acid; Cat: HY-136927, MedChemExpress) was dissolved in DMSO at a stock concentration of 20 mg/mL, aliquoted and stored at -20 °C until use. For transmigration, a concentration of 30 μM of MSA-2 in 2 ml of DMEM per well was added.

Extracellular mediator assay. Supernatants from 12 h co-cultures of H441 or H1944 cells with transmigrated human neutrophils were collected and stored at -80 °C until use. Extracellular mediators were measured by high-sensitivity chemiluminescent multiplexed assay (U-PLEX, Meso Scale Discovery), following the manufacturer's protocol. Plates were acquired on the QuickPlex SQ 120MM reader and later analyzed using Discovery Workbench 4.0 software (both from Meso Scale Discovery). For concentrations that were below the lower limit of detection, a value of half the lower limit was imputed; these values are represented with a green symbol. For concentrations that were above the higher limit of quantitation, a value of twice the higher limit was assigned; these values are represented with a blue symbol.

Flow cytometry analysis. Neutrophils were pre-incubated with Human TruStain FcX Fc blocking antibody (Clone 24G2, BioLegend) in FACS buffer at room temperature for 10 min. Then, neutrophils were incubated with fluorochrome-conjugated antibodies in the dark for 30 min at 4 °C. The staining panel included antibodies against CD63 (Clone H5C6), CD45 (Clone H130), CD16 (Clone 3G8), CD66b (Clone G10F5), CD47 (Clone CC2C6), LFA-1 (Clone m24), and the FLICA probe (FAM-YVAD-FMK, cell permeable caspase-1 substrate) all purchased from BioLegend, as well as Live Dead (Near infra-red, Cat. L10119) purchased from ThermoFisher Scientific. After incubation, neutrophils were washed three times with FACS buffer, and fixed in Lyse/Fix Phosflow (BD Biosciences). The stained samples were acquired in an Aurora Spectral Flow Cytometer (Cytek Biosciences), and the data was analyzed using FlowJo software (version 10.10, BD Biosciences).

Statistical analysis. All graphs were performed using Prism software (version 10.2, GraphPad Software). Data analysis was performed using JMP13 (SAS Institute) for statistical analysis. One-way ANOVA was used to analyze differences between the three treatments (EPZ, MS1943, and MSA-2) among both H441 and H1944 cell lines. Values of $p < 0.05$ were considered significant (* $p < 0.05$, ** $p < 0.01$, *** $p < 0.001$, and **** $p < 0.0001$).

Results

Development of a LKB1-mutant LUAD/TIN cell culture model. To determine if drugs modulating EZH2 or STING signaling can impact communication between LUAD cells and TINs, we developed a LUAD/TIN co-culture model. This model used either H441 or H1944 cells differentiated on a scaffold at air-liquid interface. Transmigration of neutrophils (1×10^6 added to each filter) across LUAD layers was driven by the LTB₄ chemoattractant, in the absence or presence of EZH2- or STING-targeting drugs and analyzed after 12 h (**Figure 3.1A**). After flow cytometry gating (**Figure 3S1**), the yield of TINs obtained across each scaffold was determined and found to range from 1×10^4 to 7×10^4 cells (**Figure 3S2**).

STING agonism alters mediator secretion in LUAD/TIN co-cultures. Among pro-neutrophil and monocyte/macrophage mediators (**Figure 3.2A**), we observed cell line-dependent differences with increased levels of G-CSF and ENA-78 and decreased level of VEGF in H1944/TIN vs H441/TIN co-cultures, which were present in both control and MSA-2 treated conditions. In addition, MSA-2 significantly increased MIP-1 beta and G-CSF levels in H1944/TIN co-cultures. Among inflammasome family mediators (**Figure 3.2B**), we observed cell line-dependent differences with increased levels of IL-18 and IL-1 α in H1944/TIN vs H441/TIN co-cultures, which were present in control but not MSA-2 treated condition. In addition, MSA-2 significantly increased IL-18 in H1944/TIN co-cultures and decreased IL-1RA in H441/TIN co-cultures. Among inflammatory mediators (**Figure 3.2C**), we observed cell line-dependent differences with increased levels of IL-6 in H1944/TIN vs H441/TIN co-cultures, which were present in control and MSA-2 treated conditions. In addition, MSA-2 significantly

increased IL-6 and TNF α in H1944/TIN co-cultures. Finally, among interferon-family mediators (**Figure 3.2D**), we observed cell line-dependent differences with increased levels of IL-29 in H1944/TIN vs H441/TIN co-cultures, which were present in control and MSA-2 treated conditions. In addition, MSA-2 significantly increased IL-29 in both H1944/TIN and H441/TIN co-cultures and IP-10 in H1944/TIN co-cultures.

STING agonism does not alter TIN phenotype in LUAD/TIN co-cultures. Flow cytometry analysis of intracellular levels of active caspase-1 (cell-permeable FLICA probe) and surface markers CD16, CD45, CD63, CD66b and LFA-1 did not reveal any difference between LKB1-mutant (H1944) and wild type (H441)/TIN co-cultures at baseline, or under MSA-2 treatment (**Figure 3.3**). Of note, however, MSA-2 seemed to reduce CD47 expression on TINs from both H441/TIN and H1944/TIN co-cultures, although this did not reach statistical significance.

EZH2 inhibition alters mediator secretion in LUAD/TIN co-cultures. Among pro-neutrophil and monocyte/macrophage mediators (**Figure 3.4A**), we observed cell line-dependent differences with increased levels of G-CSF, TRAIL and ENA-78 and decreased level of VEGF in H1944/TIN vs H441/TIN co-cultures, which were present in both EPZ6438 and MS1943 treated conditions. In addition, EPZ6438 and MS1943 both significantly increased GM-CSF and MS1943 increased MIP-1 beta in H1944/TIN co-cultures. Among inflammasome family mediators (**Figure 3.4B**), we observed cell line-dependent differences with increased levels of IL-18 and IL-1 α in H1944/TIN vs H441/TIN co-cultures, which were present in both EPZ6438

and MS1943 treated conditions. In addition, MS1943 significantly decreased IL-1 α in H441/TIN co-cultures. Among inflammatory mediators (**Figure 3.4C**), we observed cell line-dependent differences with increased levels of IL-6 and TNF α in H1944/TIN vs H441/TIN co-cultures, which were present in control and MSA-2 treated conditions. Finally, among interferon-family mediators (**Figure 3.2D**), MS1943 significantly increased IP-10 levels in H1944/TIN co-cultures compared to control condition, and in H441/TIN co-cultures compared to EPZ6438 conditions.

EZH2 inhibition alters TIN phenotype in LUAD/TIN co-cultures. Differences in secreted mediators observed with EPZ6438 and MS1943 treatments of LUAD- occurred along with altered TIN phenotype, as determined by flow cytometry analysis (**Figure 3.5**). In H441/TIN co-cultures, EPZ decreased TIN intracellular caspase-1 activity compared to control condition, and MS1943 increased TIN intracellular caspase-1 activity compared to the EPZ6438 condition. MS1943 also increased TIN surface CD63 expression in H441/TIN co-cultures compared to control and EPZ6438 conditions. In H1944/TIN co-cultures, MS1943 also increased TIN surface CD63 expression compared to control and EPZ6438 conditions. Finally, MS1943 also increased TIN surface LFA-1 expression in H1944/TIN co-cultures compared to the EPZ6438 condition.

Discussion

In this study, we established a LUAD/TIN co-culture model featuring LKB1-mutant or wild type human LUAD cells combined with transmigrated primary human blood neutrophils, extending prior work from our group [27]. We used this model to evaluate LUAD/TIN responses to drugs targeted at the EZH2 and STING pathways, which are operating directly downstream of LKB1 signaling.

Previous studies have reported LKB1 inactivation in lung cancer to be associated with EZH2 activation and subsequent epigenetic inhibition of STING expression, promoting neutrophil recruitment and mediating T-cell exclusion in LUAD [4]. It has also been observed that LKB1-mutant LUAD are associated with poorer clinical outcomes of immunotherapy due to increased PD-L1 expression and tumor mutational burden. In this study, we observed that LUAD/TIN co-cultures significantly differed in their baseline secretion profiles of several key immune mediators depending on whether LUAD cells were LKB1-mutant (H1944) or wild type (H441). Notably, we observed increased secretion of G-CSF, ENA-78, IL-18, IL-29 and IL-6 and decreased secretion of VEGF and IL1-RA in the former compared to the latter. This pattern is highly suggestive of a pro-neutrophilic, pro-inflammatory bias in LKB1-mutant LUAD, which is consistent with the *in vivo* microenvironment for this type of lung tumors.

Next, we observed that LUAD/TIN co-culture treatment with the STING agonist MSA-2 led in both LKB1-mutant and wild type models to substantially increased secretion of IL-29 (increased 27-fold compared to baseline in the former). IL-29 (also known as interferon lambda 3) is a potent mediator of epithelium/neutrophil signaling, potentiating functional activities of neutrophils (such as scavenging of debris), but also limiting their recruitment [28], which may be

beneficial in the context of LKB1-mutant LUAD. MSA-2 treatment also induced higher IP-10 secretion in LUAD-TIN co-cultures. In prior instances, IP-10 has been identified as a chemoattractant of activated T-cells into sites of inflammation [29]. Significant increase in secretion of MIP-1 β in LKB1-mutant LUAD/TIN co-cultures under MSA-2 treatment was also observed. Previous observations indicate that when neutrophils transmigrate through the basement membrane, they can secrete MIP-1 β to induce further transmigration of myeloid cells from the vasculature into inflammatory tissues [30]. Taken together, pharmacological activation of STING by MSA-2 may bypass its blockade by EZH2, inducing interferon-mediated stress responses and shifting signal intratumor signaling toward pathways (e.g., IRF3 and STAT1) that promote LUAD cell death and boost the efficacy of T cell immunotherapy [3, 31, 32].

Interestingly, when we profiled intracellular caspase-1 activity and expression of key surface markers on transmigrated neutrophils in LUAD-TIN co-cultures, we did not find significant differences between LKB1-mutant and wild type models, suggesting that they are not leading to differential functional polarization of TINs. Except for a (non-significant) decrease in CD47, MSA-2 treatment did not alter intracellular and surface markers in TINs. The fact substantial changes in mediator secretion may occur under MSA-2 treatment without altering TIN phenotype is an interesting observation that warrants further investigation.

Similarly to but also distinctly from the observed effects of direct STING activation in LUAD-TIN co-cultures by MSA-2, treatment with the EZH2 inhibitors EPZ6438 and MS1943 also led to altered secretion of several mediators. These included, for LKB1-mutant LUAD, increased IP-10 and MIP-1 β (as observed for MSA-2), and increased GM-CSF (not seen with MSA-2), while IL-29 was unchanged (unlike MSA-2). Also unlike MSA-2, MS1943 altered TIN

phenotype with an increased surface expression of CD63 indicating increased exocytosis of neutrophil elastase-rich (azurophil) granules [33]. These findings suggest that EZH2 inhibition and STING agonism may work partially but not fully along the same lines, likely because EZH2 has other targets than STING, and because STING has other regulators than EZH2.

We acknowledge several limitations to this study. First, even when our model seems to mimic some of the interplay between LKB1-mutant or wild type LUAD with TINs, we have not yet cross-validated the observed changes in mediator secretion and TIN phenotype with data from in vivo studies of LUAD. Second, while our secreted mediator screen revealed interesting results regarding IL-29 signaling as baseline difference between LKB1-mutant vs. wild type LUAD and as a highly upregulated secreted factor upon MSA-2 treatment, we do not know which cells secrete it and/or respond to it. Indeed, IL-29R is expressed on both LUAD epithelial cells and TINs, and IL-29 itself can be made by both cell types. Hence, complex autocrine/paracrine signaling may occur when IL-29 secretion is present and upregulated in LUAD/TIN co-cultures, which requires further investigation.

Over the past two decades important advancements to treat LUAD have been achieved. However, the overall survival rate remains low, especially when patients reach a metastatic stage [1]. Much work remains to be accomplished to reach a deeper understanding of the underlying pathobiology of LUAD and develop effective therapies able to overcome tumor resistance to therapeutics, whether intrinsic or extrinsic. Intrinsic resistance occurs within tumor cells as they adapt via changes in DNA damage response, gene expression, signaling, and/or immune interactions. Extrinsic resistance relates to changes in the tumor microenvironment, including but not limited to changes in T-cell activation [9, 34]. Current LUAD treatments generally aim to

target mutant genes/proteins in tumor cells or restore effector T-cell function, however, these approaches have reached limited clinical success notably in the context of LKB1-mutant tumors. Interaction between tumor cells and T-cells and innate cells like TINs (as studied here), as well as tumor-infiltrating monocytes, macrophages and eosinophils, are expected to influence immune killing of cancer cells, notably when treating cold tumors with a high innate to adaptive immune cell ratio [35, 36]. An avenue currently under investigation is the use of conventional treatments in combination with STING agonists [37-39]. Data presented here also warrant future studies to explore non-overlapping and/or synergistic effects of EZH2 inhibitors with STING agonists. Such novel combinations may yield therapies with manageable toxicity profiles and significant benefits in relation to LUAD/TIN interplay, cancer progression and patient survival.

Acknowledgments

The authors thank the Emory University Pediatrics and Winship Flow Cytometry Core, the Emory University Immunoassay Core, and Dr. Jeffrey Tomalka for assistance.

Figures

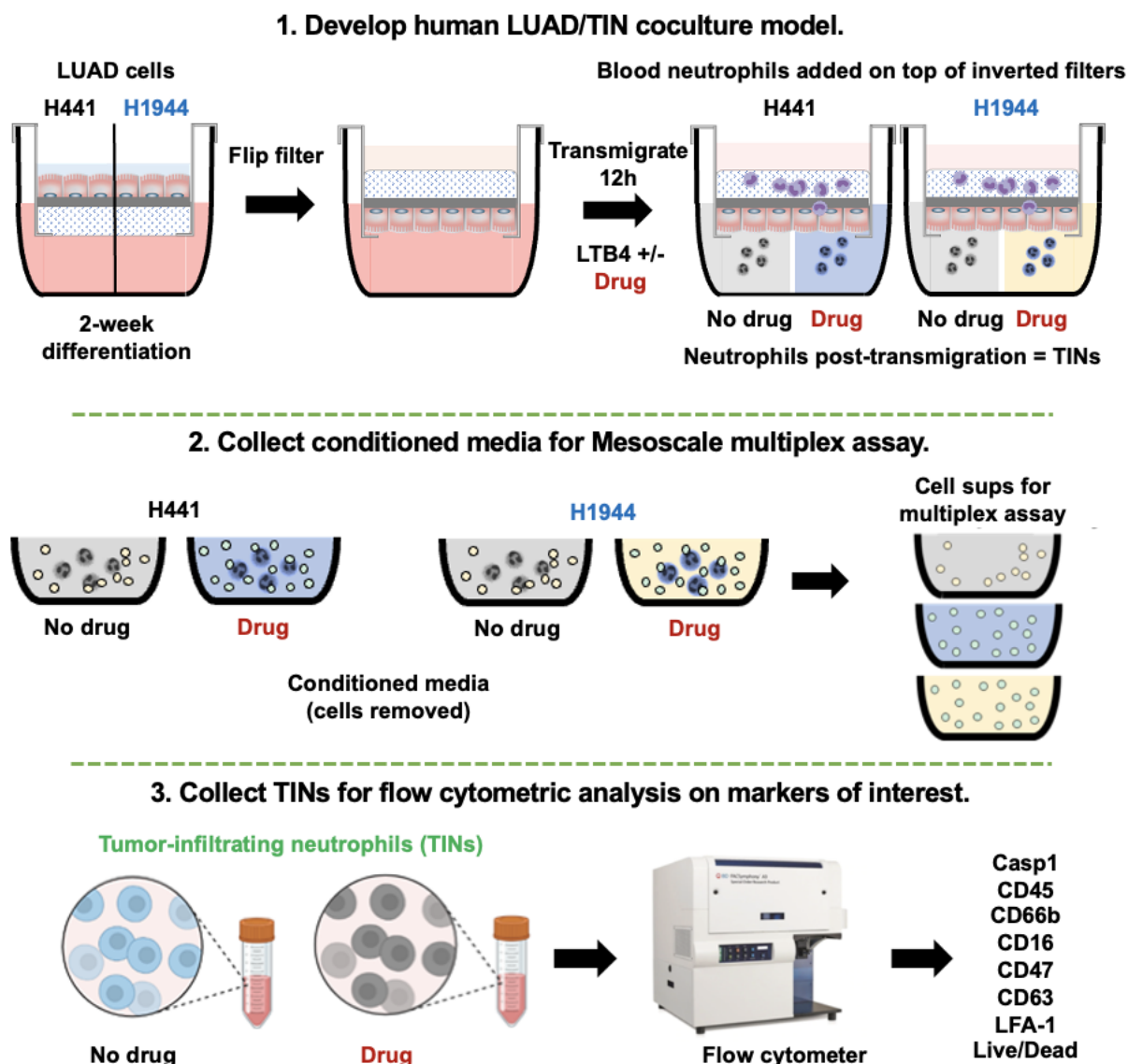
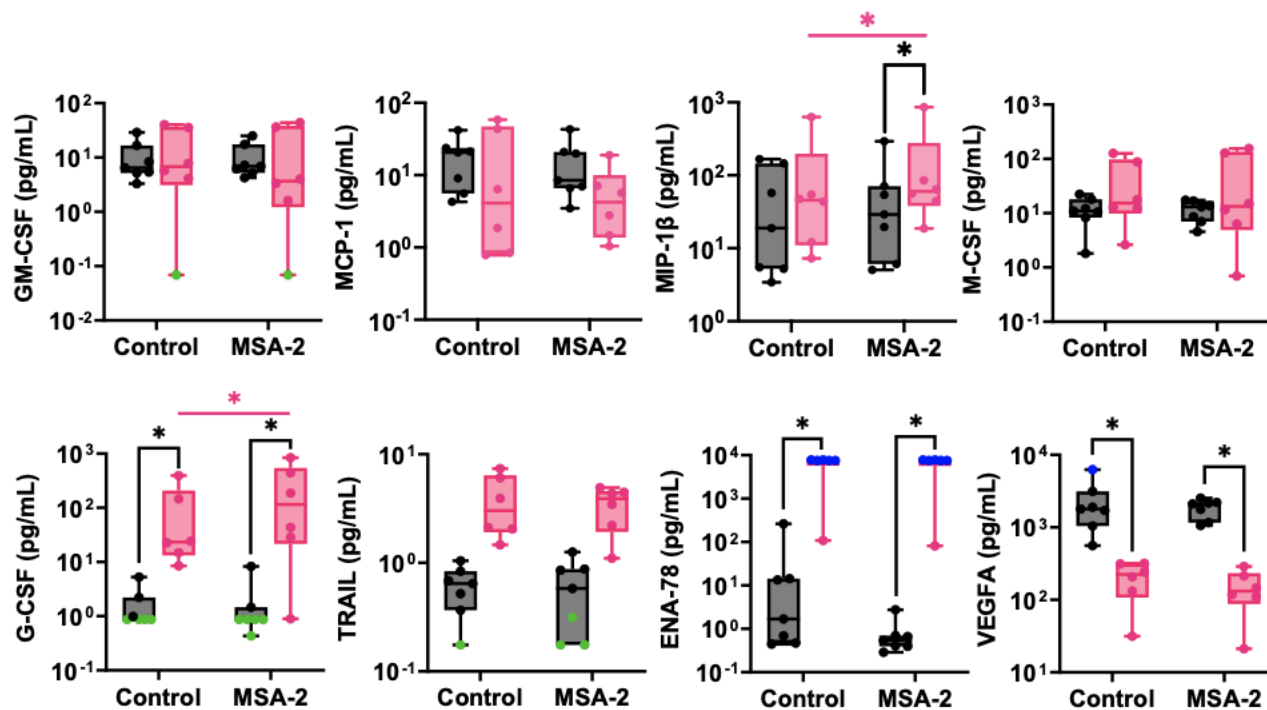
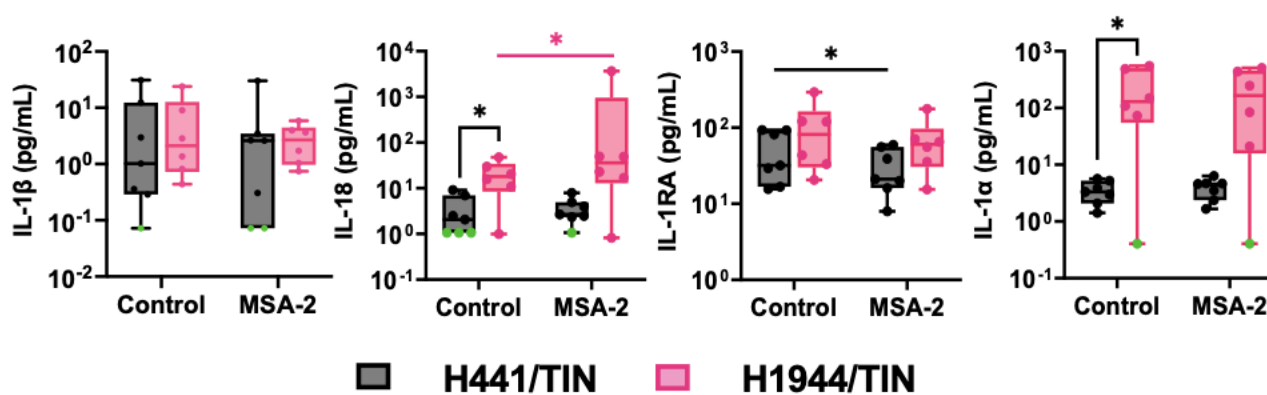


Figure 3.1. Human LKB1-mutant LUAD/TIN coculture model and analytical setup. H441 and H1944 LKB1-mutant LUAD lines were cultured at air-liquid interface on Alvetex scaffolds (Reprocell), followed by the transmigration of human blood neutrophils to generate tumor infiltrating neutrophils (TINs). The effect of EZH2- and STING-targeted drugs on the fluid secretome and TIN phenotype was analyzed.

A Pro-neutrophilic and pro-monocyte/macrophage mediators



B Inflammasome-family mediators



■ H441/TIN ■ H1944/TIN

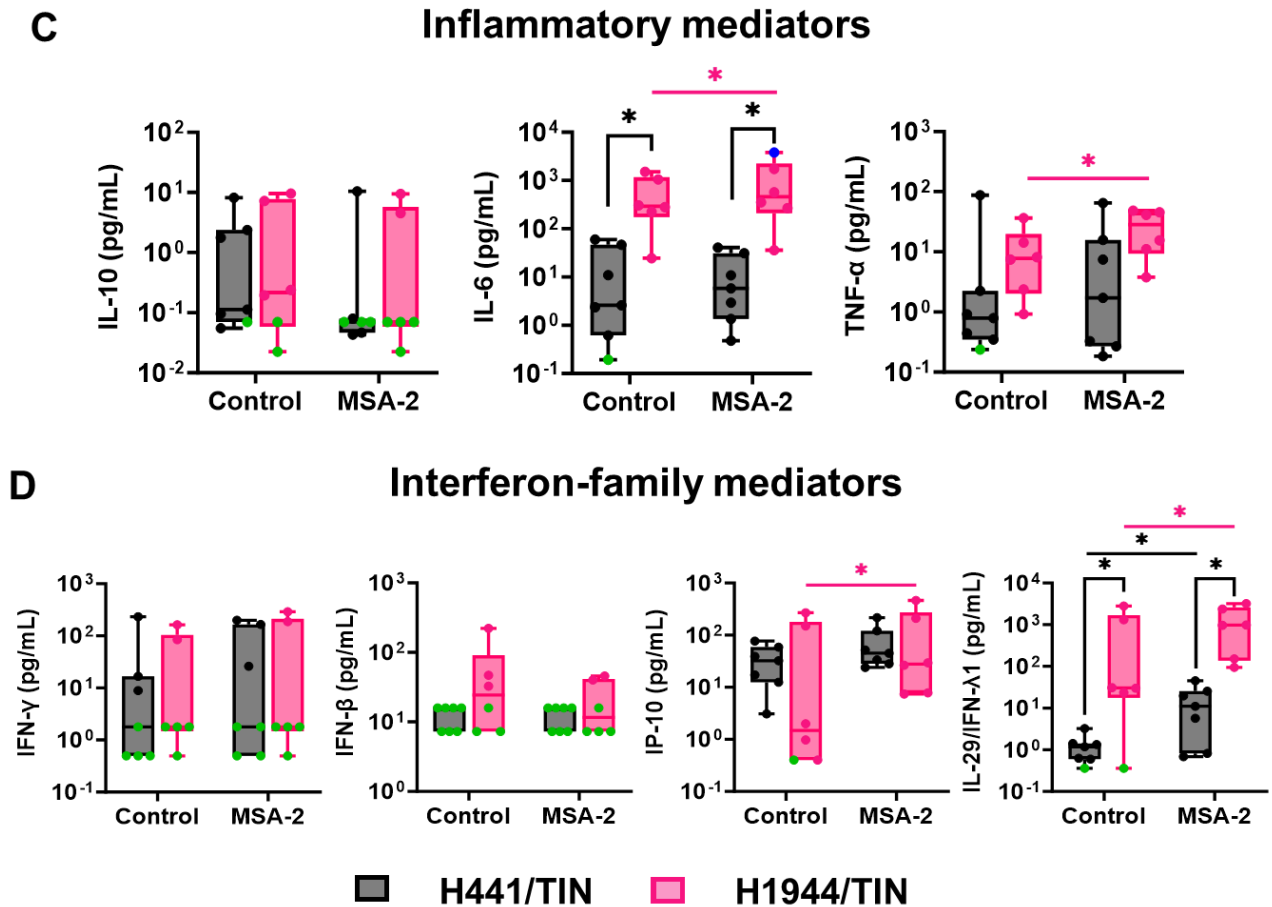


Figure 3.2. Impact of STING agonist MSA-2 on secreted mediators in LUAD/TIN co-cultures. (A-D) Human neutrophils were transmigrated through H441 (black) and H1944 (pink) LUAD lines for 12 h, using apical LTB₄, in the absence or presence MSA-2, after which co-culture supernatants were profiled for 4 families of secreted mediators using a 20-plex assay. Comparisons between H441 and H1944 cell lines and between control and MSA-2 treatment are assessed by the Wilcoxon test (N=6-7) and shown as * for p<0.05.

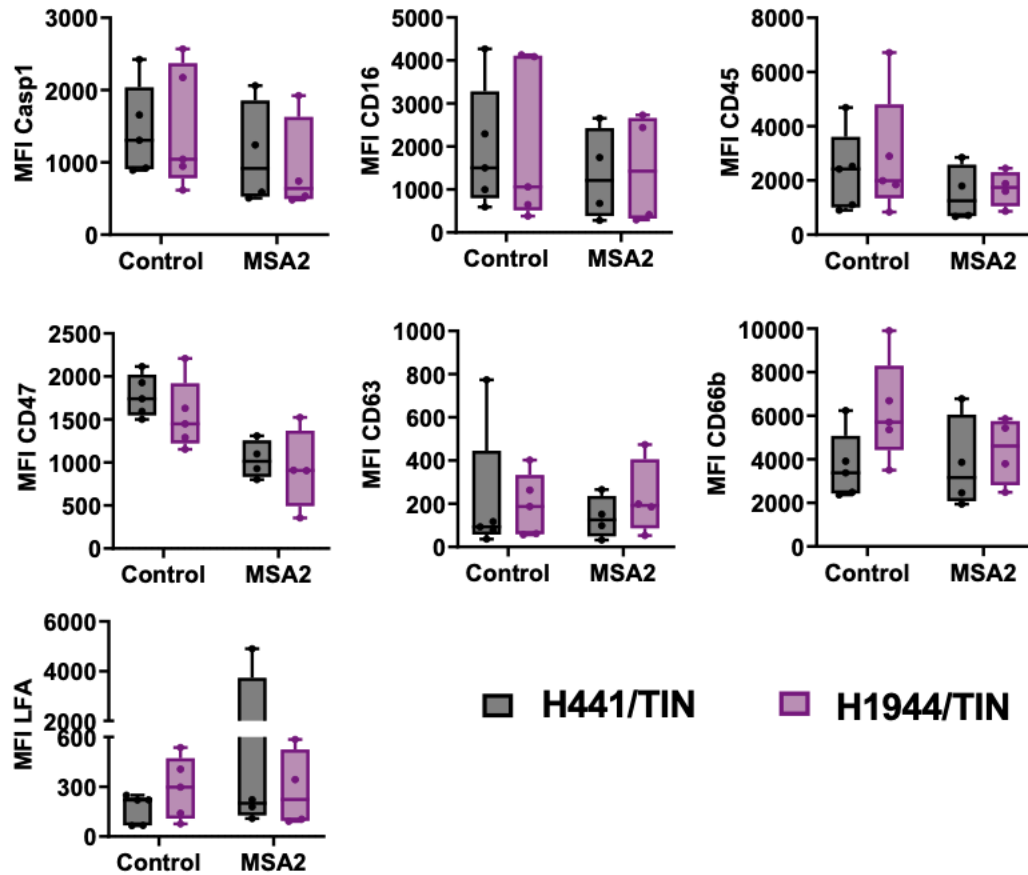
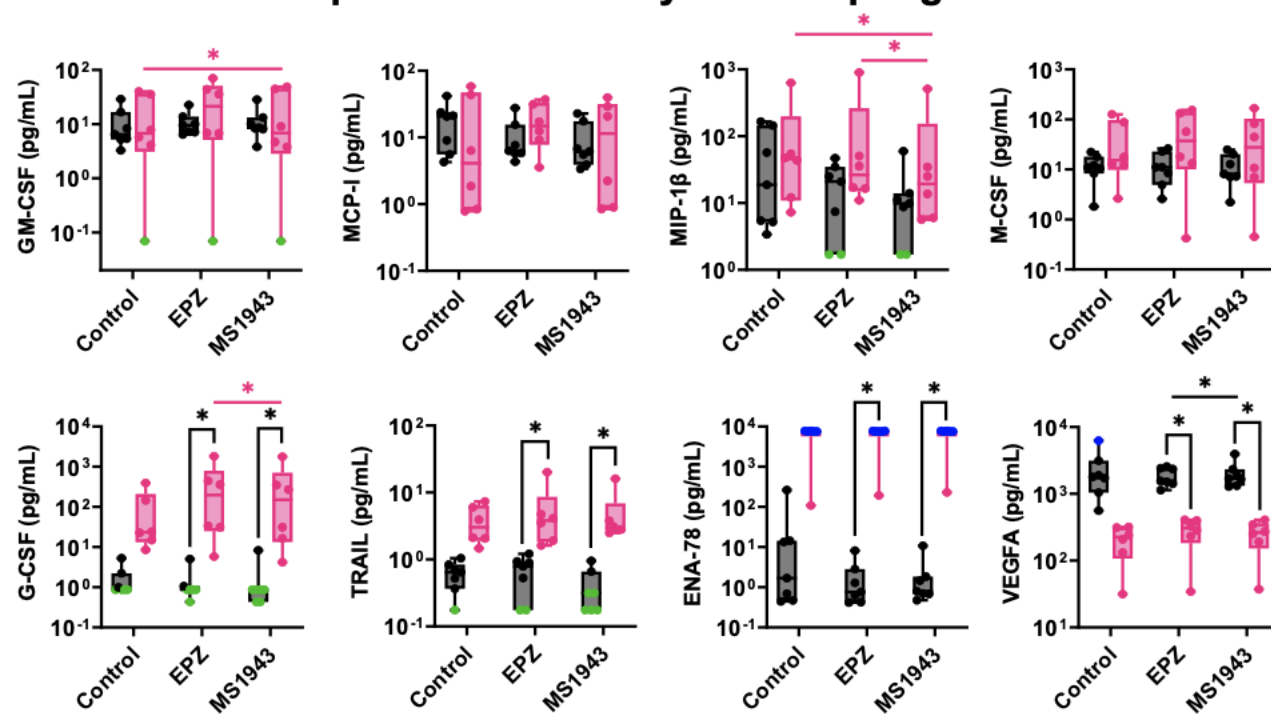


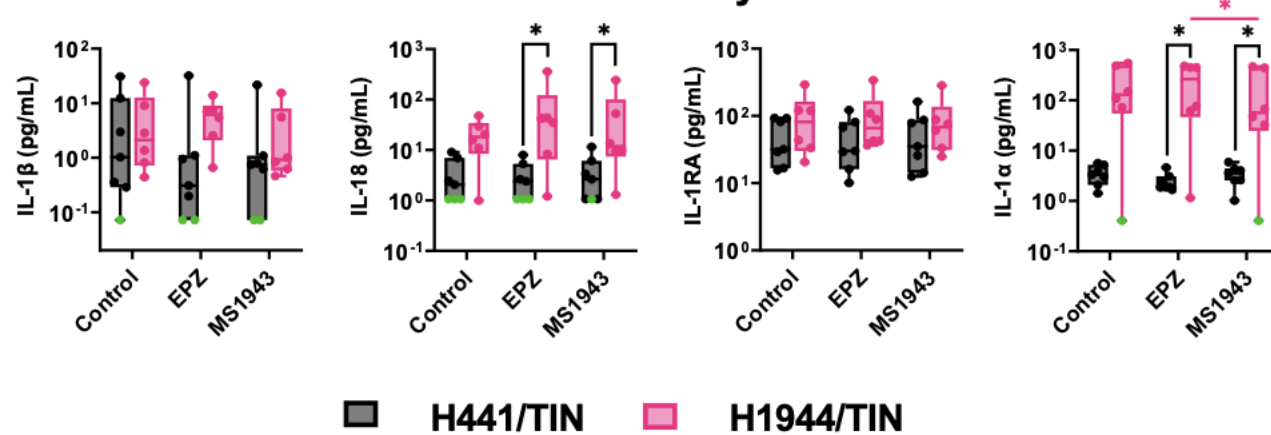
Figure 3.3. Impact of STING agonist MSA-2 on TIN phenotype in LUAD/TIN co-cultures.

Human neutrophils from healthy donors transmigrated through H441 (black) and H1944 (purple) LUAD lines into LTB₄ only (control) or LTB₄+MSA-2 (MSA-2) were subjected to flow cytometry analysis to assess activation profiles. Comparison between H441 and H1944 cell lines and between control and MSA-2 treatment was by Wilcoxon test (N=6-7).

A Pro-neutrophilic and monocyte/macrophage mediators



B Inflammasome-family mediators



■ H441/TIN ■ H1944/TIN

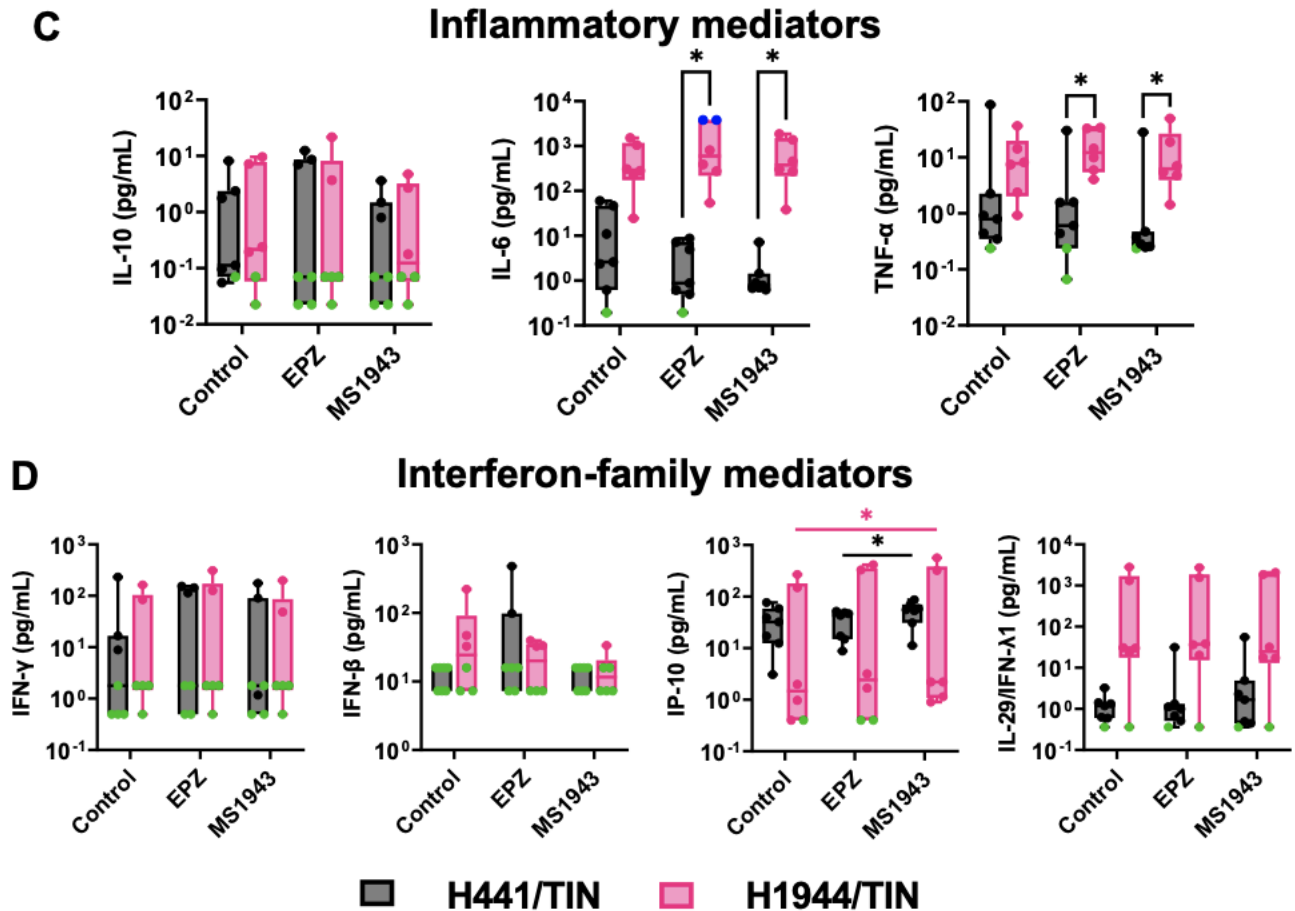


Figure 3.4. Impact of EZH2 inhibitors EPZ6438 and MS1943 on secreted mediators in LUAD/TIN co-cultures. (A-D) Human neutrophils were transmigrated through H441 (black) and H1944 (pink) LUAD lines for 12 h, using apical LTB₄, in the absence or presence of EPZ6438 (EPZ) or MS1943, after which co-culture supernatants were profiled for 4 families of secreted mediators using a 20-plex assay. Comparisons between H441 and H1944 cell lines and between control and MSA-2 treatment are assessed by the Wilcoxon test (N=6-7) and shown as * for $p < 0.05$.

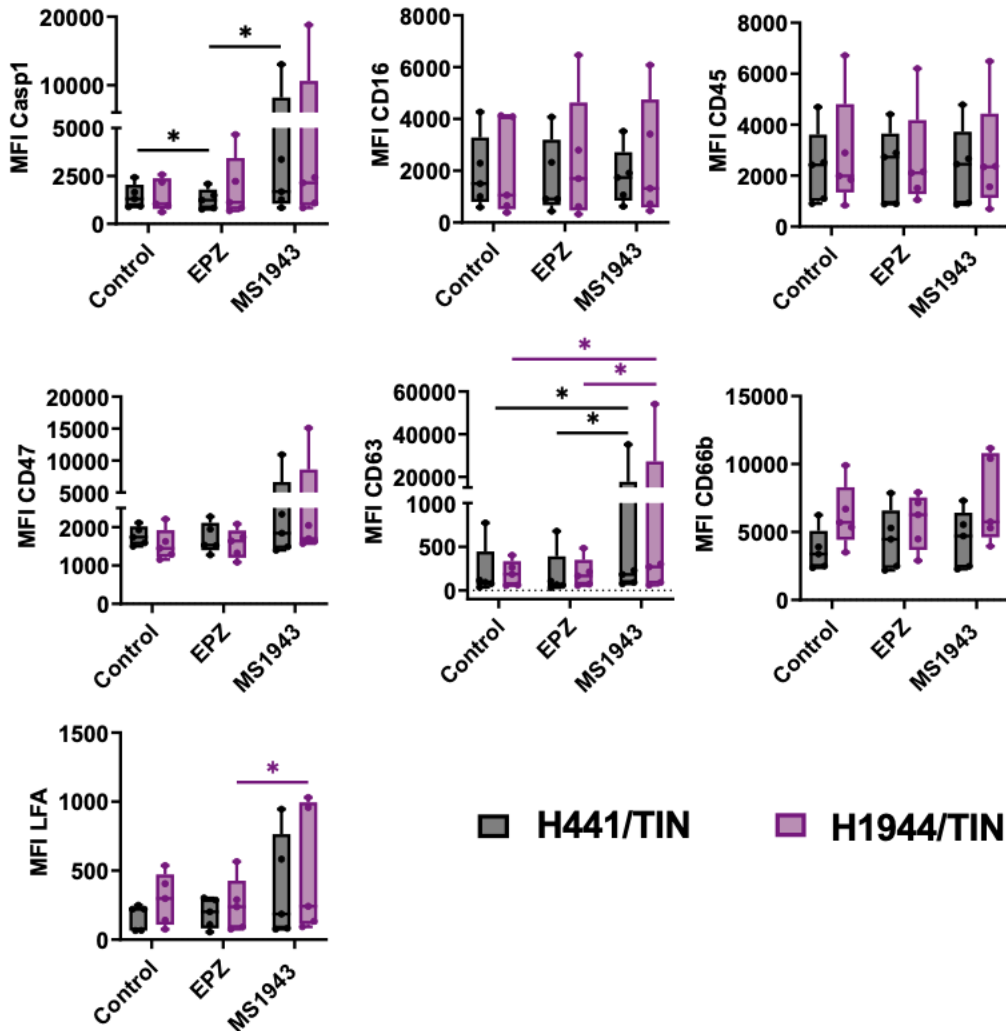
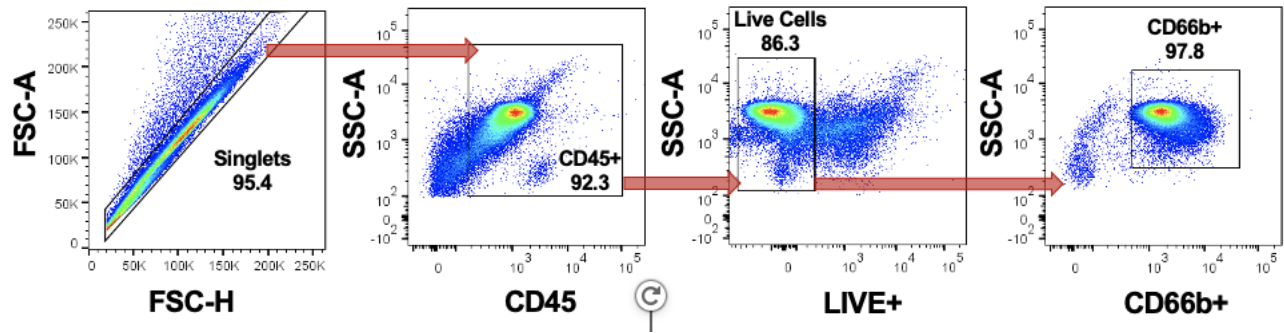
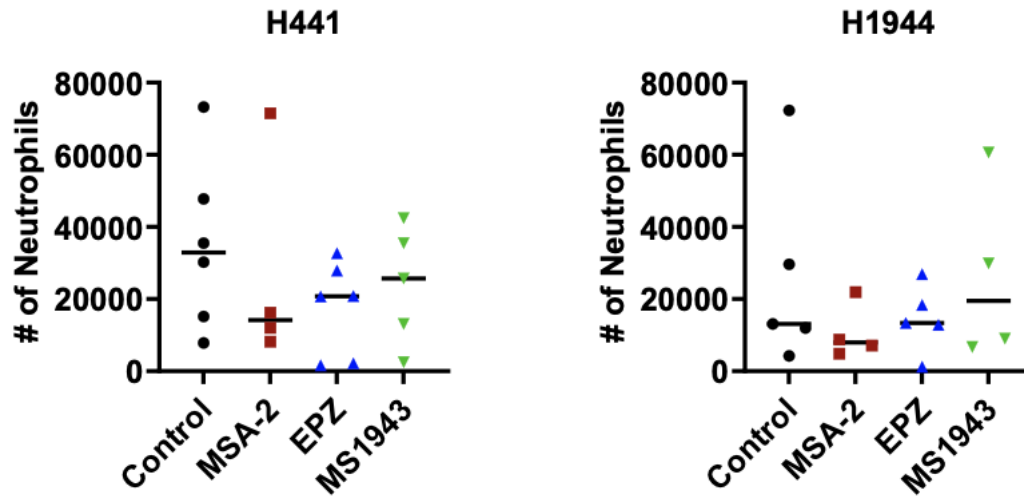


Figure 3.5. Impact of EZH2 inhibitors EPZ6438 and MS1943 on TIN phenotype in LUAD/TIN co-cultures. (A) Human neutrophils from healthy donors transmigrated through H441 (black) and H1944 (purple) LUAD lines into LTB₄ only (control), LTB₄+EPZ6438 (EPZ), or LTB₄+MS1943 (MS1943) were subjected to flow cytometry analysis to assess activation profiles. Comparison between H441 and H1944 cell lines and between control and EPZ6438 or MS1943 treatments was by Wilcoxon test (N=6-7), and shown as * for p<0.05.



Supplementary Figure 3S1. Flow cytometry strategy for gating of TINs in LUAD/TIN cocultures. After 12 h of transmigration, TINs were collected from the apical compartment and identified with sequential gates 1 (singlets), 2 (leukocytes), 3 (live cells), and 4 (neutrophils), shown from left to right.



Supplementary Figure 3S2. Quantification of TINs in LUAD/TIN cocultures. After each 12 h of transmigration, TINs were collected from the apical compartment and analyzed by flow cytometry. Shown are 6-7 independent repeats for LTB4 only (control), LTB4+MSA-2 (MSA-2), LTB4+EPZ6438 (EPZ), and LTB4+MS1943 (MS1943) conditions.

References

1. Bray, F., et al., Global cancer statistics 2022: GLOBOCAN estimates of incidence and mortality worldwide for 36 cancers in 185 countries. *CA Cancer J Clin*, 2024. **74**(3): p. 229-263.
2. Della Corte, C.M. and L.A. Byers, Evading the STING: LKB1 Loss Leads to STING Silencing and Immune Escape in KRAS-Mutant Lung Cancers. *Cancer Discov*, 2019. **9**(1): p. 16-18.
3. Kitajima, S., et al., Suppression of STING Associated with LKB1 Loss in KRAS-Driven Lung Cancer. *Cancer Discov*, 2019. **9**(1): p. 34-45.
4. Koyama, S., et al., STK11/LKB1 Deficiency Promotes Neutrophil Recruitment and Proinflammatory Cytokine Production to Suppress T-cell Activity in the Lung Tumor Microenvironment. *Cancer Res*, 2016. **76**(5): p. 999-1008.
5. Yang, L., et al., A subset of VEGFR-TKIs activates AMPK in LKB1-mutant lung cancer. *Cancer Sci*, 2023. **114**(4): p. 1651-1662.
6. Zappa, C. and S.A. Mousa, Non-small cell lung cancer: current treatment and future advances. *Transl Lung Cancer Res*, 2016. **5**(3): p. 288-300.
7. Herbst, R.S., D. Morgensztern, and C. Boshoff, The biology and management of non-small cell lung cancer. *Nature*, 2018. **553**(7689): p. 446-454.
8. Alduais, Y., et al., Non-small cell lung cancer (NSCLC): A review of risk factors, diagnosis, and treatment. *Medicine (Baltimore)*, 2023. **102**(8): p. e32899.
9. Wang, F., S. Wang, and Q. Zhou, The Resistance Mechanisms of Lung Cancer Immunotherapy. *Front Oncol*, 2020. **10**: p. 568059.

10. Sunaga, N., et al., Knockdown of oncogenic KRAS in non-small cell lung cancers suppresses tumor growth and sensitizes tumor cells to targeted therapy. *Mol Cancer Ther*, 2011. **10**(2): p. 336-46.
11. Fuca, G., et al., Modulation of peripheral blood immune cells by early use of steroids and its association with clinical outcomes in patients with metastatic non-small cell lung cancer treated with immune checkpoint inhibitors. *ESMO Open*, 2019. **4**(1): p. e000457.
12. Shaul, M.E., et al., Circulating neutrophil subsets in advanced lung cancer patients exhibit unique immune signature and relate to prognosis. *FASEB J*, 2020. **34**(3): p. 4204-4218.
13. Houghton, A.M., The paradox of tumor-associated neutrophils: fueling tumor growth with cytotoxic substances. *Cell Cycle*, 2010. **9**(9): p. 1732-7.
14. Aloe, C., et al., Emerging and multifaceted role of neutrophils in lung cancer. *Transl Lung Cancer Res*, 2021. **10**(6): p. 2806-2818.
15. Hurt, B., et al., Cancer-promoting mechanisms of tumor-associated neutrophils. *Am J Surg*, 2017. **214**(5): p. 938-944.
16. Boyero, L., et al., Primary and Acquired Resistance to Immunotherapy in Lung Cancer: Unveiling the Mechanisms Underlying of Immune Checkpoint Blockade Therapy. *Cancers (Basel)*, 2020. **12**(12).
17. Döring, G., et al., Cleavage of lymphocyte surface antigens CD2, CD4, and CD8 by polymorphonuclear leukocyte elastase and cathepsin G in patients with cystic fibrosis. *The Journal of Immunology*, 1995. **154**(9): p. 4842-4850.
18. Oberg, H.H., et al., Regulatory Interactions Between Neutrophils, Tumor Cells and T Cells. *Front Immunol*, 2019. **10**: p. 1690.

19. Cui, C., et al., Neutrophil elastase selectively kills cancer cells and attenuates tumorigenesis. *Cell*, 2021. **184**(12): p. 3163-3177 e21.
20. Gibellini, L., et al., Circulating and Tumor-Associated Neutrophils in the Era of Immune Checkpoint Inhibitors: Dynamics, Phenotypes, Metabolism, and Functions. *Cancers (Basel)*, 2023. **15**(13).
21. Shao, F.F., B.J. Chen, and G.Q. Wu, The functions of EZH2 in immune cells: Principles for novel immunotherapies. *J Leukoc Biol*, 2021. **110**(1): p. 77-87.
22. DuCote, T.J., et al., EZH2 inhibition promotes tumor immunogenicity in lung squamous cell carcinomas. *bioRxiv*, 2023.
23. Zheng, H., et al., Epigenetically suppressed tumor cell intrinsic STING promotes tumor immune escape. *Biomed Pharmacother*, 2023. **157**: p. 114033.
24. Hubaux, R., et al., EZH2 promotes E2F-driven SCLC tumorigenesis through modulation of apoptosis and cell-cycle regulation. *J Thorac Oncol*, 2013. **8**(8): p. 1102-6.
25. Gan, L., et al., Epigenetic regulation of cancer progression by EZH2: from biological insights to therapeutic potential. *Biomark Res*, 2018. **6**: p. 10.
26. Margaroli, C., et al., Transcriptional firing represses bactericidal activity in cystic fibrosis airway neutrophils. *Cell Rep Med*, 2021. **2**(4): p. 100239.
27. Dobosh, B., et al., Mass production of human airway-like neutrophils via transmigration in an organotypic model of human airways. *STAR Protoc*, 2021. **2**(4): p. 100892.
28. Steen, H.C. and A.M. Gamero, Interferon-lambda as a potential therapeutic agent in cancer treatment. *J Interferon Cytokine Res*, 2010. **30**(8): p. 597-602.
29. Cassatella, M.A., et al., Regulated production of the interferon-gamma-inducible protein-10 (IP-10) chemokine by human neutrophils. *Eur J Immunol*, 1997. **27**(1): p. 111-5.

30. Chiba, K., et al., Neutrophils secrete MIP-1 beta after adhesion to laminin contained in basement membrane of blood vessels. *Br J Haematol*, 2004. **127**(5): p. 592-7.
31. Skoulidis, F., et al., Co-occurring genomic alterations define major subsets of KRAS-mutant lung adenocarcinoma with distinct biology, immune profiles, and therapeutic vulnerabilities. *Cancer Discov*, 2015. **5**(8): p. 860-77.
32. Serrano, R., et al., Stimulatory and inhibitory activity of STING ligands on tumor-reactive human gamma/delta T cells. *Oncoimmunology*, 2022. **11**(1): p. 2030021.
33. Margaroli, C., et al., Elastase Exocytosis by Airway Neutrophils Is Associated with Early Lung Damage in Children with Cystic Fibrosis. *Am J Respir Crit Care Med*, 2019. **199**(7): p. 873-881.
34. Chae, Y.K., M.S. Oh, and F.J. Giles, Molecular Biomarkers of Primary and Acquired Resistance to T-Cell-Mediated Immunotherapy in Cancer: Landscape, Clinical Implications, and Future Directions. *Oncologist*, 2018. **23**(4): p. 410-421.
35. Qu, X., Y. Tang, and S. Hua, Immunological Approaches Towards Cancer and Inflammation: A Cross Talk. *Front Immunol*, 2018. **9**: p. 563.
36. Gregory, A.D. and A.M. Houghton, Tumor-associated neutrophils: new targets for cancer therapy. *Cancer Res*, 2011. **71**(7): p. 2411-6.
37. Tang, W., et al., Role of STING in the treatment of non-small cell lung cancer. *Cell Commun Signal*, 2024. **22**(1): p. 202.
38. Zhang, J., et al., Emerging mechanisms and implications of cGAS-STING signaling in cancer immunotherapy strategies. *Cancer Biol Med*, 2024. **21**(1): p. 45-64.
39. Low, J.T., et al., Understanding and therapeutically exploiting cGAS/STING signaling in glioblastoma. *J Clin Invest*, 2024. **134**(2).

Chapter 4: Conclusions and perspectives

Foreword

One in eight women in the United States is at risk of developing *breast* cancer including but not limited to triple-negative breast cancer (TNBC), during her lifetime. By the year 2050, it is estimated that there will be 3.2 million new breast cancer cases worldwide, each with distinct phenotypes and clinical outcomes [1]. Likewise, each year, around 230,000 people in the United States are diagnosed with *lung* cancer, including but not limited to lung adenocarcinoma (LUAD), and an estimated 135,000 patients die from the disease [2]. Patients diagnosed with these cancer subtypes represent a high-risk group due to high patient-to-patient tumor heterogeneity and a lack of specific therapeutic targets, resulting in increased rates of relapse, recurrence, and mortality. In recent years, research efforts have led to exciting progress in characterizing the molecular and immune profiles of different cancer subtypes, thereby enhancing treatment design. In addition, significant advances have been made in understanding the mechanisms of escape that allow cancer cells to survive in the face of an anti-tumor immune response, and how to counter them.

Currently, three main types of immunotherapeutic strategies are employed: 1) *passive*, which includes the infusion of monoclonal antibodies that bind to tumor-associated targets and target them for immune attack, and systemic administration of recombinant cytokines to boost immune responses; 2) *active*, which involves the administration of immune checkpoint inhibitors (ICIs) and vaccines; and 3) *adoptive*, which stimulates effector T-cell activation to eliminate cancer cells [3]. However, immunologically “cold” tumors like TNBC and LUAD typically do not respond well to immunotherapies, often due to deficiencies in immune signaling and antigen presentation [4]. Tumors also acquire antigen editing mechanisms to evade antitumor immune responses [5]. The complex mechanisms by which cancer cells escape host immune surveillance,

including cell-cell interactions with innate and adaptive immune cells, are areas of high interest in translational research.

One extrinsic factor that induces inhibition and exhaustion of T-cells in tumors is the enriched presence of tumor-infiltrating neutrophils (TINs). TINs have emerged as key participants in the complex immune landscape of cancer, both promoting and restraining tumor growth, depending on the context. In cases where TINs enable cancer pathogenesis, they have been implicated in promoting tumor proliferation by activating anabolic pathways, angiogenesis by promoting endothelial cell growth, and the formation of metastases by helping cancer cells detach from the primary tumor mass, intravasate into the circulation, then extravasate in a remote site and establish a new outpost. Consistently, a high frequency of circulating neutrophils (as measured by the neutrophil to lymphocyte ration, for example) has also been associated with poor cancer patient prognosis and response to treatment [6]. To overcome this issue, TINs are prominent candidates for the development of novel therapeutic strategies.

[EZH2, a potential TNBC therapeutic target](#)

High expression of the transcriptional repressor EZH2 in TNBC causes epigenetic silencing of target genes such as stimulator of interferon genes (STING), which impact the survival and metastatic potential of cancer cells. EZH2 expression also correlates with advanced disease stages and poor prognosis. Interestingly, EZH2 is also a key regulator of immune cell development, differentiation, and function, as well as tumor/immune cell interplay [7]. Previous studies have shown that EZH2 acts in neutrophils to modulate their mobility in response to chemotactic signals, enhancing their influx into tissue [8]. In addition, previous studies have reported that high EZH2 expression in breast epithelial cells induces anchorage-independent

growth that supports cell invasion *in vivo* through MMP-2/-9 regulation [9, 10]. Also, studies in B-cell lymphomas have shown a correlation between EZH2 mutational rate and MHC-I/II expression deficiency. While the mechanisms by which EZH2 modulates the MHC complex and other antigen presentation molecules remain unknown, this phenomenon has been observed in various cancers [11].

In this dissertation, we aimed to better understand how absence of EZH2 could directly impact tumor growth and metastasis while regulating TINs/TILs in the tumor microenvironment. In Chapter 2 (**Figure 4.1**), we used CRISPR technology to generate EZH2 KO and EZH2 OE clones from a 4T1 murine TNBC cell line.

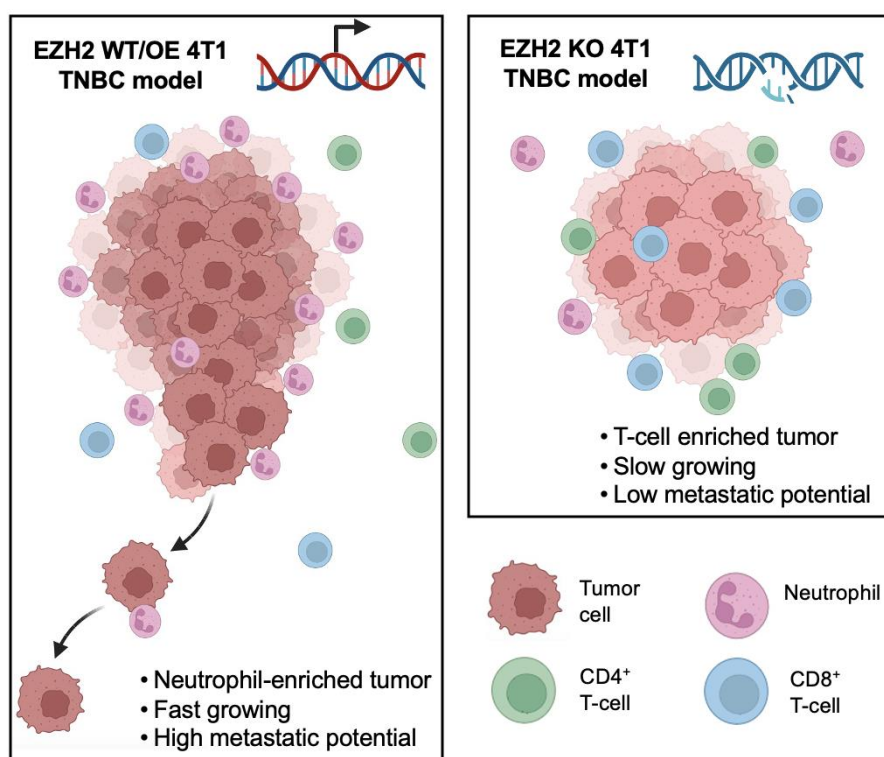


Figure 4.1. EZH2 expression influences immune cell infiltration and impacts disease progression in TNBC. High levels of EZH2 in cancer cells have shown to inhibit T-cell

infiltration, promote neutrophil enrichment in the microenvironment, and support tumor growth and metastasis. Conversely, inhibiting EZH2 expression in cancer cells resulted in increased T-cell recruitment and a significant reduction in primary tumor growth and metastatic potential.

We observed no significant changes in the replicative capacity and invasiveness of these clones compared to the wild-type cell line *in vitro*. However, we found decreased expression of multiple immune response markers in the generated clones, with intermediate levels in wild-type cells. Additionally, EZH2 KO culture supernatants showed significantly altered secretion of GM-CSF, MCP-1, and IL1 β (myeloid mediators), suggesting that complete absence of EZH2 in TNBC alters its inflammatory mediator secretome.

EZH2 overexpression is known to negatively regulate STING and the activation of interferon-stimulated genes. Therefore, chemical or genetic inhibition of EZH2 derepresses endogenous dsRNA, allowing the activation of STING and reversing resistance to checkpoint therapy [12]. Our EZH2 KO model showed a drastic reduction in tumor size and significant decreased in metastatic burden in the lungs compared to the EZH2 OE and wild-type cells. Additionally, research in other breast cancer models have shown that inhibiting EZH2 can enhance antigen presentation and increase immune infiltration into the tumor [11]. In our studies, we observed a shift in the tumor-infiltrating immune cell population in the EZH2 KO tumors. Increased percentages of tumor-infiltrating CD4⁺ and CD8⁺ T-cells and reduced percentage of TINs may have influenced cancer progression and metastatic development, leading to better outcomes in tumors lacking EZH2 expression. Our results align with other studies that have observed higher T-cell trafficking to the tumor microenvironment when EZH2 is absent.

As a therapeutic approach to tackle this specific pathway in patients with melanoma (an example of an immune-refractory, “cold” tumors), administration of the STING agonist MSA-2 has shown promising results, with enhanced antigenicity and T-cell recognition of the tumor [13]. When using MSA-2 in our TNBC model *in vivo*, we also observed therapeutic benefits in reducing tumor growth and significantly decreasing metastatic burden. Consistently, prior studies suggest a dose-dependent effect of MSA-2 on STING signaling that can enhance the maturation and antigen presentation capabilities of dendritic cells, in turn improving T-cell activation [14]. Overall, our findings indicate that altering EZH2 expression in cancer cells affects TIN recruitment, thus influencing tumor growth, metastasis, and the arrival of other immune cells into the TME. Genetic absence of EZH2 in tumor cells, coupled with STING agonism with MSA-2, can transform cold tumors into hot, T-cell-inflamed, tumors by inducing interferon and other proinflammatory mediators, and enhance anti-tumor immunity.

STING agonism and IL-29 induction are promising immunotherapeutic routes for human LUAD

In recent years, extensive scientific research has focused on creating therapies to enhance clinical outcomes for lung cancer patients. Nonetheless, significant challenges persist, including the need to identify new driver gene alterations to broaden the population that can benefit from targeted treatments. In this dissertation, we developed a novel *in vitro* co-culture model for mass-production of human TINs after transmigration through LUAD cells grown at air-liquid interface (biomimetic model). Our investigations (Chapter 3) focused on assessing the impact on LUAD/TIN co-cultures of STING agonism by MSA-2, as well as chemical inhibition of EZH2 (rather than genetic EZH2 knockout or overexpression, as done in Chapter 2, for TNBC). Previous studies using EZH2 inhibitors such as EPZ6438 and MS1943 showed no significant

impact on cancer cell growth inhibition but induced dramatic changes in interferon release, enhancing tumor cell susceptibility to T-cell-mediated killing [11]. In our study, treatment with MSA-2 resulted in high production of type III interferon IL-29 (IFN- λ 3) in LKB1-mutant, EZH2-high LUAD, suggesting that STING activation can be restored in these refractory tumors and that interferon secretion can be enhanced. Meanwhile, treatment with EZH2 inhibitors had a modest influence in the secretion of some inflammatory mediators, but failed to affect IL-29 levels, which may be caused by partially overlapping, but not total synchrony between EZH2 and STING signaling.

Interestingly, IL-29 primarily targets normal and cancerous epithelial cells, as well as tissue-recruited neutrophils and monocytes/macrophages (sole cells who bear its specific receptor subunit IL29-R1 in humans) and is considered a potential anti-tumor mediator. Other studies have reported a pro-apoptotic effect of IL-29 on cancer cells, via induction of TRAIL signaling, notably [15]. From a mechanistic perspective, it is possible that double-stranded DNA derived from dying lung cancer cells activates STING in TINs, leading to the secretion of interferons. Given that the IL-29 and its receptor may be expressed both by LUAD cells and neutrophils, an autocrine/paracrine loop could arise that may explain the 27-fold induction in IL-29 secretion in LKB1-mutant LUAD/TIN cocultures treated with MSA-2 (**Figure 4.2**) [16].

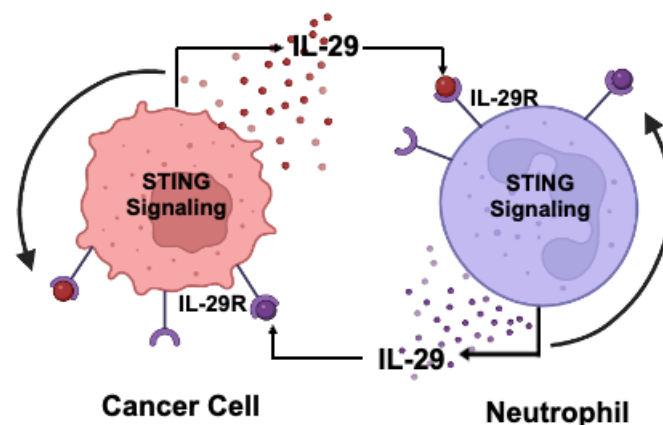


Figure 4.2. LUAD/TIN interplay shows responsiveness to STING agonist treatment through induction of IL-29. IL-29R is on cancer cells and TINs, autocrine/paracrine signaling is possible via multiple routes.

Our results suggest that the simultaneous delivery of EZH2 inhibitors in LUAD cells is not crucial for the generation of effective anti-tumor responses. However, IL29 secretion in either cancer cells or TINs could be attributed to STING activation and may be a potential therapeutic target. Additionally, studies in lung cancer patients have shown elevated levels of IL-29 in serum, suggesting its use as a diagnosis marker. Exciting discoveries indicate that IL-29 can induce cell cycle arrest and apoptosis by upregulating cyclin-dependent kinase inhibitors [17].

Concluding remarks and potential areas of future investigations

Epigenetic regulation of immunogenicity in cancer is a major obstacle to developing effective therapies [18]. Patients experience different resistance mechanisms to immunotherapy at different disease stages. Such is the case during primary resistance, when cancer cells do not respond to immunotherapy. In adaptive immune resistance, cancer cells are recognized by the

immune system but develop mechanisms to protect themselves from immune eradication. In acquired resistance, cancer initially responds to immunotherapy but eventually relapses and progresses [19]. In addition, host-related characteristics, including gut microbiome, diet, antibiotic exposure, vaccine exposure and inflammation may also impact the acquisition of tumor immune resistance [20-22]. Likewise, the immune microenvironment may lead to dampened immunotherapy responses, as it is influenced by complex tumor phenotypes and environmental factors [23]. Some phenotypes that lack immunotherapeutic responses include immune-desert (fail to evoke an immune reaction), immune-inflamed (inhibit immune cell function despite abundant infiltration), and immune-excluded (prevent immune cell infiltration) tumors [24].

Understanding the role of immune cells in cancer is essential for predicting patient outcomes through the identification of novel biomarkers and tailoring of subtype-specific therapeutic strategies. Previous studies have revealed that crosstalk between TINs and TILs at an early disease stage can lead to upregulation of costimulatory molecules on neutrophil surface, enhancing T-cell activation and proliferation [25]. Therefore, developing combination therapies that target both T-cells and other immune cells could achieve potent and durable therapeutic responses [26]. While we generated EZH2 KO and OE cell lines that allow the testing of cancer progression and metastasis in immunocompetent mice, a major unexplored avenue thus far consists in using our models to quantify EZH2 expression and inhibition of primary and metastatic tumors and associated TINs in tumor FFPE blocks via digital spatial profiling. Based on research by other groups, EZH2-mediated invasion was found to be abrogated by histone deacetylases (HDAC) inhibitors TSA and SAHA, implying that HDAC activity directly impacts the transcriptional repressor functions of EZH2 [9, 27]. For upcoming experiments, HDAC

inhibitors could be therapeutic compounds to use as controls in EZH2-expressing tumors. On the other hand, the human LUDA/TIN model we developed could be used to further investigate the effects of EZH2 inhibition by setting up a of blood neutrophils transmigrated through LUAD cells (wild-type and EZH2 KO generated by CRISPR).

For future anti-TNBC and LUAD therapeutic design, other biological variables are important to consider like metabolism and sex bias [28-30]. Studies quantifying differential expression and signaling of the EZH2/STING pathway and downstream functions in TIN-rich cancers based on sex will provide valuable information on differential mechanisms of neutrophil recruitment into the tumor, if any [31]. In addition, sex bias could impact the response of TINs to EZH2/STING modulatory drugs, leading to different pathological outcomes. Finally, while studies here focused on immune aspects of EZH2 inhibition and STING activation in cancer/TIN interplay, the metabolic effect of drugs on cancer and immune cells was not assessed, and could be a modifier of treatment effects, as seen in cancer patients with metabolic anomalies like obesity [32].

References

1. Tao, Z., et al., Breast Cancer: Epidemiology and Etiology. *Cell Biochem Biophys*, 2015. **72**(2): p. 333-8.
2. Clark, S.B. and S. Alsubait, Non–Small Cell Lung Cancer, in *StatPearls*. 2024, StatPearls Publishing.
3. Carlino, F., et al., Immune-Based Therapy in Triple-Negative Breast Cancer: From Molecular Biology to Clinical Practice. *Cancers (Basel)*, 2022. **14**(9).
4. Wang, M., et al., Therapeutic strategies to remodel immunologically cold tumors. *Clin Transl Immunology*, 2020. **9**(12): p. e1226.
5. Henriques, B., F. Mendes, and D. Martins, Immunotherapy in Breast Cancer: When, How, and What Challenges? *Biomedicines*, 2021. **9**(11).
6. Obeagu, E.I. and G.U. Obeagu, Exploring neutrophil functionality in breast cancer progression: A review. *Medicine (Baltimore)*, 2024. **103**(13): p. e37654.
7. Huang, J., et al., Easy or Not-The Advances of EZH2 in Regulating T Cell Development, Differentiation, and Activation in Antitumor Immunity. *Front Immunol*, 2021. **12**: p. 741302.
8. Kitchen, G.B., et al., The histone methyltransferase Ezh2 restrains macrophage inflammatory responses. *Faseb j*, 2021. **35**(10): p. e21843.
9. Klee, C.G., et al., EZH2 is a marker of aggressive breast cancer and promotes neoplastic transformation of breast epithelial cells. *Proc Natl Acad Sci U S A*, 2003. **100**(20): p. 11606-11.

10. Chien, Y.C., et al., EZH2 promotes migration and invasion of triple-negative breast cancer cells via regulating TIMP2-MMP-2/-9 pathway. *Am J Cancer Res*, 2018. **8**(3): p. 422-434.
11. Zhou, L., et al., Targeting EZH2 Enhances Antigen Presentation, Antitumor Immunity, and Circumvents Anti-PD-1 Resistance in Head and Neck Cancer. *Clin Cancer Res*, 2020. **26**(1): p. 290-300.
12. Morel, K.L., et al., EZH2 inhibition activates a dsRNA-STING-interferon stress axis that potentiates response to PD-1 checkpoint blockade in prostate cancer. *Nat Cancer*, 2021. **2**(4): p. 444-456.
13. Emran, A.A. and D.E. Fisher, Dual Targeting with EZH2 Inhibitor and STING Agonist to Treat Melanoma. *J Invest Dermatol*, 2022. **142**(4): p. 1004-1006.
14. Yi, M., et al., Combination of oral STING agonist MSA-2 and anti-TGF-beta/PD-L1 bispecific antibody YM101: a novel immune cocktail therapy for non-inflamed tumors. *J Hematol Oncol*, 2022. **15**(1): p. 142.
15. Ha, J.L., et al., Up and away with cervical cancer: IL-29 is a promising cytokine for immunotherapy of cervical cancer due to its powerful upregulation of p18, p27, and TRAILR1. *Med Oncol*, 2024. **41**(3): p. 65.
16. Kelm, N.E., et al., The role of IL-29 in immunity and cancer. *Crit Rev Oncol Hematol*, 2016. **106**: p. 91-8.
17. Fujie, H., et al., Antitumor activity of type III interferon alone or in combination with type I interferon against human non-small cell lung cancer. *Cancer Sci*, 2011. **102**(11): p. 1977-90.

18. Hiam-Galvez, K.J., B.M. Allen, and M.H. Spitzer, Systemic immunity in cancer. *Nat Rev Cancer*, 2021. **21**(6): p. 345-359.
19. Sharma, P., et al., Primary, Adaptive, and Acquired Resistance to Cancer Immunotherapy. *Cell*, 2017. **168**(4): p. 707-723.
20. Kioussi, D.E., et al., The Role of the Gut Microbiome in Cancer Immunotherapy: Current Knowledge and Future Directions. *Cancers (Basel)*, 2023. **15**(7).
21. Huang, X.Z., et al., Antibiotic use and the efficacy of immune checkpoint inhibitors in cancer patients: a pooled analysis of 2740 cancer patients. *Oncoimmunology*, 2019. **8**(12): p. e1665973.
22. Wang, F., S. Wang, and Q. Zhou, The Resistance Mechanisms of Lung Cancer Immunotherapy. *Front Oncol*, 2020. **10**: p. 568059.
23. Chen, D.S. and I. Mellman, Elements of cancer immunity and the cancer-immune set point. *Nature*, 2017. **541**(7637): p. 321-330.
24. Chae, Y.K., M.S. Oh, and F.J. Giles, Molecular Biomarkers of Primary and Acquired Resistance to T-Cell-Mediated Immunotherapy in Cancer: Landscape, Clinical Implications, and Future Directions. *Oncologist*, 2018. **23**(4): p. 410-421.
25. Eruslanov, E.B., et al., Tumor-associated neutrophils stimulate T cell responses in early-stage human lung cancer. *J Clin Invest*, 2014. **124**(12): p. 5466-80.
26. Johansen, P., et al., Antigen kinetics determines immune reactivity. *Proc Natl Acad Sci U S A*, 2008. **105**(13): p. 5189-94.
27. Varambally, S., et al., The polycomb group protein EZH2 is involved in progression of prostate cancer. *Nature*, 2002. **419**(6907): p. 624-9.

28. Xiao, T., et al., Hallmarks of sex bias in immuno-oncology: mechanisms and therapeutic implications. *Nat Rev Cancer*, 2024. **24**(5): p. 338-355.
29. Costa, A.R., et al., The Sex Bias of Cancer. *Trends Endocrinol Metab*, 2020. **31**(10): p. 785-799.
30. Martinez-Reyes, I. and N.S. Chandel, Cancer metabolism: looking forward. *Nat Rev Cancer*, 2021. **21**(10): p. 669-680.
31. Uppala, R., et al., HERC6 regulates STING activity in a sex-biased manner through modulation of LATS2/VGLL3 Hippo signaling. *iScience*, 2024. **27**(2): p. 108986.
32. Margaroli, C., et al., The immunosuppressive phenotype of tumor-infiltrating neutrophils is associated with obesity in kidney cancer patients. *Oncoimmunology*, 2020. **9**(1): p. 1747731.